Old Dominion University

ODU Digital Commons

Biological Sciences Theses & Dissertations

Biological Sciences

Spring 5-2023

Landscape Genetics of the Gulf Coast Tick, *Amblyomma maculatum*

Sara Simmons Benham
Old Dominion University, sabenham425@gmail.com

Follow this and additional works at: https://digitalcommons.odu.edu/biology_etds

🟠 Part of the Ecology and Evolutionary Biology Commons, Entomology Commons, and the Genetics Commons

LANDSCAPE GENETICS OF THE GULF COAST TICK, *AMBLYOMMA MACULATUM*

by

Sara Simmons Benham
B.S. March 2012, Oregon State University
M.S. July 2017, Southeastern Louisiana University

A Dissertation Submitted to the Faculty of
Old Dominion University in Partial Fulfillment of the
Requirements for the Degree of

DOCTOR OF PHILOSOPHY

ECOLOGICAL SCIENCES

OLD DOMINION UNIVERSITY
May 2023

Approved by:

Holly D. Gaff (Director)

David T. Gauthier (co-Director)

Wayne Hynes (Member)

Andrea Varela-Stokes (Member)

Tom Allen (Member)

ABSTRACT

LANDSCAPE GENETICS OF THE GULF COAST TICK, *AMBLYOMMA MACULATUM*

Sara Simmons Benham
Old Dominion University, 2023
Co-Directors: Dr. Holly Gaff
Dr. David Gauthier

Connectivity among populations helps to maintain genetic diversity, population stability, and resilience. The Gulf Coast tick, *Amblyomma maculatum*, is a vector of the pathogen *Rickettsia parkeri*. Persistence of tick populations with high rates of *R. parkeri* infection poses health risks to humans and animals. Mitochondrial haplotypes were characterized by sequencing a fragment of the mitochondrial 16S rRNA gene. A comparative study of *A. maculatum* and *Amblyomma americanum* was conducted to identify similar and unique patterns between the species within the same region. Next, I compared *A. maculatum* sites across three different regions of the United States. This work examined diversity and connectivity between and among *A. maculatum* populations to resolve questions about the process of range expansion and population establishment. The first research aim was to characterize the genetic diversity within *A. maculatum* populations and infer connectivity among populations. These population genetics comparisons revealed that Gulf Coast tick populations showed signs of isolation compared to *A. americanum* populations, which have higher gene flow. One *A. maculatum* population was dominated by an otherwise rare haplotype, an unusual pattern that signaled a possible founder effect from a long-distance drop-off. Given the apparent isolation and unusual dominance within one unique population, a landscape analysis was completed by examining remote-sensing data to determine correlations between environmental variables and *A. maculatum* populations for the purpose of identifying suitable and unsuitable habitat that could influence patterns of movement and barriers to gene flow. None of the environmental variables had clear correlations with *A. maculatum* population presence, so barriers could not be identified. Finally, an agent-based model was created to simulate recurrent introductions of Gulf Coast ticks in rasterized models of several field study sites. Propagule pressure was positively

associated with haplotype richness, whereas edge patches had a negative effect on richness. The simulation results suggested that limited immigration as well as landscape configurations could explain rare patterns of low diversity.

ACKNOWLEDGMENTS

TABLE OF CONTENTS

LIST OF TABLES

LIST OF FIGURES

Figure   Page

CHAPTER 1

INTRODUCTION

The burden of tick-borne disease (TBD) in the United States presents a serious threat to public health (Sonenshine, 2018). Understanding the ecology of TBDs, particularly the environmental drivers that can influence host and tick population dynamics, thus influencing disease spread, is an important complement to clinical work and biomedical research focusing on the pathogen. Population dynamics and range expansions of ticks are especially critical to understand if we intend to manage and control TBDs. Models that forecast mosquito-borne illness risks (e.g. Barker, 2019) offer examples of remote-sensing applications and the use of geospatial tools to address problems in the study of vector-borne disease. A similar approach that incorporates environmental data with tick and pathogen surveillance can be useful to understand TBD risks, with some modifications to use methods and spatio-temporal scales appropriate for ticks. The basic premise of the work proposed here is that different environmental variables can affect both tick and host populations. Quantifying those variables that contribute most to changes in tick populations and geographic extent, by considering the unique ecology of a focal tick species, can aid the development of better forecasting and surveillance models for TBD.

The Gulf Coast tick (GCT), *Amblyomma maculatum*, is a vector of the bacterial pathogen *Rickettsia parkeri*, the causative agent of *R. parkeri* rickettsiosis in humans, a disease previously known as Tidewater spotted fever (Paddock et al., 2004). Spotted fever rickettsiosis (SFR) is a diagnostic term that refers to disease caused by several *Rickettsia* spp. pathogens. Rocky Mountain spotted fever (RMSF), caused by the agent *R. rickettsii*, is a severe illness that has led to fatalities in about 3.4% of laboratory-confirmed cases in the United States since the 1980s (Paddock et al., 1999). In contrast, *R. parkeri* rickettsiosis

typically causes less severe disease than RMSF. Disease caused by *R. parkeri* is most often differentiated from RMSF by the appearance of an eschar at the site of the tick bite, which can reveal *R. parkeri* in tissue biopsies (Paddock et al., 2008). No fatalities have been associated with *R. parkeri* rickettsiosis (Biggs et al., 2016). The incidence of SFR has been increasing, with higher incidences in states that lie in the southeastern and central United States. The regions with human cases of SFR generally overlap with the GCT range in many areas, an ecological indication that GCTs are currently contributing to caseloads by transmitting *R. parkeri* to humans. In fact, cases of *R. parkeri* rickettsiosis identified outside of the documented GCT range in 2014 (Herrick et al., 2016) prompted further investigation and ultimately new collection records for GCTs from Arizona and New Mexico (Allerdice et al., 2017; Hecht et al., 2020). These additional collections strengthen the connection between the presence of GCTs and a rising incidence of *R. parkeri* rickettsiosis.

Amblyomma maculatum populations have expanded north from the species' historic range in the southeastern United States and northern Gulf Coast (Teel et al., 2010). This trend of range expansion has been accompanied by remarkable disparities in the geographical pattern of *R. parkeri* prevalence. Populations along the northeastern margins of this range, specifically in the Mid-Atlantic region, have 41.5–55.7% *R. parkeri* prevalence (Fornadel et al., 2011; Nadolny et al., 2014; Paddock & Goddard, 2015; Wright et al., 2011), compared to about 8–40% prevalence in southern states (Paddock & Goddard, 2015). This prompts the question, what is the influence of geography on this vector-pathogen system? This question must be answered for each part of the system: the animal host, the tick vector, and the pathogen. Although these components are interconnected, the first step to understanding this system comprehensively is to understand the effects of geography on each part independently.

1.1 RESEARCH AIMS

The aim of this work is to explore the relationship between the tick vector, GCT populations in this case, and spatial landscape patterns. Prior attempts to evaluate environmental influences on GCTs have used a species distribution modeling approach to explore distributions of tick specimens of the *A. maculatum* species complex collected across multiple continents (Cuervo et al., 2021). Niche conservatism is generally apparent across species and morphotypes, with niche differentiation observed between several groups that may lead to speciation. However, that work did not explore the mechanics at work within populations at smaller geographic and temporal scales that contribute to the broader patterns observed in realized niches. Specifically, the question remains how movement of ticks, via hosts, could be directed or interrupted by geography, including environmental factors. How does movement on smaller scales contribute to population mixing or isolation, and thus the exchange of pathogens that might inhabit these population?

Here I propose a set of research questions that will focus on understanding tick population mixing using a landscape genetic analysis. This analysis will consider changes in populations and habitats within short time frames, for example across a single decade. This time period is relevant to understanding how environment influences population expansion and establishment in new areas. The landscape genetics approach will include: 1) genetic connectivity patterns derived from population genetics analyses 2) analysis of remotely-sensed environmental variables that describe habitat associations of the tick, and 3) agent-based modeling and simulation to compare simulated theoretical and empirical data.

1.2 KEY CONCEPTS AND TERMS

Connectivity – Evidence of gene flow between populations, inferred from estimates of genetic structure or explored directly by looking at covariance among populations using Population Graphs (Dyer & Nason, 2004), resistance analyses (McRae, 2006), or random walk theories based on Sewall Wright's fitness landscapes (Wright, 1932).

Drop-off – In tick biology, a drop-off refers to a single tick or cohort leaving a host after completing a bloodmeal. The term is often used in the context of a tick present in isolation, or in a location distant from the source population, which has been moved there by a host.

Expansion front – A reference to the geographic area at the extent, or margins, of a species distribution during an ongoing range expansion.

Fixation/Fixation index – Fixation is lack of allelic diversity within a population resulting from ecological, demographic, or evolutionary effects. Fixation indices, such as F_{ST}, G_{ST}, and ϕ_{ST}, are used to calculate differences in heterozygosity between populations, or between hierarchical groups (F_{SC} and F_{CT}). These indices report a value from 0–1 where 0 indicates shared alleles between populations and 1 indicates fixation, inferring populations are completely isolated from each other. Significantly non-zero values in between 0–1 are evidence of fixation.

Founder effect – A founder effect describes the influence of a small group of first-generation individuals on the genetic diversity of subsequent generations in a population. The founder effect is often described in relation to phenotypes that have adverse effects on the fitness of later generations as a result of fixation, but can also be used to describe any evidence of

fixation of apparently neutral genetic variants as a result of non-evolutionary processes such as genetic drift or bottlenecks.

Genetic distance – A measure derived from mathematical models that use categorical genotypes (i.e. a classification such as haplotype) or the base-pair sequences to estimate proximity in the lineages of individuals or populations. Many models exist to estimate genetic distance, most often using assumptions about mutation rates to infer relationships or connectivity.

Genetic diversity – In population genetics, genetic diversity is typically measured through mathematical indices based on genotype classes (i.e. haplotypes) or sequences within the same species. The basic components of diversity are: 1) composition, the identity, e.g. haplotype; 2) richness, the number of unique identities within a population; 3) evenness, the proportions or frequency of each identity in relation to the others. Some patterns of genetic diversity can be associated with historical, population-level events such as demographic expansion or contraction, and connectivity between populations.

Genetic structure – The appearance of clades or clustering among populations, regions, or other *a priori* groups. The most common measures of structure in population genetics, derived from F_{ST}, use fixation indices to estimate the probability of two populations or groups being connected through gene flow based on relative heterozygosity among alleles.

Haplotype – A classification of genotypes based on genetic sequences along a specific portion of DNA. Variants that make up the DNA sequence of a haplotype tend to be inherited as a whole, which enables ancestral and population genetic inferences. Haplotypes here are classified based on single base-pair variations.

Heterozygosity – A measure of gene diversity. Heterozygosity is calculated as shown in Equation 1:

$$H = \frac{n}{n-1}\left(1 - \sum_{i=1}^{k} p_i^2\right) \tag{1}$$

where p is the frequency of an allele for all alleles i through k, for a population of size n.

Landscape – An area that includes a mix of environmental conditions, e.g. a core habitat and the surrounding environment, which are expected to have different effects on an outcome of interest (Gergel & Turner, 2017).

Landscape genetics – An integrative set of methods or techniques used to relate genetic distances to geographic or ecological distance to identify barriers to gene flow. Landscape genetics typically implies a shorter time period than phylogeography, and is often used to measure species adaptation or non-evolutionary genetic responses to rapid changes in the landscape.

Niche conservatism – The retention of traits that enable a species to occupy a specific niche over time.

Patch – In landscape ecology, a patch refers to a contiguous area of similar habitat within a broader heterogeneous landscape. In agent-based modeling, a patch is the smallest spatial unit represented, more similar to the grain in landscape ecology. When necessary, a patch in the landscape ecology sense will be called a "habitat patch".

Propagule pressure – A concept in invasion biology that describes the number of individuals and introduction events that accompany a species invasion. Propagule pressure is an important component of establishment success in non-native species.

Sensitivity analysis – A test of model parameters to identify the direct effects and relative influence of inputs on the measured outcomes of a model.

Succession – The ecological progression of vegetation from open habitat to a climax community over time in the absence of disturbance. Climax communities vary by region, but are typically mixed or deciduous forests in temperate regions of the United States. A classic example of succession is "old field succession", which describes a transition from a field or pasture to a dense forested area after maintenance or grazing pressure discontinues.

CHAPTER 2

COMPARATIVE POPULATION GENETICS OF *AMBLYOMMA MACULATUM* AND *AMBLYOMMA AMERICANUM* IN THE MID-ATLANTIC UNITED STATES

PREFACE

The content of this chapter is adapted with permission from Benham, S. A., H. D. Gaff, Z. J. Bement, C. Blaise, H. K. Cummins, R. Ferrara, J. Moreno, E. Parker, A. Phan, T. Rose, S. Azher, D. Price, and D. T. Gauthier. 2021. "Comparative Population Genetics of *Amblyomma maculatum* and *Amblyomma americanum* in the Mid-Atlantic United States." *Ticks and Tick-borne Diseases* 12: 101600. Copyright 2021. Elsevier. The manuscript can be found online at https://doi.org/10.1016/j.ttbdis.2020.101600

2.1 INTRODUCTION

The Gulf Coast tick, *Amblyomma maculatum*, and the lone star tick, *Amblyomma americanum*, are hard ticks (Family: Ixodidae) that occur primarily in the southeastern United States. Both *A. americanum* and *A. maculatum* are three-host, non-nidicolous ticks that are known to bite humans; however, ecological differences include host utilization at different life stages and suitable habitats (Childs & Paddock, 2003; Nadolny & Gaff, 2018*b*; Paddock & Goddard, 2015). Adults of both *A. maculatum* and *A. americanum* parasitize large mammals such as humans, cattle (*Bos taurus*), dogs (*Canis familiaris*), coyotes (*Canis latrans*), and white-tailed deer (*Odocoileus virginianus*) (Nadolny & Gaff, 2018*b*; Paddock & Goddard, 2015). Immature *A. maculatum* are most frequently collected

from hosts such as rodents and small birds (Paddock & Goddard, 2015) but rarely by flagging or dragging (Goddard, 2007). *Amblyomma americanum* strongly prefers large-mammal hosts at all life stages, and so *A. americanum* larvae and nymphs can be readily collected by flagging vegetation (Childs & Paddock, 2003).

Geographic range expansions of human-biting tick species present a public health challenge. Little is currently known about the source of new populations, the mechanisms by which new populations become established, and how these factors influence pathogen persistence (Sonenshine, 2018). Across their geographic range, *A. maculatum* adults are typically collected in open habitats with sparse canopy cover, especially sites where early- to mid-successional vegetation is maintained by regular disturbance, such as mowing, grazing, wind and wave activity, hurricanes, or fire (Gleim et al., 2016; Nadolny & Gaff, 2018*a*; Teel et al., 2010). *Amblyomma maculatum* tick populations are likely restricted to habitat that can support both rodent populations for immature life stages and larger mammals for successful adult feeding. In contrast, *A. americanum* are collected from multiple habitat types and are associated with high densities of white-tailed deer and other large mammals (Childs & Paddock, 2003).

Historically, *A. maculatum* populations occurred throughout the southern United States within 240 km of the Gulf of Mexico and southern Atlantic coastlines (Teel et al., 2010). The occurrence of *A. maculatum* south of the United States border overlaps with the closely related *Amblyomma triste*, but with clear morphological and genetic distinctions (Lado et al., 2018). Despite an apparent *A. maculatum*-*A. triste* overlap in parts of the southernmost range of *A. maculatum* (Lado et al., 2018), expansion of members of this species complex into the United States Mid-Atlantic region currently appears to be restricted to *A. maculatum*. *Amblyomma americanum* has likely been established in Virginia since the 1910s (Springer et al., 2014) and established in larger populations by the 1970s, such that a multi-year population study (> 10,000 ticks collected) could be carried out within two sites located

in Piedmont and Tidewater areas of Virginia over a three-year period (Sonenshine & Levy, 1971). Populations of *A. americanum* in the Northern Atlantic states, such as Maine, have been documented only since the 1990s (Springer et al., 2014). This paper focuses on the expansion of *A. maculatum* along the United States Atlantic coastline, particularly the current leading edge of this expansion in Virginia, in comparison to *A. americanum*, which has been established in this area for many more decades.

Newly recorded populations of *A. maculatum* in Virginia are associated with higher prevalence of the human pathogen *Rickettsia parkeri*, than has been reported inthe historical range along the southeastern US coastline. Reported prevalence of *R. parkeri* in Virginia by county ranges from 37 to 56%, (Fornadel et al., 2011; Nadolny et al., 2014), whereas prevalence in the historic range along the Gulf Coast is generally lower, ranging between 8 and 40% (Paddock & Goddard, 2015). *Rickettsia parkeri* is an obligate intracellular endosymbiont associated with *A. maculatum* that has been identified as the causative agent of *R. parkeri* rickettsiosis, also called Tidewater spotted fever.

The biotic and abiotic factors involved in apparently increased prevalence of *R. parkeri* in the invasion range of *A. maculatum* are unknown. Information on local- and broad-scale patterns of *A. maculatum* dispersal will likely be informative on this subject; however, previous studies have been equivocal in this area. In the most recent work, Nadolny et al. (2015) examined sites in three Mid-Atlantic states (North Carolina, Virginia, Maryland), Southern Appalachia (Kentucky and Tennessee), and Mississippi using an mtDNA marker. Nearly all sites, including those in close spatial proximity, were significantly different from one another with respect to haplotype composition, and no clear overall population structure of *A. maculatum* was resolved. This lack of spatial structuring indicates that long-range dispersal may be important in *A. maculatum* expansion since it appears that closely spaced populations of *A. maculatum* are not routinely intermixing. One potential test of this concept is to compare the connectivity of *A. maculatum* in study sites with that of *A. americanum*

from the same sites. *Amblyomma americanum* population connectivity has not previously been explored in Virginia; however, several previous studies in other locations suggest that *A. americanum* readily disperses over short distances, and that populations are highly connected at state-wide scales (Mixson et al., 2006; Trout et al., 2010).

In this study, we compare the population genetics of *A. maculatum* and *A. americanum* ticks within same study sites in southeastern Virginia. We expected to observe low genetic variation among *A. americanum* at these sites, particularly those not separated by distinct geographic barriers, whereas we hypothesized low connectivity among *A. maculatum* at all study sites.

2.2 MATERIALS AND METHODS

2.2.1 SAMPLE COLLECTION

Unfed questing adult ticks were collected by flagging at eight sites within eastern and central Virginia, northeastern North Carolina, and three Virginia barrier islands between 2015 and 2018 (Figure 1.). Ticks were identified by morphology (Keirans & Lacombe, 1998; Sonenshine, 1979) and stored at -20°C. Sites were selected based on locations where both *A. maculatum* and *A. americanum* were present during surveillance sweeps prior to this study. The active season for adult *A. maculatum* in Virginia typically extends from May through August. Transects were established and flagging was conducted bi-weekly from April through October at these sites: VB2, DN1, NC1, TP1, BI2, CH1. In addition, two nearby barrier islands (BI1 and BI3) along the Eastern Shore of Virginia were included in this comparative analysis because sample sizes were large enough to consider *A. maculatum* on BI1 and *A. americanum* on BI3. Samples were collected from barrier island sites twice per year (June and July) in both 2015 and 2016, and once each year (June) in 2017 and 2018.
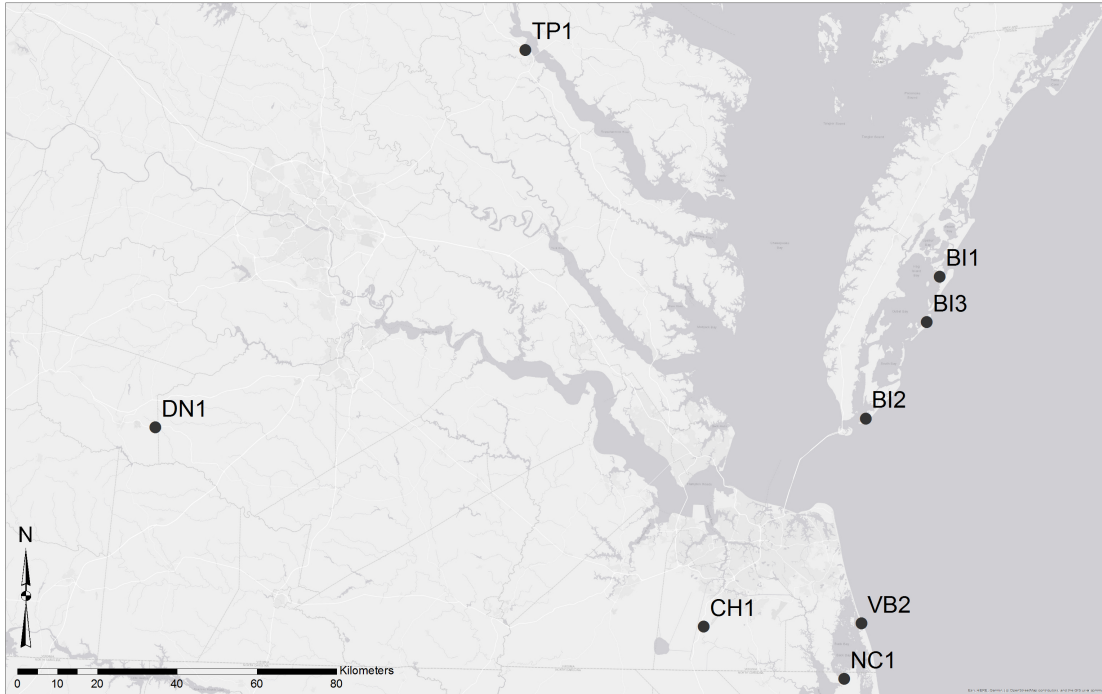
FIGURE 1. Locations of study sites in Virginia and North Carolina. Site codes are intended to de-identify sensitive locations. Codes are generally derived from geographic boundaries or features, e.g. barrier islands sites are "BI". Figure and legend adapted from Benham et al. (2021) with permission.

2.2.2 DNA EXTRACTION AND PURIFICATION

Each adult tick was bilaterally dissected. One half was stored at -80°C, and the other half was extracted for DNA. Tick halves were placed individually in 2 mL microcentrifuge tubes containing a single 5 mm and 150 mg of 1 mm glass beads and were disrupted in a beadmill

(BioSpec Products, Inc., Bartlesville, OK) at setting 4500 rpm for 45 s. After mechanical disruption, DNA was extracted using the GeneJET Genomic DNA Purification kit (Thermo Fisher Scientific, Waltham, MA) according to manufacturer's instructions, eluting to a final volume of 200 µl.

2.2.3 POLYMERASE CHAIN REACTION

A portion of the mitochondrial 16S gene was amplified in 15 µL PCR reactions. Reactions included 1X EconoTaq PLUS GREEN mastermix (Lucigen, Alexandria, MN), and 1µM each F/R primer: 16S+1.aa 5'- CTGCTCAATGAATTATTTAAATTGCTGT -3' [modified from (de la Fuente et al., 2001; Nadolny et al., 2015)], and Aa_6993F 5'- TCCAACATCGAGGTCGCAAA-3. Two µL of DNA template was added to all reactions, with ddH$_2$O added instead of DNA to no-template controls. Thermal cycling conditions were 95°C for 3 min, 30 cycles of 95°C for 30 s, 52°C for 45 s, and 72°C for 1 min, and final extension cycle at 72°C for 7 min (Nadolny et al., 2015).

2.2.4 SEQUENCING

Amplicons were visualized on 1.5% agarose gels. Correctly sized products were purified using ExoSAP-IT according to manufacturer's directions (Affymetrix Ltd., Santa Clara, CA). Purified amplicons were then sequenced using BigDye Terminator v3.1 sequencing reactions with the same 16S forward and reverse primers used for amplification (Applied Biosystems, Foster City, CA) on an Applied Biosystems 3130xl sequencer.

2.2.5 SEQUENCE CURATION

Haplotypes were assigned to individual ticks by generating consensus sequences from chromatograms with at least two bidirectional unambiguous coverage of the 16S rRNA gene. Fragment sizes analyzed included 216–218 base pairs from *A. maculatum* and 250–252 base

pairs from *A. americanum*. Nucleotide sequences were aligned and curated for each sample using Geneious R9 (https://www.geneious.com [Kearse et al. 2012]). Consensus sequences were compared against the NCBI nr databases using BLAST to match identical sequences (Altschul et al., 1990). Three novel *A. maculatum* haplotypes, MAC37–39 were submitted to GenBank (Clark et al., 2016) (Accession numbers MK749996, MK749997, MK749998, respectively).

2.2.6 POPULATION GENETIC STRUCTURE AND CONNECTIVITY

We started exploring population genetic structure first with a temporal analysis to understand whether populations within a site were changing substantially from on year to the next. We considered previously reported data from Nadolny et al. (2015) for CH1 and VB2 in our analyses, as we had additional archived *A. maculatum* samples from VB2, and *A. americanum* specimens from the same sites and similar time period to add for comparison. Initially, a matrix was created listing haplotypes by site and year for both *A. maculatum* and *A. americanum* using the R packages haplotyper and sidier (Muñoz-Pajares, 2013; Simondi et al., 2016) to sort consensus alignments generated in Geneious. Sites with fewer than five haplotyped adult ticks in any year were excluded from all analyses (Tables 3. and 4.). An initial AMOVA and pairwise ϕ_{ST} analysis was run in Arlequin v. 3.5 (Excoffier & Lischer, 2010). Where no significant temporal variation was identified, individuals were pooled by site across all years for further analysis. Spatial population genetic structure and connectivity were evaluated for pooled populations using pairwise ϕ_{ST} and AMOVA. AMOVA was performed using Tamura-Nei distance with 20000 permutations to explore the effect of population groupings on global variance (F_{ST}), as well as among groups (F_{CT}) and among populations (F_{SC}). For both species, we explored mainland/island groups, as well as coastal, inland and island comparisons to test for significant structure (F_{CT}) based on these geographic categories. We also used a Mantel Test to explore isolation by distance.

2.2.7 GENETIC DIVERSITY ANALYSIS

ChaoJost estimated diversity and observed Simpson's diversity were generated with the R package SpadeR, using bootstrapping to obtain confidence interval for both values (Chao et al., 2016). Sample coverage, Chao1 and ACE estimators were generated from SpadeR and reported for each site to estimate sample completeness.

2.2.8 NON-METRIC MULTIDIMENSIONAL SCALING

We visualized the genetic distances using non-metric multidimensional scaling (NMDS), which optimizes placement of points through an iterative process using a pairwise distance matrix. NMDS plot distances were calculated separately for *A. maculatum* and *A. americanum* from the Tamura-Nei pairwise ϕ_{ST} matrices using the Euclidean distance formula for NMDS in Primer v6 (Clarke & Gorley, 2006). NMDS was performed for 50 restarts. Single linkage hierarchical cluster analysis identified nearest-neighbor distances between clusters. The clustering distances displayed in the ordinations are based on the cluster analysis and correspond to the significant spatial structure (F_{CT}) in the AMOVA analyses. Minimum stress was set to 0.01.

2.3 RESULTS

2.3.1 POPULATION GENETIC STRUCTURE AND CONNECTIVITY

Temporal variation

Both *A. americanum* and *A. maculatum* populations were largely stable within sites across years. AMOVA analysis of temporal variation in *A. americanum* sites demonstrated non-significant temporal ($F_{SC} = 0.001$; $p = 0.16$; $df = 2$) and spatial variation ($F_{CT} = 0.085$; $p = 0.229$; $df = 6$) when groups were defined by sites with years pooled for the

temporal analysis, rather than the maximized spatial grouping (Section 2.3.1). No pairwise comparisons of ϕ_{ST} within-sites and among years were significant. Samples were consequently pooled by site. For *A. maculatum*, AMOVA of individual years grouped by site similarly demonstrated nonsignificant temporal (F_{SC} = -0.008; p = 0.71; df = 7), but significant spatial variation (F_{CT} = 0.215; p = 0.0004, df = 7). Although temporal variation was non-significant overall, pairwise ϕ_{ST} comparisons indicated BI1 2016 differed from BI1 2015 and 2018 samples ($p < 0.05$). This site also differed markedly from the other two years in diversity and composition (Section 2.3.2). BI1 samples from 2015 and 2018 were consequently pooled, and BI1 2016 was removed from the analysis. All other pairwise comparisons of *A. maculatum* within sites and among years were non-significant where multi-year data were available.

Spatial structure

Both *Amblyomma* species showed evidence of genetic differences among populations, but clear spatial structure was only observed in *A. americanum*. Among-groups structure (F_{CT}) was maximized for *A. americanum* when the two barrier island sites were considered one group (F_{CT} = 0.19, 19.40% of variance; p = 0.047). Further, pairwise ϕ_{ST} values for *A. americanum* indicated that two barrier island sites BI2 and BI3 were not significantly different from each other, but were distinct from all other sites except DN1 (n = 7) when adjusted for false-discovery rates (FDR) using a two-stage sharpened method (Benjamini et al., 2006) (Table 1.). In contrast, maximal F_{CT} for *A. maculatum* occurred when sites VB2, BI1 and DN1 were grouped, and other sites were individual (F_{CT} = 0.24; 24.06% of variance; p = 0.03; df = 4). Pairwise ϕ_{ST} values indicated *A. maculatum* populations between most sites were genetically distinct (Table 2.) after FDR adjustment. The AMOVA results did not support a grouping of sites by mainland or island groups, nor by any other clear geographic barriers. Neither species exhibited isolation by distance at this scale.

TABLE 1. Tamura-Nei distance-based pairwise ϕ_{ST} matrix for *A. americanum* with FDR-adjusted q values. Pairwise ϕ_{ST} values are in the lower triangle, and q values are in the upper triangle. Significant q values and corresponding ϕ_{ST} after FDR adjustment are in bold.

	NC1 $(n = 43)$	CH1 $(n = 23)$	VB2 $(n = 18)$	DN1 $(n = 7)$	TP1 $(n = 16)$	BI3 $(n = 17)$	BI2 $(n = 10)$
NC1	*	0.521	0.435	0.521	0.41	**0.003**	**0.027**
CH1	-0.005	*	0.15	0.521	0.365	**0.008**	**0.027**
VB2	-0.001	0.015	*	0.41	0.3	**0.004**	**0.014**
DN1	-0.035	-0.04	0.005	*	0.719	0.365	0.365
TP1	0	0.009	0.027	-0.088	*	**0.042**	**0.039**
BI3	**0.198**	**0.199**	**0.203**	0.03	**0.139**	*	0.521
BI2	**0.15**	**0.163**	**0.163**	0.013	**0.14**	-0.033	*

Table and legend adapted from Benham et al. (2021) with permission.

TABLE 2. Tamura-Nei distance-based pairwise ϕ_{ST} matrix for *A. maculatum* with FDR-adjusted q values. Pairwise ϕ_{ST} values are in the lower triangle, and q values are in the upper triangle. Significant q values and corresponding ϕ_{ST} after FDR adjustment are in bold.

	NC1 ($n = 42$)	CH1 ($n = 82$)	VB2 ($n = 50$)	DN1 ($n = 46$)	TP1 ($n = 42$)	BI1 ($n = 71$)	BI2 ($n = 20$)
NC1	*	**0.014**	**0**	**0.002**	**0**	**0**	0.039
CH1	**0.038**	*	**0**	**0.009**	**0**	**0**	**0.022**
VB2	**0.197**	**0.117**	*	0.032	**0**	0.12	**0.005**
DN1	**0.079**	**0.05**	0.027	*	**0**	0.101	0.105
TP1	**0.444**	**0.42**	**0.644**	**0.521**	*	**0**	**0**
BI1	**0.159**	**0.106**	0	0.004	**0.597**	*	**0.022**
BI2	0.038	**0.056**	**0.134**	0.007	**0.606**	0.0689	*

Table and legend adapted from Benham et al. (2021) with permission.

2.3.2 GENETIC DIVERSITY

Amblyomma maculatum populations were more diverse at NC1, less diverse at TP1, and generally similar in diversity measures to *A. americanum* populations from other sites (Tables 3. and 4.). The uniquely low diversity associated with the *A. maculatum* population at TP1 stood out compared to other *A. maculatum* populations. This site persistently differed from all other sites in diversity measures (Table 3.), as well as ϕ_{ST} (Table 2.) because of the overwhelming presence of a single haplotype that was not present at any other site in Virginia. This haplotype (MAC6) had been reported only from Kentucky and Mississippi in prior work, in which it was initially identified (Nadolny et al., 2015).

Temporal variation in diversity was only observed in BI1 between 2015 and 2016 samples

(Table 3.). Site BI1 in 2016 was unique from other BI1 years because a single, common haplotype (MAC16) dominated the data (72% of sample relative abundance), with only two other haplotypes present in that sample. We concluded that BI1 was undersampled in 2016, or suffered from another sampling artifact, since BI1 samples were otherwise diverse. Haplotype composition differed in VB2 during the year 2016, compared to 2010 and 2014 samples, in that 90% of the haplotypes sampled in 2016 were not present in samples from the same site during prior years. These years were pooled, however, based on non-significant genetic distance among years.

TABLE 3. *Amblyomma maculatum* haplotypes by year collected from sites throughout Virginia and eastern North Carolina. Site codes are intended to de-identify sensitive locations. Codes are generally derived from geographic boundaries or features, e.g. barrier islands sites are "BI". Years are indicated in the second part of each sample ID, e.g. VB2_10 describes site: VB2, and year: 2010.

	MAC16	MAC17	MAC38	MXHR2	MAC20	MAC15	AZ1614	MAC8	MAC12	AZ1663	MAC10	MAC6	MAC35	MAC21	MAC36	MAC23	MAC27	USA21B	MAC30	AZ1640	MAC37	MAC2	MAC39	Totals
VB2_10	2	4						3																9
VB2_11		3			1			1																5
VB2_12	7	8			2	2		7											1					27
VB2_16		1														4				4				9
VB2	**9**	**16**			**3**	**2**		**11**								**4**			**1**	**4**				**50**
DN1_17	2		1	1			4			1														9
DN1_18	8	2		1	2		5	5		3							2			6	1	1	1	37
DN1	**10**	**2**	**1**	**2**	**2**		**9**	**5**		**4**							**2**			**6**	**1**	**1**	**1**	**46**
BI1_15	21	11				3	4	11		3						1			1					55
BI1_16**	2	1						8																11
BI1_17*								2																2
BI1_18	5	3		1			1	4								2								16
BI1	**26**	**14**		**1**		**3**	**5**	**17**		**3**						**3**			**1**					**73**
NC1_17						1	1	6	1		2			3		1	1	1	3					20
NC1_18		1	1				4	7			1			2		1	1			4				22
NC1		**1**	**1**			**1**	**5**	**13**	**1**		**3**			**5**		**2**	**2**	**1**	**3**	**4**				**42**
TP1_18							**1**	**3**					**37**						**1**					**42**
BI2_16*	2							1																3
BI2_17	5	1	1	2				6	1							4								20
BI2_18*	1				1			1								1								4
BI2	**8**	**1**	**1**	**2**				**8**	**1**							**5**								**23**
CH1_11	7	1			3	2	1	7	10			3			6					3				43
CH1_12	13				1		5	4	9					2	3				2					39
CH1	**20**	**1**			**4**	**2**	**6**	**11**	**19**			**3**		**2**	**9**				**2**	**3**				**82**
GRAND TOTAL																								358

*Samples were removed from the analyses if $n < 5$. Bold indicates site totals included in the analyses.

**Sample BI1_16 was removed from the analysis as described in Section 2.3.1.

Table and legend adapted from Benham et al. (2021) with permission.

TABLE 4. *Amblyomma americanum* haplotypes by year collected from sites throughout Virginia and eastern North Carolina. Site codes are intended to de-identify sensitive locations. Codes are generally derived from geographic boundaries or features, e.g. barrier islands sites are "BI". Years are indicated in the second part of each sample ID, e.g. VB2_11 is the sample from the site VB2 and the year 2011.

	AA01	AA02	AA03	AA04	AA05	AA06	AA07	AA08	AA09	AA10	AA11	AA12	AA13	AA14	AA15	AA23	AA16	AA17	AA18	AA19	AA20	AA21	AA22	Totals
VB2_11*	1																1							2
VB2_14	7			1	1				1						1		3					1	1	16
VB2	**8**			1	1				1						1		4					1	1	**18**
DN1_18	**4**							1				1					1							**7**
BI3_17	**4**											7	1				2			1	2			**17**
NC1_17	14						1	2									4	1		1				23
NC1_18	12											2		2			3		1					20
NC1	**26**						1	2				2		2			7	1	1	1				**43**
TP1_18	**10**							2				1					1				1	1		**16**
BI2_17	2	1									1	2												6
BI2_18	2											1						1						4
BI2	**4**	1									1	3					1							**10**
CH1_12	5		1									1												7
CH1_14	9			1	1													3				1	1	16
CH1	**14**		1	1	1							1						3				1	1	**23**
GRAND TOTAL																								134

*Samples were removed from the analyses if $n < 5$. Bold indicates site totals included in the analyses.

Table and legend adapted from Benham et al. (2021) with permission.

2.3.3 NON-METRIC MULTIDIMENSIONAL SCALING

Ordination of *A. americanum* populations (Figure 2.) showed the single-linkage clustering of island sites apart from mainland sites with ϕ_{ST} distances < 0.01 (Section 2.3.1: Spatial structure). The distances displayed were chosen to highlight the minimum clustering distances that match the significant *A. maculatum* groups resulting from the AMOVA analysis. Geographic structure is not apparent in *A. maculatum*. TP1 is unique, as the distance from the nearest neighbor (CH1) is much greater ($\phi_{ST} = 0.42$) than the minimum distances joining all other sites ($\phi_{ST} < 0.04$).
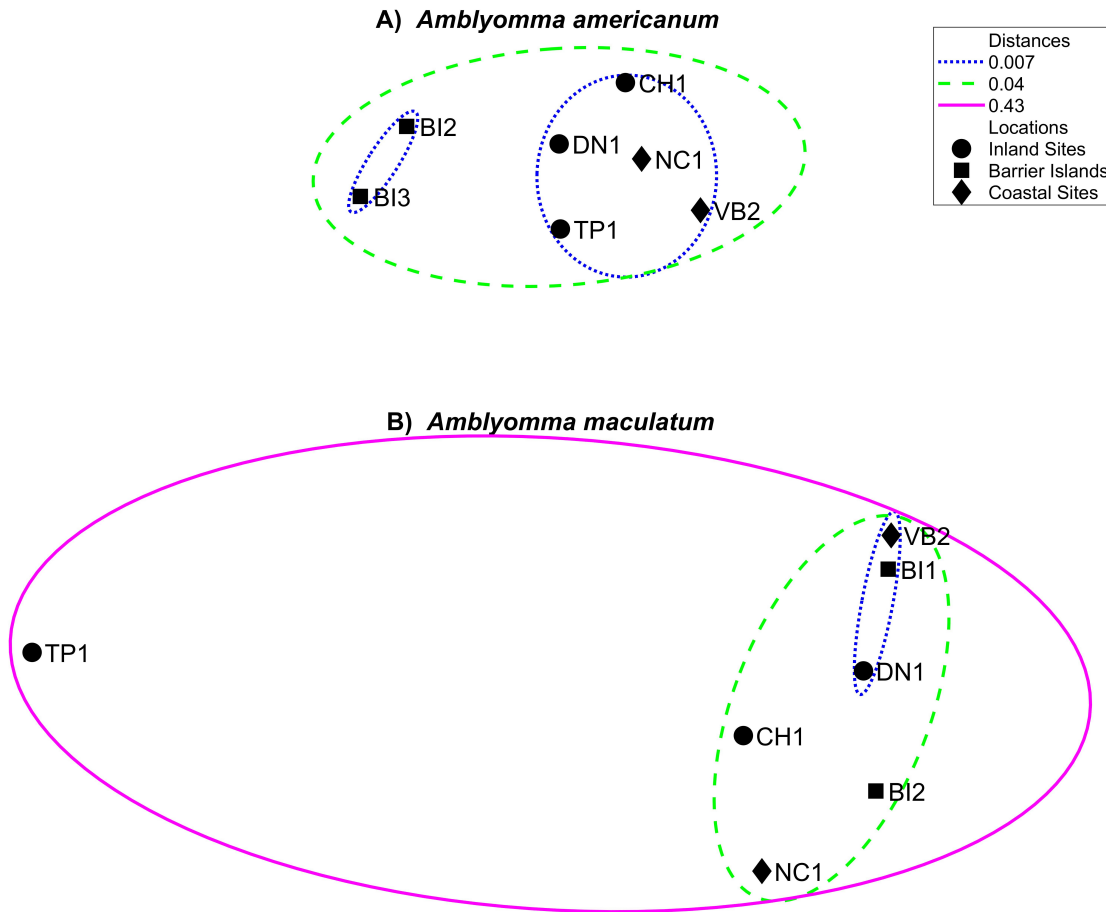
FIGURE 2. Ordination of genetic distances between sites based on A) *A. americanum* and B) *A. maculatum* 16S fragment sequences. Site codes are intended to de-identify sensitive locations. Codes are generally derived from geographic boundaries or features, e.g. barrier islands sites are "BI". Dotted lines identify distances from the single linkage hierarchical clustering analysis that correspond to maximized grouping in the AMOVA results. Dashed lines show that all sites are linked below $\phi_{ST} = 0.04$, except TP1 in the *A. maculatum* plot. The solid ellipse highlights the distance of TP1 from all other sites in the *A. maculatum* plot. Figure and legend adapted from Benham et al. (2021) with permission.

2.4 DISCUSSION

2.4.1 POPULATION ESTABLISHMENT AND CONNECTIVITY

Pairwise genetic structure was significant between most *A. maculatum* sites, suggesting multiple Virginia populations with little gene flow between them, in contrast with relatively few significant pairwise ϕ_{ST} values for *A. americanum*. *Amblyomma maculatum* populations in Virginia do not therefore appear to be well-connected, even at spatial scales where migration of individuals among *A. americanum* populations is apparent. The data also presented unexpected findings that improve our understanding of the biology of both *Amblyomma* species. The first, most striking pattern in the mtDNA data was at site TP1, where we identified one dominant haplotype within a much less diverse population compared to other sites. TP1 is a grassland managed with annual or semi-annual prescribed burning and adjacent to a riparian forest-wetland complex near the Rappahannock River. A single *A. maculatum* was first flagged from this site in 2014 as part of a statewide survey (2012–present), along with a single adult male collected from a roadkilled deer. No *A. maculatum* were collected from this site again until 2017 when, again, one adult male was flagged. In 2018, 83 adults were collected from the site. This increase resulted in part from increased sampling frequency during June and July, however, overall density of ticks during 2018 was higher for each single sampling event. Compared to prior years, an average of 11.8 ticks were collected on each of 7 sampling events in 2018, whereas no single sampling event yielded more than one individual in any previous year. Interestingly, the dominant haplotype (MAC6) at this site in 2018 had not been previously observed from any other site in Virginia, during any other year of sampling between 2010 and 2018 (Nadolny et al., 2015). This haplotype was rarely observed (4/370; 1.1% of total ticks) in a previous study, and then only from Mississippi and Kentucky and not from North Carolina, Delaware, or Maryland

(Nadolny et al., 2015). We conclude that the population at TP1 was established between 2013 and 2018 following the drop-off of one or more MAC6 females. The first generation likely occurred in or before 2016, leading to a substantial cohort of MAC6 adults in 2018.

Dominance of a single mitochondrial haplotype in *A. maculatum* populations is atypical in studies thus far, yet the presence of this pattern at TP1 indicates that new populations can arise largely from a single maternal lineage. Further, the dominance (88%) of a regionally unique haplotype is suggestive of a long-distance founding event. This lends support to the hypothesis that some *A. maculatum* populations are established via long-distance dispersal, with important implications for movement of *R. parkeri* across these same distances. The appearance of a single founding lineage at the TP1 site strongly contrasts with the otherwise high haplotype diversity within Virginia sites observed for both *A. maculatum* and *A. americanum* in the current study, and in previous population genetic studies of *A. maculatum* (Nadolny et al., 2015). Our results are consistent with prior work that suggests that *A. maculatum* populations typically arise where there is high propagule pressure from multiple sources on ecologically permissive sites, leading to high-diversity populations with distinct haplotype compositions (Nadolny & Gaff, 2018*b*), but we have also found that a founder effect can be observed in sites where either immigration is reduced or reproductive success is limited to few individuals, leaving the signature of a predominantly single-lineage population.

Whereas *A. maculatum* demonstrated little to no clear regional connectivity, regular mixing among *A. americanum* populations appears common, as indicated by non-significant differences in haplotype frequencies among many sites. This regional homogeneity is consistent with previous state-level studies of the lone star tick (Mixson et al., 2006; Trout et al., 2010). The only remarkable pattern we observed in *A. americanum* was a significant structure identified between mainland and barrier island populations in the AMOVA analysis. The Chesapeake Bay presents a substantial barrier (at least 17 km of open water) to

movement of large mammals from the mainland to the peninsula of the Eastern Shore of Virginia. Therefore, this pattern is likely driven by host preference of *A. americanum.*

2.4.2 TEMPORAL VARIATION IN GENETIC STRUCTURE

Temporal variation within sites was not expected, because we assumed that cohorts from earlier years would contribute substantially to subsequent generations consistent with the 2–3 year life cycle of *Amblyomma* ticks. We looked for temporal patterns, however, because of the possibility that high turnover or propagule pressure could contribute to punctuated shifts in genetic structure or composition among years. Most sites for both *A. maculatum* and *A. americanum* were temporally stable, as evidenced by pairwise ϕ_{ST} values and F_{SC} from AMOVA when groups were defined by multiple sample years within the same site. VB2 displayed a notable shift in haplotype frequency in *A. maculatum* between the years 2014 and 2016 (Section 2.3.1- POPULATION GENETIC STRUCTURE AND CONNECTIVITY, Temporal variation). This shift may have resulted from immigration to the site via drop-offs from hosts, but no clear source population, host, or distance could be determined. Alternatively, this relatively small sample from VB2 2016 might indicate a phenomenon of substructure within the local site that led to shift at that transect between years. Although *A. maculatum* juveniles have been collected from migratory birds (Florin et al., 2014), population establishment appears to be associated with habitat that supports rodent hosts for immature ticks (Cumbie et al., 2020; Nadolny & Gaff, 2018*b*). Therefore, substructure within a site might reflect short-distance dispersal of immature ticks on rodent hosts. Genetic substructure could be particularly distinct if sibling cohorts tend to cluster during host-seeking, for example questing together as larval masses (e.g. Leal et al., 2020). Although this type of clustering has not been definitively observed among adults in the field, observations of immature *A. americanum* in the lab and field, and *A. maculatum* larvae and nymphs raised from colonies in the lab suggest that *Amblyomma* cohorts may quest together

in all life stages leading up to adulthood. This observation leads to a second consideration regarding the mechanisms of population establishment. Long-distance dispersal of siblings may occur if spatial clustering means siblings are more likely to feed together, either as immatures feeding on migrating birds, or adults feeding on large mammals. Such behavior could contribute to a founder effect, as we saw at TP1, in sites where adult female siblings feed in clusters, then drop off together, leading to a population founded predominantly by a single maternal lineage. In these instances, some half-sibling or unrelated females may be present such that additional mitochondrial haplotypes would also be represented in the new population. A different pattern would be expected if more frequent drop-offs occur in high host-traffic sites, or if there is no relationship between relatedness and clustered feeding. In this case, even newly established populations could be highly diverse.

2.4.3 GENETIC MARKERS

Mitochondrial loci are useful in comparative studies to uncover congruency, or the lack thereof, in the spatial genetic structure among different taxa (Bowen et al., 2014). Initial mtDNA studies can help in determining which additional molecular tools will help to answer unresolved questions about the biology of the system. Among the tools available, new molecular technologies, such as RADseq and other reduced representation techniques (e.g. Monzón et al., 2016), provide a large volume of information about individual genotypes, vastly increasing genetic resolution within populations. Multi-locus genotypic data can identify relatedness among individuals and can also be used in conjunction with individual-based modeling to understand the mechanisms driving genetic patterns observed at the population level (Landguth et al., 2012). Given that we have identified a population of *A. maculatum* that appears to be the result of a founder event based on mtDNA, a deeper look at the genetic diversity within mitochondrial haplotype backgrounds would be appropriate to understand whether these individuals are indeed closely related, and if the

founder effect is apparent across a larger number of loci.

2.4.4 CONCLUSIONS

The establishment of new *A. maculatum* populations appears, at least in part, to be a result of long-distance dispersal events. Shorter-distance regional dispersals seem likely given the host utilization of adult *A. maculatum* but these short-distance dispersals do not sufficiently homogenize genetic structure in the region. In contrast, *A. americanum* populations in this region display higher connectivity, with some structure imposed by the geographical barrier of the Chesapeake Bay. Genetic structure of *Amblyomma* ticks in southeastern Virginia is consistent with novel *A. maculatum* populations formed by drop-off events resulting from long-distance host migration, and regional dispersal of *A. americanum* on hosts restricted by water barriers.

CHAPTER 3

SPATIOTEMPORAL ANALYSIS OF INTRASPECIFIC DIVERSITY IN *AMBLYOMMA MACULATUM* POPULATIONS

3.1 INTRODUCTION

The Gulf Coast tick (GCT), *Amblyomma maculatum*, has been undergoing an expansion of its North American range. A steady increase in the number of populations identified beyond the historic extent, along the United States (U.S.) Gulf Coast region (Teel et al., 2010), indicates a clear, progressive spread into northern latitudes. Established populations have been reported in Virginia for over a decade. An adult GCT was associated with the first confirmed diagnosis of Tidewater Spotted Fever (Paddock et al., 2004), now more commonly called *Rickettsia parkeri* rickettsiosis. Within the last decade the known distribution of Gulf Coast ticks has also expanded, in order of reported establishment, to Delaware, Arizona, Illinois, Connecticut, and New York (Bajwa et al., 2022; Florin et al., 2014; Herrick et al., 2016; Molaei et al., 2021; Phillips et al., 2020; Wright et al., 2011). The ongoing expansion of GCT range prompts public health concerns because GCT is a vector of two pathogens of medical and veterinary importance, *Rickettsia parkeri* and *Hepatozoon americanum*, and can acquire and transmit *Ehrlichia ruminantium* in the lab (Paddock & Goddard, 2015). *Rickettsia parkeri* is a pathogen of particular concern for humans because it has been identified as a causative agent of spotted fever rickettsiosis (SFR) (Paddock et al., 2004). Reports of SFRs in humans are not typically diagnosed by causative agent because commonly-used serological tests do not distinguish between different species of spotted fever group rickettsiae (Heitman et al., 2019). Delaware, North Carolina, and Virginia all have an

annual incidence of > 15 infections per one million people (CDC, 2019). North Carolina and Virginia are among the five states that make up more than 50% of human cases of SFR in the United States, alongside Arkansas, Missouri, and Tennessee. High incidences of SFR, combined with high *R. parkeri* prevalence in ticks collected in emergent populations throughout the Mid-Atlantic U.S. (Nadolny et al., 2014) have prompted studies aiming to identify the sources of and patterns driving GCT expansion into new regions.

Population genetics is one tool for uncovering some of the underlying mechanisms of this range expansion, including a fundamental question of how introductions occur and the patterns of connectivity among populations. Connectivity can facilitate exchange of genetic diversity in both the ticks and the pathogens. A "drop-off" in tick biology refers to a single tick or cohort leaving a host, typically in a location some distance from the source population. Not all drop-offs contribute to a population. Drop-offs are important to population establishment or gene flow only after ticks feed to repletion and then successfully produce offspring. Long-distance dispersal of adults ticks on hosts, followed by drop-offs appears to contribute to successful population establishment. Benham et al. (2021) described a GCT population in which population genetic analyses indicated a founder event, likely a drop-off of a single successful female, based on the genetic patterns as well as the population history at the site. Such populations would have genetic identities in common with a source population. Depending on the number of genetically distinct individuals in the initial drop-off and the ongoing immigration of new individuals to a site (i.e. propagule pressure during a species invasion or range expansion), the founder's genetics might dominate the population. At least one population could have been founded by a single female from an initial drop-off, where an apparent founder effect was observed (Benham et al., 2021). Here I investigated how haplotype diversity changed or remained stable in this population in subsequent years, and whether newly established GCT populations in other geographic regions show similar genetic signals. I hypothesized that newly established populations should exhibit dominant

haplotypes and/or low haplotype diversity. I also included two additional years of data collection from sites with active populations in the Mid-Atlantic to complete a temporal analysis of change in genetic signatures over time.

We followed mitochondrial 16S haplotyping methods (Benham et al., 2021; Nadolny et al., 2015) to haplotype individual ticks collected from North American populations in Virginia, Delaware, and Illinois, with the latter two containing GCT populations that have only been observed within the last 5 years. Mitochondrial DNA (mtDNA) 16S rRNA gene fragments provide a means to track intraspecific diversity across time and space. Population structure and connectivity can be readily evaluated using mtDNA, insofar as researchers remain aware of some of the limitations and assumptions of using this marker. The major limitation of mtDNA, in general, is that it is specific to the maternal lineage, thus the paternal contribution is not considered. The reproductive biology of metastriate ticks ameliorates this concern, in that mating occurs on-host. In GCTs specifically, females begin feeding where conspecific males have already initiated feeding (Teel et al., 2010). Based on this mating behavior, the male parent of any offspring is likely to be from a location near where the female originated, even in the cases of long-distance host migration. If both parents are from the same source population, I did not anticipate a significant loss of genetic information relevant to intraspecific diversity as I focused on maternal lineages and excluded paternal DNA.

Three key assumptions guide the development of the founder hypothesis here: 1) male drop-offs at a new location are less informative than female drop-offs if adult ticks are the primary founders of new populations, because males will die within weeks of mating, with no further interactions, 2) paternal mitochondrial leakage occurs infrequently in GCTs (Nadolny et al., 2015) and 3) migration of reproducing adult GCTs on large animals promotes successful invasion (Nadolny & Gaff, 2018a). Following these assumptions, I demonstrated how tracking maternal lineages (mtDNA) can clarify mechanisms of population establishment by revealing patterns that can be used to infer how many females have

successfully contributed to the established population. Female ticks that are infected with the pathogen *R. parkeri* can transmit the bacteria to offspring via transovarial transmission (Wright et al., 2015), which means infected females can contribute to *R. parkeri* prevalence in subsequent generations. Greater genetic diversity within tick populations may have a significant effect on *R. parkeri* prevalence, although the direction of that effect (i.e. positive or negative) is unknown. Diversity within vertebrate host communities has been associated with negative effects on pathogen prevalence, with some controversy regarding this dilution effect (Huang et al., 2016). However, whether any similar effect can be seen as a result of intraspecific diversity is yet to be determined. Ultimately, high prevalence of *R. parkeri* in ticks is likely an important component of exposure to humans, thus a risk to public health. Although the relationship between tick diversity and pathogen prevalence is not yet clear, establishing the patterns of diversity in ticks and what these patterns imply about the populations over time is an essential first step to investigate the broader question. Here, I continued to explore mtDNA because a substantial collection of mtDNA haplotypes exists from across the range of *A. maculatum*, which facilitated this spatial and temporal analysis as well as comparison to prior work.

This study focused on mitochondrial 16S rRNA gene fragment haplotype markers to measure intraspecific genetic diversity in populations of the sexually-reproducing metastriate species *A. maculatum*. I characterized diversity in existing populations, considering spatiotemporal stability and variation. The temporal analysis considered change in diversity measures over time to look for significant shifts or trends. The spatial analysis included a deeper look at dissimilarity among sites, as well as overall connectivity based on population haplotype frequencies.

3.2 MATERIALS AND METHODS

3.2.1 COLLECTION

Collection methods in Virginia continued as described in prior work (Benham et al., 2021; Nadolny et al., 2015). Mid-Atlantic tick samples were collected as part of a surveillance project at Old Dominion University that has been ongoing since 2008. Flagging is conducted year-round, with bi-weekly sampling during the GCT active season (April through October). A total of seven populations from Virginia were included in this analysis, including a historical population (CH0) with individuals collected between 2010 and 2013. DNA samples from four populations in Illinois and three populations in Delaware were obtained from personnel at University of Illinois (Phillips et al., 2020) and Delaware Technical Community College (Maestas et al., 2020). In total, I evaluated ticks from fifteen sampling locations ("sites") three higher level groups ("regions"), which were Virginia, Delaware and Illinois (Figure 3.). The spatial analysis pertains to this collection of sites.
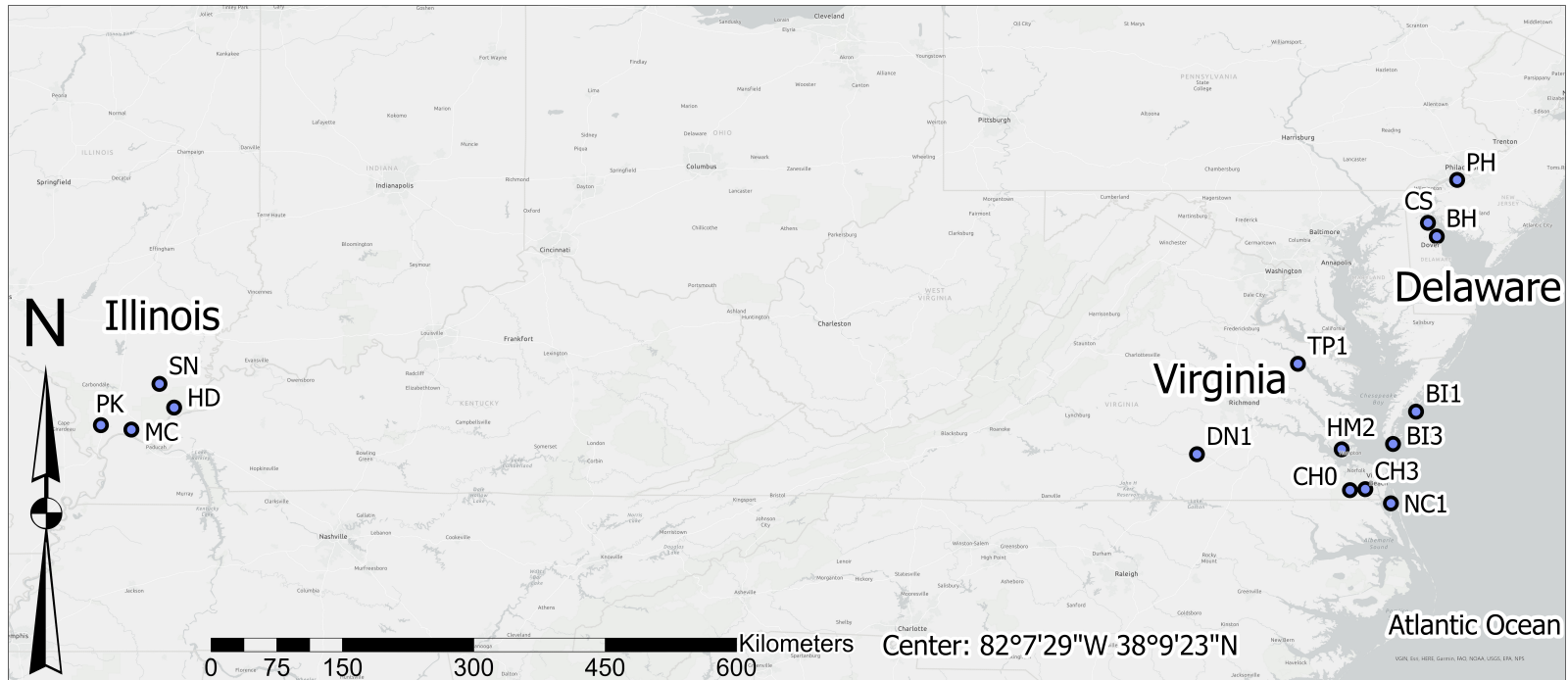
FIGURE 3. *Amblyomma maculatum* collection sites in Virginia, Delaware, and Illinois. Site codes are intended to de-identify sensitive locations. Codes are generally derived from geographic boundaries or features, e.g. barrier islands sites are "BI". Illinois and Delaware site codes are prefixed with "IL" and "DE" in the text.

A separate temporal analysis was completed for the seven sites in Virginia by partitioning populations based on year of collection. The population HM2 was excluded from the temporal analysis because the site was added to the surveillance project in 2020 and we only had one year of sampling data. In addition, two years of sampling from CH0 (2010, 2013) were excluded because only one tick was collected in each of these years. The remaining site/year combinations had a minimum of 8 individuals haplotyped.

Temporal diversity and similarity in Virginia

The sites and years that were included in the temporal analysis were CH3, 2019–2020; BI1, 2018–2019; NC1, 2017–2019; TP1, 2018 and 2020; and CH0, 2011–2012. Two sites (TP1 and DN1) did not have enough individuals collected and haplotyped in 2019 to obtain diversity estimates using the package SpadeR (Chao et al., 2016) in R 4.2.1 (R Core Team, 2023), so only basic statistics are reported for these sites. The primary purpose of the temporal analyses was to examine the null hypothesis that sites did not have significant differences in any diversity measures from year to year. Failing to reject the null would justify pooling data and assuming that a single year of data in the spatial dataset would be representative of a population. Further, following up on year-to-year dynamics would support intepretations about genetic stability in these populations, particularly at the site that showed an initial founder effect.

Subsampling within three sites

Subsampling occurred in 2019 within three sites where GCTs were collected within the site, but beyond the original transect. These three sites included two barrier island sites (BI1 and BI3) subsampled by flagging five distinct clusters of woody vegetation that were separated by an open, grassy habitat matrix. Vegetation clusters were naturally occurring and separated from each other by approximately 30 m. An additional transect was added

to the site TP1, approximately 600 m from the transect established in 2018. Variation in vegetation structure between transects at this site was less pronounced than at the barrier islands. The grassy matrix between barrier island vegetation clusters was flagged to account for presence, but no ticks were collected in this habitat. The hypothesis was that haplotypes cluster at a fine scale, for example between transects or sampling units within sites. Clustering would indicate that siblings tend to remain together across life stages and increase the likelihood that closely-related ticks (e.g. ticks of the same haplotype) would colonize a site together as a founding group, leaving the signature of a dominant haplotype on site.

3.2.2 HAPLOTYPING

Haplotypes were identified by curating sequences and searching NCBI (BLAST) (Altschul et al., 1990) for 100% pairwise matches along a 225 base pair (bp) sequence of the mitochondrial 16S gene. I followed methods from prior work (Benham et al., 2021; Nadolny et al., 2015), but used a slightly longer bp fragment to accurately align sequences with insertions or deletions. The haplotyped region ranged from 216 to 218 bp (Benham et al., 2021).

3.2.3 INTRASPECIFIC DIVERSITY

A haplotype-by-site matrix was generated by grouping population by site and year to calculate dissimilarity in SpadeR. I also derived a genetic distance matrix using Tamura-Nei genetic distances to calculate ϕ_{ST} in Arlequin based on FASTA sequences sorted by site. Similarly, a haplotype-by-site × year matrix was created for the temporal dataset, which was then analyzed with the same methods, except without considering connectivity. I repeated the same process for subsampling, using only the sites and transects mentioned in Section 3.2.1.

I used SpadeR to generate dissimilarity and diversity statistics along with estimators of sample coverage. I examined population evenness using two evenness indices: E_Q (Equation 2) and E_{var} (Equation 3). Both E_Q and E_{var} were selected because these indices calculate evenness independent of richness (Smith & Wilson, 1996), whereas Simpson's evenness is a classic measure included for comparison. Evenness indices E_Q, E_{var}, and Simpson's evenness were calculated in the R package codyn (Hallett et al., 2020), using the following equations for E_Q, E_{var}:

$$E_Q = -2/\pi \ arctan(b'), \tag{2}$$

$$E_{var} = 1 - 2/\pi \ arctan\left\{ \sum_{s=1}^{S} \left(ln(x_s) - \sum_{t=1}^{S} ln(x_t)/S \right)^2 \Big/ S \right\} \tag{3}$$

where b' in Equation 2 is the slope of the log abundance by the rank of abundance.

For each population in the dataset, rank-abundance curves were fitted to models by plotting log abundance (y) against haplotype rank (x), then using least squares regression to determine the model fit using the radfit routine in the R package vegan (Oksanen et al., 2022). Rank-abundance models are used primarily to identify dominance of a species or class (e.g. haplotype) in relation to overall diversity in a sample, where the relative steepness of the slope can be interpreted in terms of ecological or evolutionary processes (Whittaker, 1965; Wilson, 1992). Here, rank-abundance model fitting was used to compare and contrast patterns of dominance, identify populations that appear to deviate from the general patterns observed, and apply ecological insights to explain underlying processes that could be contributing to differing patterns. The analysis was applied here to intraspecific diversity, rather than community diversity, which requires a different interpretation. However, some basics can be inferred from the overall picture of dominance/diversity. The radfit algorithm fits each sample to five different rank-abundance models: Null (broken-stick), Preemption,

Lognormal, Zipf, and Zipf-Mandelbrot. The models and ecological interpretations for different model fits are discussed primarily in relation to plants (Whittaker, 1965; Wilson, 1992). A null model fits a random distribution of haplotypes, and would be expected if all haplotypes arrive at the same time and succeed according to random probabilities. Preemption models, also called geometric series or Motomura models (Whittaker, 1965), are common in difficult to moderately harsh environments with relatively limited (low to moderate) richness. A Zipf or Zipf-Mandelbrot model fit is typically observed when serial introductions occur, such as successional shifts in plant communities (Wilson, 1992).

Two analyses of variance relevant to population genetics were used to examine hierarchical structure based on genetic distance (analysis of molecular variance, AMOVA) and dissimilarity. The AMOVA algorithm in Arlequin (Excoffier & Lischer, 2010) calculates genetic distances from haplotype sequences and partitions the variances by hierarchical groups (Site and Region) (Excoffier et al., 1992). For a PERMANOVA design, I used a second set of distance matrices that was generated in the packages 'gstudio' (Dyer, 2014a, A) using the amova distance method and Horn dissimilarity ($C_{1,2}$) from SpadeR. I used the R package vegan to evaluate dispersion and perform a PERMANOVA test on the effects of Site and Region separately.

3.2.4 STRUCTURE AND CONNECTIVITY

Population Graphs (Dyer & Nason, 2004) are used here to explore the overall connectivity among sites. We inferred in Benham et al. (2021) that GCT populations had little connectivity in the Mid-Atlantic based on significantly non-zero ϕ_{ST} results, but I wanted to explore this further with more geographic regions included. Population Graphs were generated for spatial groups using the R package popgraph (Dyer, 2014b). In contrast to AMOVA and PERMANOVA, which have a similar hierarchical structure, Population Graphs do not require an *a priori* grouping, but instead this graph approach creates a network of

populations based on covariances between site pairs (Dyer & Nason, 2004). A Population Graph consists of nodes and edges that form a network showing pairwise connectivity between populations based on genetic covariance. Nodes are the populations studied and edges are derived from the genetic covariances between populations. Conditional graph distance (cGD) denotes the shortest distance between populations, which implies higher gene flow either between the two populations, or indirectly via a third (i.e. source) population. Saturation and degree of the graphs were considered in evaluation (Dyer et al., 2010). Saturation occurs when all of the nodes are connected to one another, in contrast with nonsaturated networks, in which at least one edge is missing between nodes. Degree is a measure of the number of edges connecting to a node.

3.3 RESULTS

A total of 41 unique haplotypes were identified among 15 populations, including the historical population CH0. Unique haplotypes per population ranged from 6 to 17. Compared to previous reports (Benham et al., 2021; Ketchum et al., 2009; Nadolny et al., 2015), 13 novel haplotypes were identified. Of these 13, five were collected only in Virginia, five only in Illinois, one was detected in both Virginia (BI3) and Illinois, and two were collected only in Delaware. Overall, diversity was high among all samples. Sample coverage was estimated to be between 68 and 97% (Table 5.). A non-metric dimensional scaling (NMDS) ordination of Tamura-Nei genetic distances illustrates pairwise relationships between populations (Figure 4.).

TABLE 5. Diversity estimates for each population. Values are: n = number of individuals, H = haplotypes, Cov. = sample coverage, Chao1 = Chao 1 minimum richness estimator (Chao, 1984), ACE = abundance-based coverage estimator (Chao & Lee, 1992), s.e. = standard error, Shannon = Shannon diversity index, E_Q and E_{var} = evenness indices (Smith & Wilson, 1996). Site codes are intended to de-identify sensitive locations. Codes are generally derived from geographic boundaries or features, e.g. barrier islands sites are "BI". Illinois and Delaware site codes are prefixed with "IL" and "DE".

	n	H	Cov.	Chao1	s.e.	ACE	s.e.	Shannon	s.e.	E_Q	E_{var}
ILSN	48	13	0.92	16.90	5.20	16.30	3.30	9.84	1.04	0.24	0.62
ILMC	42	9	0.93	11.90	4.40	10.70	2.40	7.06	0.44	0.20	0.54
ILPK	33	11	0.88	18.80	11.30	14.20	3.40	8.70	1.28	0.27	0.67
ILHD	49	8	0.96	10.00	3.70	9.00	2.10	5.45	0.62	0.18	0.46
DECS	12	6	0.75	8.80	4.10	8.40	3.30	5.26	0.53	0.32	0.78
DEPH	54	11	0.93	14.90	5.20	15.00	4.20	6.26	0.92	0.19	0.47
DEBH	22	6	0.86	10.30	6.90	10.60	6.10	3.53	0.90	0.20	0.48
NC1	82	17	0.94	29.30	16.90	19.80	2.90	11.63	1.11	0.21	0.55
BI1	70	9	0.96	12.00	4.00	12.60	4.60	5.61	0.46	0.17	0.37
BI3	21	8	0.81	15.60	11.10	12.80	5.40	6.06	1.03	0.26	0.65
HM2	16	6	0.88	7.90	3.50	7.20	1.90	5.11	0.98	0.29	0.72
TP1	73	7	0.97	9.00	3.70	9.00	2.80	2.71	0.43	0.14	0.31
DN1	35	13	0.86	15.40	2.90	17.80	4.60	9.05	1.50	0.23	0.68
CH3	54	11	0.87	31.60	16.90	39.40	29.20	5.72	0.23	0.18	0.38
CH0	84	12	0.99	12.20	0.50	12.50	1.00	8.14	0.86	0.19	0.53
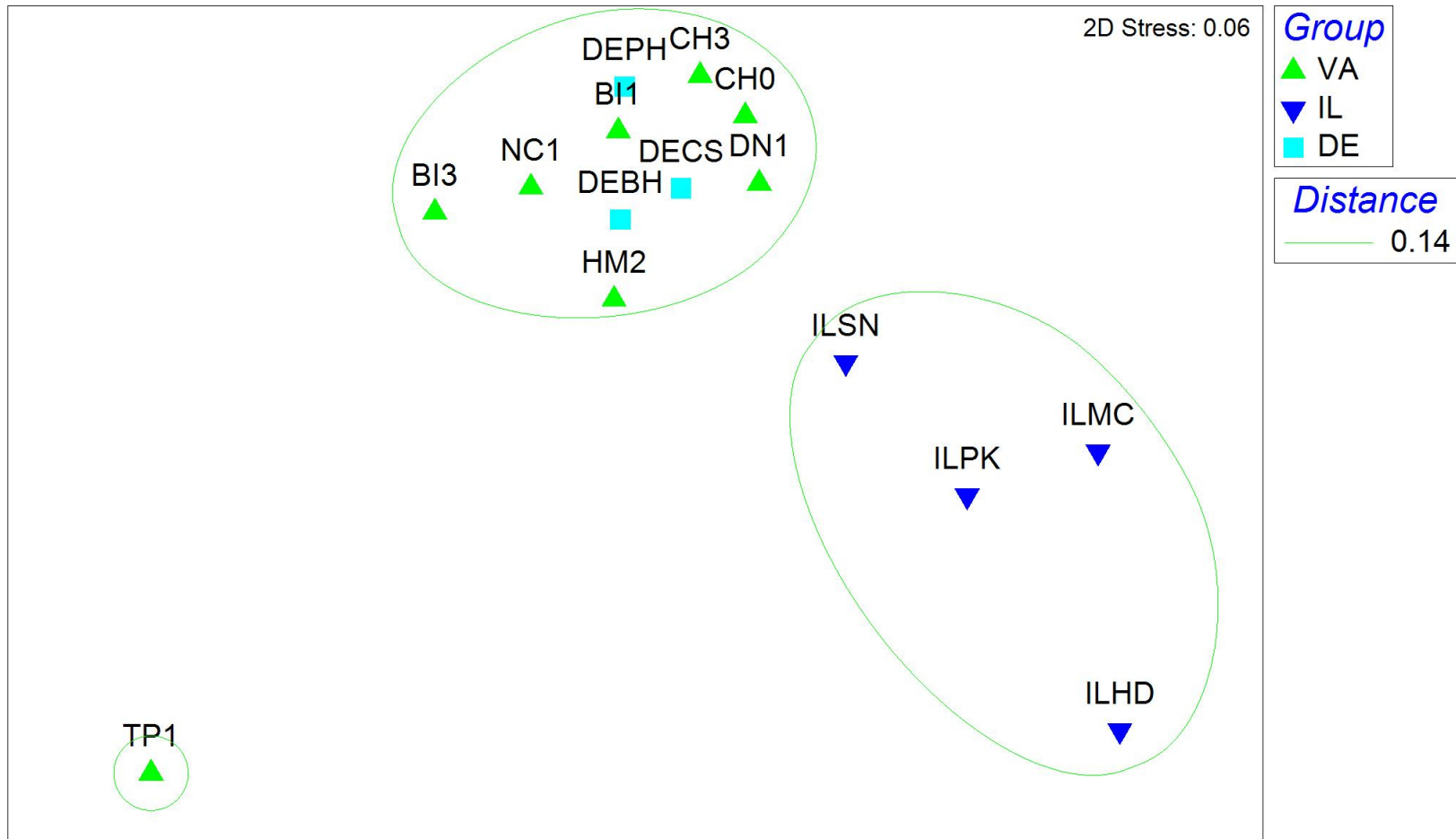
FIGURE 4. Non-metric dimensional scaling ordination of genetic distances from the spatial dataset. Regional groupings are indicated by shape and color of icons. Site codes are intended to de-identify sensitive locations. Codes are generally derived from geographic boundaries or features, e.g. barrier islands sites are "BI". Illinois and Delaware site codes are prefixed with "IL" and "DE". Solids lines identify clusters from a single-linkage hierarchical cluster analysis based on Tamura-Nei distances < 0.14, for which distances among clustered populations were non-significant in AMOVA results.

3.3.1 INTRASPECIFIC DIVERSITY

The most abundant haplotypes overall were MAC8, MAC9, and MAC16. Virginia site TP1 stood out in that the most dominant haplotype collected from this site, MAC6, made up roughly 73% of the total abundance with no significant changes in diversity or evenness among years (Table 6.). A Delaware site, DEBH, was dominated by MAC8, which made up 59% of the total abundance. The dominant haplotype in the remaining sites ranged from 20 to 43% of total abundance in those sites. On average, the most abundant haplotype from any given site comprised approximately 35% of total abundance, with a median of 31%.

The appropriate model fit for rank-abundance curves was selected using AIC values (Table 7.). Hereafter, "fit" refers to selected fit. The majority of the sites fit a null, or broken stick model of haplotype distributions. Several sites fit a preemption or Zipf model. The Zipf model follows the proportion of the dominant haplotype, possibly resulting from serial introductions as described in Section 3.2.3. The sites that fit this model were: DN1, TP1, and DEPH. The sites CH3 and DECS both fit a preemption model, likely because of low richness which could be a result of poor habitat quality or, alternately, poor sample coverage (particulary DECS, see Table 5.).

The diversity profiles show that the three sites that fit a Zipf model of haplotype dominance appear to have different underlying reasons for fitting this model rather than a null model. DN1 stands out because of a relatively high species richness for the abundance, which leads to an even sample with much uncertainty in estimated species richness. In contrast, TP1 and DEPH are both driven by the dominance of a single haplotype, MAC6 and MAC9 respectively, that cause deviation from the null model. DECS has the greatest evenness and TP1 has the least (Table 5.).

TABLE 6. Diversity estimates for temporal dataset. Values are: $n =$ number of individuals, $H =$ haplotypes, Cov. $=$ sample coverage, Chao1 $=$ Chao 1 minimum richness estimator (Chao, 1984), ACE $=$ abundance-based coverage estimator (Chao & Lee, 1992), s.e. $=$ standard error, Shannon $=$ Shannon diversity index, $E_Q =$ evenness index (Smith & Wilson, 1996). Site codes are intended to de-identify sensitive locations. Codes are generally derived from geographic boundaries or features, e.g. barrier islands sites are "BI". Illinois and Delaware site codes are prefixed with "IL" and "DE".

	n	H	Cov.	Chao1	s.e.	ACE	s.e.	Shannon	s.e.	E_Q
					Diversity Estimators					
NC1 2017	34	15	0.74	37.40	19.60	36.20	15.50	10.35	1.86	0.28
NC1 2018	19	9	0.68	23.20	12.80	19.20	10.60	6.94	0.33	0.22
NC1 2019	29	10	0.86	13.90	5.10	14.80	4.80	7.33	1.06	0.26
BI1 2018	16	6	0.88	6.90	2.10	7.10	1.70	5.22	0.64	0.28
BI1 2019	54	7	0.96	8.00	2.20	8.00	1.70	4.67	0.45	0.16
TP1 2018	46	5	0.94	7.90	4.30	13.70	4.80	2.00	0.13	0.14
TP1 2019	8	4	–	–	–	–	–	–	–	0.31
TP1 2020	19	5	0.84	7.80	4.20	12.60	11.70	2.76	0.29	0.19
DN1 2017	10	5	0.70	9.10	6.50	10.30	7.00	3.89	1.00	0.29
DN1 2018	17	10	0.71	13.90	4.60	14.20	3.60	9.03	1.28	0.40
DN1 2019	8	6	–	–	–	–	–	–	–	0.381
CH3 2019	34	11	0.79	34.80	30.20	25.30	13.10	6.86	1.43	0.22
CH3 2020	20	4	1.00	4.00	0.50	4.00	0.50	3.28	0.42	0.26
CH0 2011	44	10	0.96	12.00	3.70	10.90	1.40	8.00	0.93	0.23
CH0 2012	38	8	0.97	8.20	0.70	8.60	1.10	5.98	0.84	0.22

TABLE 7. Model fit results for rank-abundance curves. Par(1,2,3) = parameters 1, 2, and 3, Dev = deviance, AIC = Aikake information criterion, BIC = Bayesian information criterion. Site codes are intended to de-identify sensitive locations. Codes are generally derived from geographic boundaries or features, e.g. barrier islands sites are "BI". Illinois and Delaware site codes are prefixed with "IL" and "DE".

Site	Par 1	Par 2	Par 3	Dev	AIC	BIC
BI1						
Null				4.97	**35.24**	**35.24**
Preemption	0.35			3.56	35.83	36.03
Lognormal	1.53	1.20		3.10	37.35	37.75
Zipf	0.42	-1.22		6.43	40.70	41.09
Mandelbrot	2.40E+108	-52.42	118.19	3.53	39.80	40.39
BI3						
Null				1.62	**22.57**	**22.57**
Preemption	0.30			1.00	23.95	24.03
Lognormal	0.69	0.87		1.07	26.02	26.18
Zipf	0.36	-0.98		1.047	26.00	26.16
Mandelbrot	20.96	-2.56	4.03	0.71	27.66	27.90
CH0						
Null				4.24	**45.16**	**45.16**
Preemption	0.25			2.38	45.3028	45.79
Lognormal	1.55	0.96		4.60	49.52	50.49
Zipf	0.32	-0.99		7.97	52.89	53.86
Mandelbrot	Inf	-419	1468	2.28	49.20	50.66

TABLE 7 Continued.

Site	Par 1	Par 2	Par 3	Dev	AIC	BIC
CH3						
Null				14.05	44.77	44.77
Preemption	0.35			6.77	**39.49**	**39.88**
Lognormal	0.94	1.26		9.67	44.39	45.19
Zipf	0.43	-1.31		10.24	44.96	45.76
Mandelbrot	12824	-4.90	7.41	5.71	42.43	43.62
DN1						
Null				4.92	38.89	**38.89**
Preemption	0.21			4.61	40.58	41.14
Lognormal	0.64	0.90		2.56	40.53	41.66
Zipf	0.31	-0.98		0.86	**38.83**	39.96
Mandelbrot	0.31	-0.98	6.55E-06	0.86	40.83	42.53
HM2						
Null				1.06	**17.41**	**17.41**
Preemption	0.31			0.40	18.76	18.55
Lognormal	0.82	0.69		0.33	20.68	20.26
Zipf	0.36	-0.81		0.75	21.10	20.68
Mandelbrot	Inf	-8.90E+06	2.58E+07	0.18	22.53	21.90
NC1						
Null				4.87	**57.32**	**57.32**
Preemption	0.17			6.47	60.92	61.75
Lognormal	1.18	0.93		2.64	59.09	60.76
Zipf	0.26	-0.91		4.35	60.80	62.47
Mandelbrot	0.60	-1.23	1.09	4.02	62.48	64.98

TABLE 7 Continued.

Site	Par 1	Par 2	Par 3	Dev	AIC	BIC
TP1						
Null				39.05	61.79	61.79
Preemption	0.62			11.15	35.88	35.83
Lognormal	1.02	2.10		5.40	32.14	32.03
Zipf	0.71	-2.20		0.97	**27.71**	**27.60**
Mandelbrot	0.71	-2.20	7.53E-07	0.97	29.71	29.54
DEBH						
Null				3.88	**20.17**	20.17
Preemption	0.50			2.08	20.38	20.17
Lognormal	0.70	1.38		1.53	21.83	21.41
Zipf	0.58	-1.63		0.24	20.53	**20.12**
Mandelbrot	0.58	-1.63	5.31E-06	0.24	22.53	21.91
DECS						
Null				2.40	**17.37**	**17.37**
Preemption	0.28			1.14	18.12	17.91
Lognormal	0.60	0.52		0.95	19.92	19.51
Zipf	0.31	-0.62		1.23	20.21	19.79
Mandelbrot	Inf	-1.29E+08	4.81E+08	0.78	21.75	21.13
DEPH						
Null				7.71	40.16	40.16
Preemption	0.32			5.10	39.55	39.95
Lognormal	0.97	1.23		2.47	38.92	39.72
Zipf	0.43	-1.29		1.70	**38.16**	**38.95**
Mandelbrot	0.72	-1.53	0.43	1.62	40.07	41.27

TABLE 7 Continued.

Site	Par 1	Par 2	Par 3	Dev	AIC	BIC
ILHD						
Null				1.76	**27.82**	**27.82**
Preemption	0.35			1.71	29.78	29.86
Lognormal	1.40	1.08		1.48	31.55	31.71
Zipf	0.41	-1.15		3.42	33.49	33.65
Mandelbrot	2.33E+272	-112.76	261.72	1.66	33.72	33.96
ILMC						
Null				4.5583	**32.71**	**32.71**
Preemption	0.24			4.10	34.24	34.44
Lognormal	1.33	0.75		3.79	35.93	36.33
Zipf	0.29	-0.78		6.21	38.36	38.76
Mandelbrot	Inf	-6.39E+05	2.45E+06	3.73	37.88	38.47
ILPK						
Null				2.25	**32.74**	**32.74**
Preemption	0.21			1.03	33.52	33.92
Lognormal	0.87	0.73		0.97	35.46	36.25
Zipf	0.27	-0.81		1.71	36.19	36.99
Mandelbrot	9.90E+06	-5.74	20.41	0.78	37.27	38.47
ILSN						
Null				2.26	**40.18**	**40.18**
Preemption	0.20			1.10	41.02	41.59
Lognormal	1.03	0.80		1.54	43.44	44.59
Zipf	0.26	-0.83		3.24	45.17	46.30
Mandelbrot	Inf	-6.04E+07	2.82E+08	0.92	44.84	46.53

Temporal analysis

Considering the six sites included in the temporal analysis, 4/6 experienced a net loss of haplotypes over time (Table 8.). For two of those sites that had multiple years included, losses had a greater impact on richness than years in which there was a gain, particularly at NC1. Overall the change in haplotype rank was generally low, meaning losses and gains tended to occur among rare haplotypes with little impact on the rank structure (Table 8.). Therefore, stability appeared to be the general rule from year to year, absent major disturbances.

TABLE 8. Pairwise change in site diversity measures from year-to-year. Diversity measures include haplotype gains and losses, and changes in haplotype richness, rank, and evenness. Site codes are intended to de-identify sensitive locations. Codes are generally derived from geographic boundaries or features, e.g. barrier islands sites are "BI".

Year 1	Year 2	Site	Δ Richness	Δ Evenness	Δ Rank	Gains	Losses
11	12	CH0	-0.167	-0.018	0.215	0.167	0.333
18	19	BI1	0.111	-0.322	0.247	0.333	0.222
19	20	CH3	-0.636	0.114	0.190	0.000	0.636
17	18	DN1	0.455	0.144	0.198	0.545	0.091
18	19	DN1	-0.308	0.014	0.243	0.231	0.538
17	18	NC1	-0.375	0.000	0.234	0.063	0.438
18	19	NC1	0.083	-0.042	0.278	0.250	0.167
18	19	TP1	-0.167	0.519	0.167	0.167	0.333
19	20	TP1	0.143	-0.317	0.265	0.429	0.286

Some of the haplotype losses, for example CH3 (2019–2020) and TP1 (2018–2019), likely resulted from disturbances such as fire and successional change, respectively. Population

decline followed a prescribed burn in early 2019 at TP1, after which population and haplotype richness rebounded, and evenness dropped because the haplotype MAC6 recovered nearly in proportion to its prior dominance. The population at CH3 declined as the tree canopy developed. No GCTs were found in collections from CH0 and NC1 populations after 2014 and 2019, respectively. The decline at CH0 after 2014, when only 7 ticks were collected, coincided with successional change (Nadolny, 2016), whereas frequent mowing had suppressed or extirpated the GCT population at NC1.

Subsampling

Though much more data need to be collected, there appeared to be no apparent pattern in haplotype distribution, clustering or otherwise, at scales finer than the site level. Sample sizes for each cluster or transect were low, yet each sample with more than two individuals had more than one haplotype present (Table 9.). Sample sizes were generally too small to calculate useful diversity statistics.

TABLE 9. Subsampling collection summary. n = number of individuals and H = number of haplotypes. Site codes are intended to de-identify sensitive locations. Codes are generally derived from geographic boundaries or features, e.g. barrier islands sites are "BI".

Site	Transect	n	H
BI1	1	5	4
BI1	2	24	6
BI1	3	10	3
BI1	4	8	3
BI3	1	1	1
BI3	2	2	1
BI3	3	5	5
BI3	4	7	6
BI3	5	7	3
TP1	2	3	3
TP1	3	4	2
TP1	4	1	1

3.3.2 STRUCTURE AND CONNECTIVITY

The AMOVA showed significant ($p > 0.001$) regional population structure in terms of variance at all levels of a hierarchical analysis, but most of the variance occurred within populations (77.17%), rather than among populations (8.72%), or among regions (14.11%). Likewise, a single-linkage hierarchical cluster analysis based on Tamura-Nei distances demonstrated visual clustering by region. These clusters were overlaid on the original NMDS plot for visualization (Figure 4.). Similarly, the PERMANOVA results were

significant for regions and populations (Region, $F = 8.96$, $p < 0.001$; population, $F = 8.91$, $p < 0.001$). Delaware samples were significantly more dispersed (DE = 7.748, IL = 6.309, VA = 7.125) than either Virginia or Illinois ($p = 0.26$ and $p = 0.23$). Dispersion between Virginia and Illinois was not significantly different ($p = 0.77$).

Finally, the connectivity analysis based on the Popgraph network model showed a high degree of interconnectivity among populations, even across regions (Figure 5.). Some general patterns were observed, but there are many exceptions. The graph was nonsaturated, meaning that not all populations were connected. However, at least one population in each region was connected to one in another region in this population graph. When one looks at cGD (Figure 6.), populations generally have the shortest pairwise distances between populations within the same region, although the historic population CH0 and the unusual site TP1 stood out. Greater pairwise distances were generally apparent between Illinois populations and others. However, DEBH and DN1 both had relatively short cGD with ILSN compared to other populations in their respective regions. Similar results were evident in the Tamura-Nei genetic distances, which generally reported significantly non-zero pairwise distances between Illinois populations and the other regions (Table 10.).
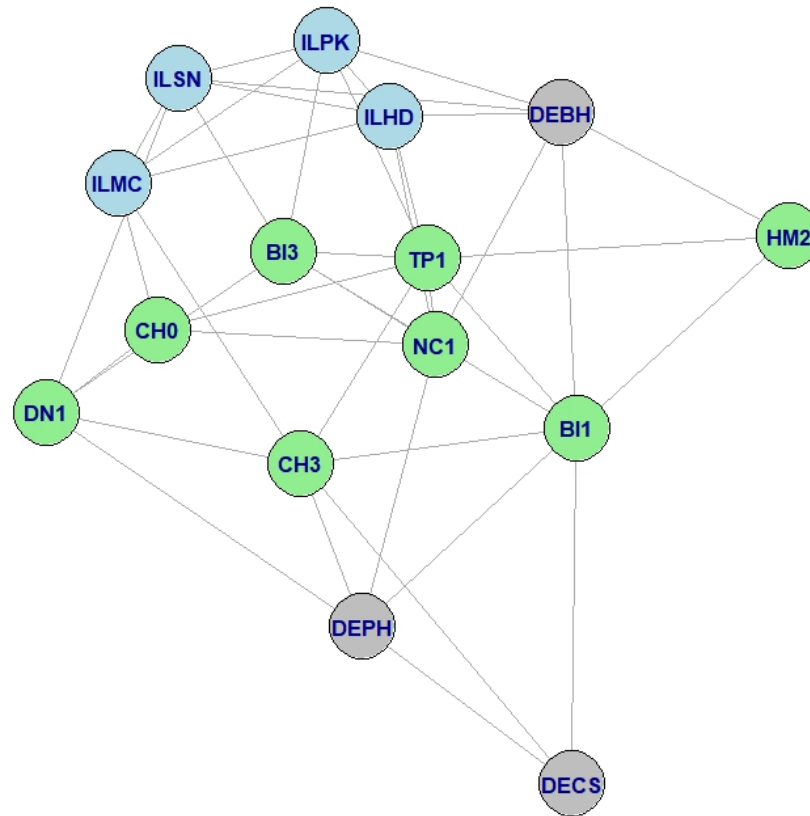
FIGURE 5. A Population Graph for 15 *A. maculatum* populations. Site codes are intended to de-identify sensitive locations. Codes are generally derived from geographic boundaries or features, e.g. barrier islands sites are "BI". Illinois and Delaware site codes are prefixed with "IL" and "DE".

	DEBH	DECS	DEPH	CH0	BI1	BI3	CH3	DN1	NC1	HM2	TP1	ILHD	ILMC	ILPK	ILSN
DEBH	0.000	2.880	3.210	5.660	1.580	3.820	3.800	4.840	2.860	2.490	5.190	3.360	5.480	2.840	2.510
DECS	2.880	0.000	1.360	5.640	1.300	3.540	1.100	2.990	4.000	3.400	5.730	6.240	4.290	5.720	5.380
DEPH	3.210	1.360	0.000	4.290	1.630	3.870	1.830	1.630	2.650	3.730	6.060	6.320	5.010	6.050	4.020
CH0	5.660	5.640	4.290	0.000	5.910	5.170	4.590	2.650	2.800	7.650	4.950	6.470	3.370	6.640	5.040
BI1	1.580	1.300	1.630	5.910	0.000	2.240	2.220	3.260	4.280	2.100	4.430	4.940	5.400	4.420	4.090
BI3	3.820	3.540	3.870	5.170	2.240	0.000	4.450	2.520	2.920	4.340	5.040	5.740	5.610	3.320	2.640
CH3	3.800	1.100	1.830	4.590	2.220	4.450	0.000	1.940	4.480	4.320	4.850	6.410	3.180	6.450	4.330
DN1	4.840	2.990	1.630	2.650	3.260	2.520	1.940	0.000	4.280	5.360	6.790	5.500	5.120	5.180	2.390
NC1	2.860	4.000	2.650	2.800	4.280	2.920	4.480	4.280	0.000	5.340	4.920	3.670	6.170	5.700	5.360
HM2	2.490	3.400	3.730	7.650	2.100	4.340	4.320	5.360	5.340	0.000	2.700	5.850	7.500	5.330	4.990
TP1	5.190	5.730	6.060	4.950	4.430	5.040	4.850	6.790	4.920	2.700	0.000	5.510	8.030	5.120	7.670
ILHD	3.360	6.240	6.320	6.470	4.940	5.740	6.410	5.500	3.670	5.850	5.510	0.000	3.220	2.990	3.110
ILMC	5.480	4.290	5.010	3.370	5.400	5.610	3.180	5.120	6.170	7.500	8.030	3.220	0.000	3.270	2.970
ILPK	2.840	5.720	6.050	6.640	4.420	3.320	6.450	5.180	5.700	5.330	5.120	2.990	3.270	0.000	2.790
ILSN	2.510	5.380	4.020	5.040	4.090	2.640	4.330	2.390	5.360	4.990	7.670	3.110	2.970	2.790	0.000

FIGURE 6. Pairwise conditional graph distances between populations, where larger values indicate greater distances. Site codes are intended to de-identify sensitive locations. Codes are generally derived from geographic boundaries or features, e.g. barrier islands sites are "BI". Illinois and Delaware site codes are prefixed with "IL" and "DE".

TABLE 10. Tamura-Nei distance-based pairwise ϕ_{ST} matrix for *A. maculatum* with FDR-adjusted q values. Pairwise ϕ_{ST} values are in the lower triangle, and q values are in the upper triangle. Site codes are intended to de-identify sensitive locations. Codes are generally derived from geographic boundaries or features, e.g. barrier islands sites are "BI". Illinois and Delaware site codes are prefixed with "IL" and "DE".

	ILSN (n=48)	ILMC (n=42)	ILPK (n=33)	ILHD (n=49)	DECS (n=12)	DEPH (n=54)	DEBH (n=24)	NC1 (n=82)	BI1 (n=70)	BI3 (n=21)	HM2 (n=16)	TP1 (n=73)	DN1 (n=35)	CH3 (n=54)	CH0 (n=84)
ILSN	*	**0.019**	0.237	**0.000**	0.164	**0.000**	0.087	**0.000**	**0.000**	**0.000**	0.144	**0.000**	0.093	**0.010**	**0**
ILMC	**0.058**	*	0.156	**0.019**	**0.010**	**0.000**	**0.000**	**0.000**	**0.000**	**0.000**	**0.000**	**0.000**	**0.010**	**0.000**	**0**
ILPK	0.017	0.022	*	0.161	**0.043**	**0.000**	**0.010**	**0.000**	**0.000**	**0.000**	**0.035**	**0.000**	**0.019**	**0.000**	**0**
ILHD	**0.156**	**0.094**	0.035	*	**0.000**	**0.000**	**0.000**	**0.000**	**0.000**	**0.000**	**0.000**	**0.000**	**0.000**	**0.000**	**0**
DECS	0.037	**0.165**	**0.114**	**0.266**	*	0.688	0.685	0.623	0.867	0.227	0.380	**0.000**	0.662	0.867	0.394
DEPH	**0.100**	**0.229**	**0.184**	**0.333**	-0.029	*	0.291	0.121	0.249	0.058	0.211	**0.000**	0.207	0.240	0.164
DEBH	0.042	**0.184**	**0.121**	**0.273**	-0.026	0.008	*	0.720	0.548	0.394	0.379	**0.000**	0.243	0.196	0.186
NC1	**0.097**	**0.239**	**0.201**	**0.365**	-0.016	0.019	-0.014	*	0.361	0.359	0.227	**0.000**	0.072	0.051	**0.019**
BI1	**0.073**	**0.218**	**0.185**	**0.354**	-0.040	0.008	-0.011	0.001	*	0.107	0.257	**0.000**	0.283	0.392	**0.027**
BI3	**0.128**	**0.285**	**0.210**	**0.352**	0.043	0.067	-0.002	0.010	0.042	*	0.144	**0.000**	**0.027**		**0.027**
HM2	0.052	**0.171**	**0.133**	**0.279**	-0.002	0.033	0.003	0.020	0.017	0.064	*	**0.000**	0.249	0.182	0.134
TP1	**0.348**	**0.504**	**0.437**	**0.529**	**0.371**	**0.332**	**0.310**	**0.293**	**0.333**	**0.305**	**0.210**	*	**0.000**	**0.000**	**0**
DN1	0.032	**0.121**	**0.104**	**0.254**	-0.027	0.016	0.017	0.039	0.006	0.117	0.021	**0.386**	*	0.539	0.227
CH3	0.075	**0.188**	**0.167**	**0.325**	-0.045	0.010	0.027	0.031	0.001	0.104	0.037	**0.379**	-0.007	*	0.065
CH0	0.087	**0.185**	**0.157**	**0.307**	0.001	0.017	0.026	**0.035**	**0.031**	**0.089**	0.041	**0.326**	0.014	0.026	*

3.4 DISCUSSION

A single drop-off of an adult female tick might not be a rare event, but subsequent population establishment from a lone drop-off is apparently uncommon. Propagule pressure, which can be defined as a combination of propagule size and frequency (Wittmann et al., 2014) undoubtedly influences the likelihood of population establishment. Although data are lacking with regard to host movement, population sizes, and tick dispersal behaviors to adequately describe propagule pressure of GCTs during this range expansion, genetic data presented here support the inference that the frequency of drop-offs along the northern margins of the GCT range is high enough to establish genetically diverse populations. This likely helps to overcome the limitations imposed on new populations that can be caused by low numbers and genetic diversity among founding adults such as Allee effects, demographic stochasticity, and genetic stochasticity. These data fit with a broader trend in invasion biology, that establishment success and range expansion is primarily a numbers game (Blackburn et al., 2017).

Previous work haplotyping GCT from southeastern Virginia indicated substantial diversity at most sampling sites with the marked exception of TP1, which was dominated by a single haplotype MAC6 that was not previously detected within Virginia (Benham et al., 2021). New populations of GCT have recently established in Illinois and Delaware (Florin et al., 2014; Phillips et al., 2020). I hypothesized that these new populations may exhibit low haplotype diversity consistent with a founder event, as was postulated for TP1. However, this hypothesis was not supported, and instead both Delaware and llinois populations resembled higher diversity of the Virgnia populations, other than TP1, without a clearly dominant lineage such as that observed at TP1. These findings suggest that clear founder effects reflected by dominance of individual haplotypes may be an exception rather than a rule for newly established GCT populations. Importantly, this also indicates that

establishment of GCT populations in areas where they were previously undetected results from transplantation of multiple female ticks of different maternal lineages on short temporal scales. Given the high reproductive potential of individual GCT females (Nadolny & Gaff, 2018*b*), a single female could successfully found a population that would then be dominated by that founding haplotype even if continued introductions bring new haplotypes to the site in subsequent years. In general, it appears that the initial introduction in many of these new populations includes multiple haplotypes from different females. These results suggest that substantial propagule pressure is contributing to the current GCT range expansion. Source populations are likely as diverse or more diverse than these newly established populations if new populations experience a bottleneck. However, further investigation within the historical range is needed to confirm this, as existing evidence is limited in regions such as Arkansas, Kansas, Mississippi, Oklahoma, and Texas where haplotype characterization has been based primarily on single-strand conformation polymorphism studies with limited sequencing and, in some cases, small sample sizes (Ferrari et al., 2013; Ketchum et al., 2009; Nadolny et al., 2015; Trout et al., 2010).

Following-up on the site TP1 where we first noticed the founder effect (Benham et al., 2021) showed that even after a population recovery following a prescribed burn in 2019, the haplotype MAC6 remains dominant. The recovery of MAC6 as a dominant haplotype suggests that ongoing propagule pressure from outside populations is limited and that this site might be isolated within the metapopulation. If this population is isolated, this could provide the opportunity to develop a case study for elimination, which could be measured in terms of how well the existing lineages persist after experimental control efforts. TP1 is a unique population across multiple measures. For example, this site has both low evenness, as explored through rank-abundance models, and low richness relative to the population size and estimated sample coverage. These unique patterns persist across years. Although abundance declined in 2019 after fire, a rebound of the same overall diversity pattern

was observed, along with recording several haplotypes that were either new to the site, or previously unreported.

Disturbance such as fire appears not to be a major destructive event for a GCT population, given the recovery of the population at TP1 in 2020 with the same overall genetic composition and diversity patterns that existed prior to the 2019 burn. Rather, fire is likely conducive to maintaining conditions that allow GCT populations to persist. GCT are able to evade deleterious effects of low-intensity managed burns well enough to rapidly recover, as seen in the TP1 population. In contrast, canopy closure can completely eliminate populations (Nadolny, 2016). In the broader surveillance project, we have not yet identified a population re-emerging within a site where an earlier population had previously disappeared as a result of canopy closure. The progress of ecological succession in the Mid-Atlantic Coastal Plain ecoregion typically leads to a permanent habitat shift unless a major, habitat-altering disturbance occurs to reset the system.

At TP1, where the question about a founder effect lingers, the next step is to continue exploring these questions by comparing mtDNA to alternative genetic markers at the population level. Genetic markers such as microsatellites and single-nucleotide polymorphisms (SNPs) can clarify relationships between individuals of the same haplotype to determine relatedness and inbreeding. Work to develop useful microsatellites and test these in populations is ongoing (Allerdice, 2021), while advances in mitochondrial genome sequencing (Brenner & Raghavan, 2021) and sequencing of the full GCT genome (Ribeiro et al., 2022) show promise for developing novel genomic markers that can help resolve some remaining questions about the nature of GCT geographic expansion.

Future work should incorporate field collections aimed at estimating propagule pressure as it relates to geographic region and host movement. Such efforts include collecting ticks from hosts and continuing to seek new populations both within the historic range and in areas of recent expansion. Ecological modeling will be an important component of any such

study to compare empirical data to theory and understand constraints in the system. Finally, the development of new markers will expand the types of questions that can be asked about these dynamic populations. New genetic tools and models for ecological inference developed specifically for ticks can help integrate different bodies of knowledge that are essential for controlling GCT invasions.

CHAPTER 4

EVALUATION OF REMOTE SENSING TO IDENTIFY GULF COAST

TICK HABITAT

4.1 INTRODUCTION

Expert assessment of habitat is an important predictor of *A. maculatum* presence or absence in the field. Typically, experts identify *A. maculatum* habitat by looking for key indicators of late primary succession, similar to the shrub and sapling stage of old field succession (Nadolny & Gaff, 2018*b*; Teel et al., 2010). This stage of succession is when woody growth just begins, but woody shrub and tree height remain below approximately 2–4 m and the canopy has not yet closed. *Amblyomma maculatum* habitats can have different historical land uses. In the Mid-Atlantic, coastal and dune habitats, as well as old fields, overgrown park edges, and powerline right-of-ways are often targeted to search for *A. maculatum* presence. Evidence of frequent disturbances such as fire, mowing, and coastal wind and wave activity can also be indicators of conditions that reset habitat to earlier successional stages. *Amblyomma maculatum* populations can invade or recover in these sites, given a period of 1–2 years of vegetation recovery following the disturbance (Gleim et al., 2016; Nadolny & Gaff, 2018*b*; Teel et al., 2010).

Changes in vegetation composition can be measured through both categorical variables, such as land use and land cover classes (LULC), and numeric variables, for example the normalized difference vegetation index (NDVI) and changes in soil organic composition. LULC classes provided by the Chesapeake Bay Program incorporate high resolution land cover data, which primarily shows the type of vegetation present along with hydrology,

combined with data about human use to distinguish between natural succession and actively-managed croplands or extractive areas (CBPO, 2022). Whereas LULC models rely primarily on static spatial imagery, NDVI values can be collected across a time range relevant to the study to show site vegetation dynamics, particularly vegetation stress, inter-annual change, and annual phenology patterns. Values can range from -1 to 1, with negative values indicating water bodies and positive values associated with vegetation. One of the limitations of NDVI is that the index is sensitive to bare soil, which measures around 0, and becomes saturated at higher values, which narrows the difference between healthy vegetation of different types. An example of saturation is the relatively narrow distance between golf course grass (around 0.7 NDVI on Landsat 8 Surface Reflectance) and forest (around 0.9 NDVI) (Huang et al., 2021). Lower values, between 0–0.7 can indicate more bare soil in the pixel or stressed/sensecent vegetation, or in some cases, cloud cover or sensor errors.

NDVI is calculated (Equation 4) by extracting red (R) and near-infrared (NIR) spectral imagery from the 8 or 11 available spectral bands from Landsat 7 ETM+ or Landsat8 OLI satellites, respectively. Each band monitors a different wavelength emitted from the Earth's atmosphere or surface. The MODIS Terra instrument monitors 36 bands, from which processed NDVI bands are available for download from the U.S. Geological Survey (USGS) LP DAAC (Didan, 2021).

$$NDVI = \frac{NIR - R}{NIR + R} \tag{4}$$

This chapter includes an analysis of both types of data to evaluate the relationship between these remotely-sensed variables and the presence of *A. maculatum* populations collected from the field across eastern Virginia and northeastern North Carolina.

Among tick species collected in the Mid-Atlantic region of the United States (U.S.), *A. maculatum* are relatively rare, with densities an order of magnitude less than the density

of the American dog tick (Nadolny & Gaff, 2018*b*), *Dermacentor variabilis*, which can be collected alongside *A. maculatum* or in similar habitat where *A. maculatum* are not present *Amblyomma maculatum* are often not present even where they might be expected based on habitat conditions, geographic range, and/or the presence of nearby populations. As a result, *A. maculatum* are typically located in patchy distributions. The most common host species of *A. maculatum* in Virginia and the Mid-Atlantic more broadly are not completely known, but immature ticks are often collected on rodents and small mammals (Nadolny & Gaff, 2018*b*), including several species of mice and rats, as well as meadow voles (*Microtus pennsylvanicus*), in Virginia and North Carolina (Cumbie et al., 2020). The relatively short distances these host animals travel may contribute to both the patchiness and the apparent lack of connectivity between *A. maculatum* populations (Benham et al., 2021; Nadolny et al., 2015) if ticks are spending most of their immature life stages on these smaller animals.

To aid in ongoing surveillance of *A. maculatum* habitat, the goal was to develop a reliable way to use remote sensing to aid in the detection of potential *A. maculatum* habitat in the Mid-Atlantic region. To understand how landscape affects *A. maculatum* presence on a meso-scale (regional) rather than broader (continental) or finer (site-level) scales, a set of variables had to be chosen that would have enough variation at the desired scale to discriminate between suitable and unsuitable habitat, without high correlation between variables. LULC and NDVI were selected as the most likely habitat variables to make this distinction remotely. The working hypothesis was an expectation that *A. maculatum* habitat is sufficiently unique that remote sensing could be used to distinguish areas that are suitable for *A. maculatum*.

4.2 MATERIALS AND METHODS

4.2.1 FINE-SCALE TEMPORAL CHANGE

Fine-scale habitat change was examined at one site in Chesapeake, Virginia (scale: approximately 1:5,000) where one historical *A. maculatum* population was documented (Nadolny, 2016). The time period of interest included the point at which an established population was identified to the time that population was locally extirpated. This period coincided with the transition from a working crop to a fallow field, and finally to an early stage, closed-canopy forest (Nadolny, 2016). Initial empirical data collected from the field (Nadolny, 2016) was followed up here using remote sensing variables to help determine how such landscape transitions might be monitored remotely in the future. Initally, National Land Cover Database (NLCD) (Yang et al., 2018) images accessed through ArcGIS Pro 3.0 (Esri, 2022) were reviewed to identify the time when the transition was detected in land cover classes. NLCD data are available at a resolution of 30 m. Land cover classes were expected to be a relatively coarse temporal measure, as it takes years to compile and analyze imagery for classification. To look at a finer temporal scale, a series of harmonized Landsat NDVI values were used to visualize 30 m resolution NDVI change over years 2000–2016 for the month of August, which was typically near the peak NDVI value. Harmonized values (Roy et al., 2016) were used because the time span began before the operation of Landsat 8 OLI satellite. The time frame considered (years 2000–2016) includes the transition, with several additional years evaluated both before and after the *A. maculatum* population was observed.

An underlying assumption of this analysis was that the habitat change observed on the ground can adversely affect populations of one or more key hosts, and this led to the decline of the tick population between 2010 and 2014 (Nadolny, 2016). Mammal trapping

and observations from the ground occurred as early as 2005 (Nadolny, 2016). The contrast between the habitat during years when *A. maculatum* were present and the period of decline will help to establish indicator variables that can be used to discriminate between suitable and unsuitable habitat. The completeness of the historical dataset related to this site was not reproducible at other sites. However, this analysis can provide a foundation for long-term monitoring of populations occupying habitat subject to disturbance or successional change. The methods can then be applied more broadly to other sites at the same scale to better understand the sensitivity of population presence to habitat indicators that can change over time.

4.2.2 REMOTE-SENSING TO IDENTIFY INDICATORS OF HABITAT AT THE REGIONAL SCALE

Collection sites were determined using three databases from the ongoing active tick surveillance program at Old Dominion University. The goal for site selection was to include the maximum number of *A. maculatum* sites, based on population presence, which could be contrasted with sites that were sampled within the same databases, but where *A. maculatum* populations could not be considered established. The Centers for Disease Control and Prevention (CDC) considers tick populations established when six or more ticks of a single life stage or ticks from more than one life stage are collected from a site in a 12-month period (Dennis et al., 1998). For *A. maculatum*, I based the definition of an established population on adult numbers because immature ticks are rarely collected by flagging. Two types of sites were considered unoccupied by *A. maculatum*: spatial points where *A. maculatum* have been collected but do not meet the population criteria given above and points where a site has been sampled at least three times but no *A. maculatum* have been collected. The presence of four other tick species was considered and included in a occupancy matrix to evaluate whether sampling was sufficient to identify a population of any tick species, and also to draw

inferences about different habitat associations among different species. The five species were: *A. maculatum, A. americanum, Ixodes affinis, I. scapularis*, and *D. variabilis*. Sites without any tick populations were excluded from the analysis.

To classify sampling locations (spatial points) by population presence, two definitions of population establishment were used here to compare the effect of different standards for classifying collections as a population. In processing location data here, a strict definition of an established population (≥ 6 adults) was compared to a more relaxed definition of two adults from the same site in the same year. The rationale for this comparison was that *A. maculatum* are relatively rare compared to other species, therefore a population standard that applies to other species may not be entirely appropriate.

The three databases used to identify sites were the regular Field Study data from 2017–2020, State Sweep data, and the Maculatum Hunt database. The Field Study data are collected via regular sampling year round according to seasonal schedules. Sampling begins bi-weekly in April of each year through November. After November, sites are sampled monthly. State Sweep data differs from regular flagging data in that the objective of State Sweep was to maximize spatial coverage across the state of Virginia by flagging each county at a single time point during the active season for most tick species. State Sweep data considered here were drawn from 2017 and 2018. Part of the purpose for this project was to identify new sites to be included in the regular flagging database, particularly those where *A. maculatum* or other species of interest are collected. Starting in 2019, the Maculatum Hunt database superceded State Sweep to identify *A. maculatum* populations specifically. This database includes sites that were typically only sampled once per year, including sites that are difficult to access, like the barrier islands off the Eastern Shore of Virginia. Since sampling frequency varied for the sites, species matrices were reduced to presence/absence based on the population definition of presence.

Landscape variables that were considered include: 1 m Chesapeake Bay Land Use/

Land Cover datasets from 2018 (CBPO, 2022), 19 biologically relevant climate (bioclim) variables, including mean annual temperature and mean annual precipitation (Fick & Hijmans, 2017), and elevation at 1 km resolution, 250 m resolution soils tiles from the International Soil Reference and Information Center (organic carbon density, soil organic carbon in fine particles, and soil water pH) (Hengl et al., 2017), 2019 global forest canopy height (30 m) (Potapov et al., 2020) and MODIS Terrra NDVI. Bioclim variables and soil grid data were extracted from raster datasets using the geodata package (Hijmans et al., 2022) in R 4.2.2 (R Core Team, 2023). The MODIS (MOD13A1.061) Terra Vegetation Indices 16-Day Global 500m (Didan, 2021) were visualised and data tables generated using Google Earth Engine software. MODIS satellite images were available across the 2017–2020 time period in 16-day intervals, so these were reduced to identify the annual peak NDVI during the active season for *A. maculatum*. Correlations between environmental variables were inspected by using the ggcorr function in the package GGally (Schloerke et al., 2021) in R 4.2.2.

4.2.3 DATA SOURCES AND PROCESSING

All spatial points were thinned to include one observation per 0.5 km resolution for each species (Figure 7.). This resolution preserves nearby transects that have distinctly different vegetation and different tick species collected. Sites were excluded where coordinates were unavailable or there was low confidence in the specific area flagged, for example if coordinates for a site showed a building or impervious structure, or a generic location pin for a site.
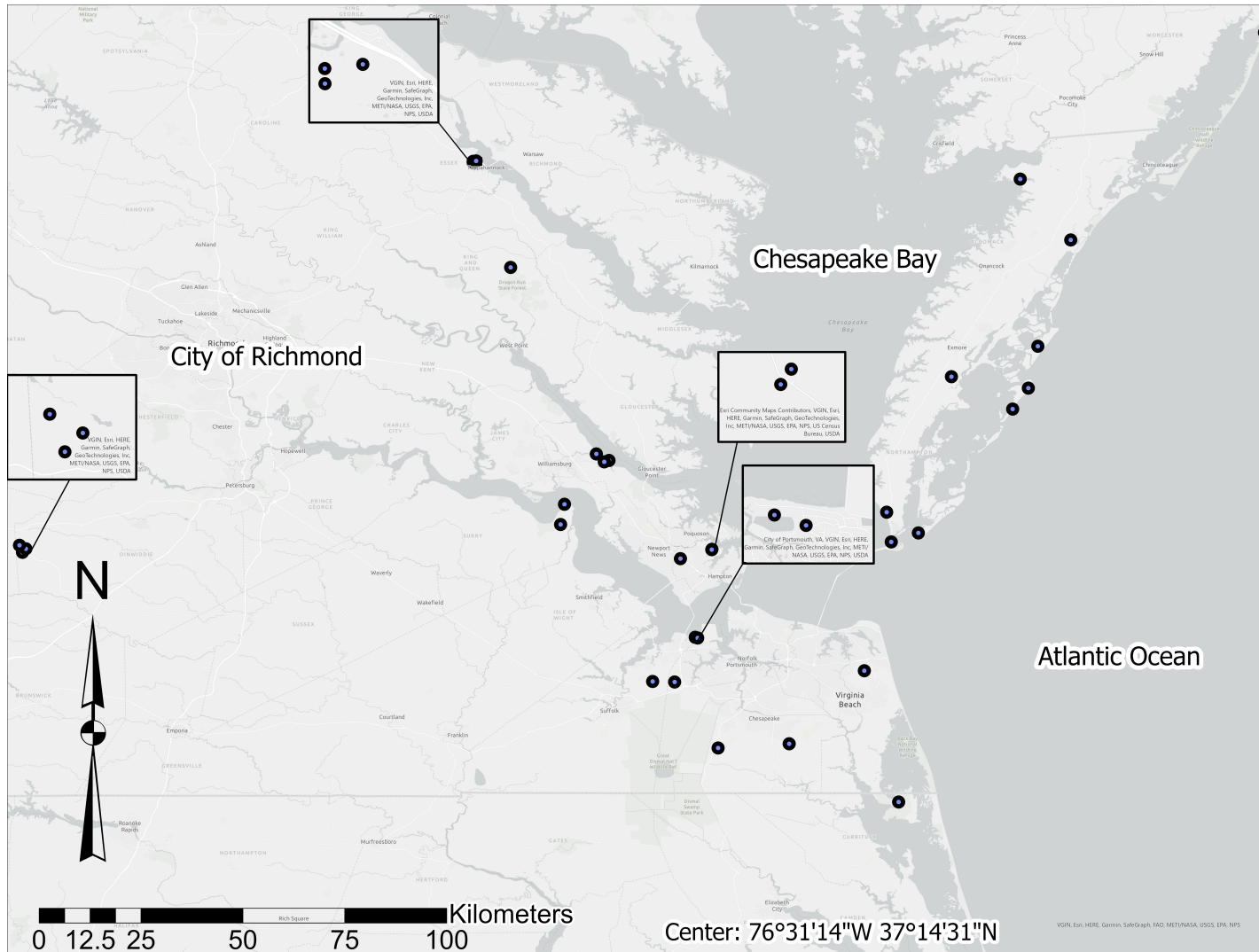
FIGURE 7. Sampling locations from thinned spatial points. Points include sites where *A. maculatum* were present or where *A. maculatum* were absent, but a population of at least one other species (*A. americanum, I. affinis, D. variabilis,* or *I. scapularis*) was present.

The bioclim, soil, and elevation variables were evaluated for correlation to select independent variables. LULC classes were extracted from spatial points based on the LULC class at the origin of the transect and the most frequent cover class within 50 m and 250 m buffers. NDVI values were obtained for each point using MODIS NDVI, which were available at a minimum resolution of 500 m. To evaluate finer-scale NDVI values, Landsat 8 OLI spectral bands were used to calculate NDVI at 30 m, the minimum resolution available. The intra-annual median value was calculated for each year (2017–2020) for the active season (June–August). NDVI median statistics were generated in Google Earth Engine.

Statistical analyses were done in R using base R and the lme4 package (Bates et al., 2022). A Bernoulli generalized linear mixed-effects model (GLMM) was produced using the function glmer in lme4 package. The binomial family was used with the complementary log-log link function because of the proportionately high number of zeroes (80%) in the year-to-year data. The default logit link function was used only for *A. americanum*, which had about equal number of presences and absences. True zeroes were only included for site and year combinations in which a site was flagged and a population of at least one tick species was present. This was done to minimize zero-inflation by excluding sites that were flagged but had no populations of any species. Presence by site and year were used to model the relationship between *A. maculatum* populations and NDVI values. For all other variables, only presence by site was used with a generalized linear model (function glm in base R), not split temporally for individual years, because the chosen variables did not have a temporal dimension aside from being the most recent estimate available for the time period of interest.

4.3 RESULTS

4.3.1 FINE-SCALE TEMPORAL CHANGE

The transition from crop to forest at CH0 was documented as a land cover class change between the NLCD 2008 and NLCD 2011 datasets (Figure 8.) (Dewitz, 2021), with no changes between the 2006 and 2008 land cover datasets. Land use change coincided with the transfer of the property from a private landowner to The Nature Conservancy as part of the Great Dismal Swamp conservation project.
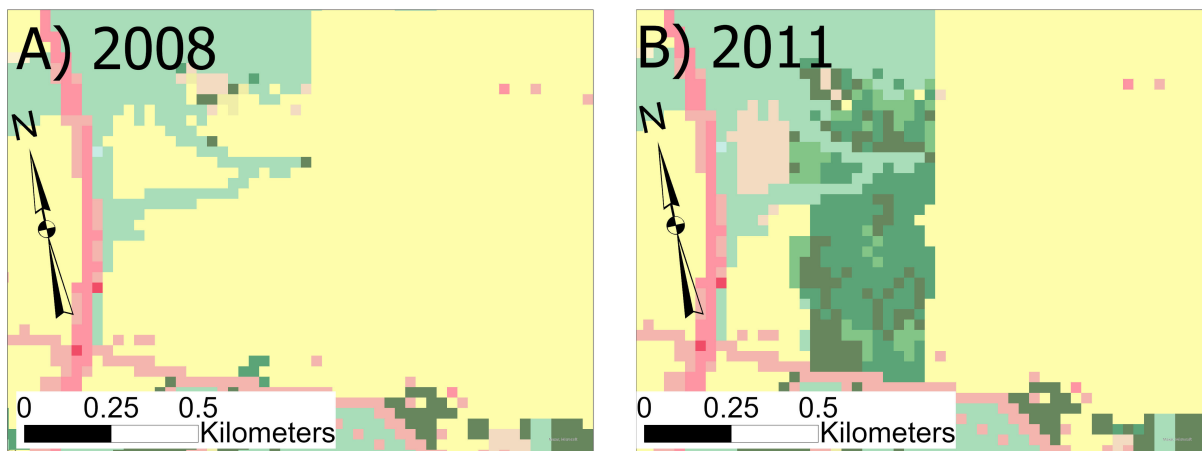
FIGURE 8. Images showing the land cover class transition of a site in Chesapeake, Virginia (CH0). The site transitioned from Cultivated Crop to a combination of Deciduous Forest, Evergreen Forest, and Mixed Forest from the National Land Cover Database (NLCD) (Dewitz, 2021)

An evaluation of MODIS NDVI values during the same time period showed the lowest NDVI around years 2000 and 2004, followed by an increase from around 0.6 in 2004 to

over 0.9 by 2016 (Figure 9.). Between 2006 and 2009, NDVI values remained relatively steady around 0.75 before rising to consistently > 0.8 thereafter. *Amblyomma maculatum* collections in this time period spanned from 2010–2014 after which the population rapidly disappeared from the site. No *A. maculatum* have been collected since 2014 (Nadolny, 2016), despite regular flagging of this location.

The shift in NDVI values between 2005 and 2014 showed that successional change observed on the ground during sampling translates to a relatively narrow increase in NDVI, compared to the overall scale of the index (-1 to 1). A trend across the entire time period (2000–2016) was apparent using both Landsat 5 TM and Landsat 7 ETM+ bands to calculate NDVI. The time period that coincided with the land cover class change, 2008–2011, experienced a net NDVI index change of +0.054 for the average during the active season. With ongoing monitoring, species like *I. affinis*, *A. americanum* and *D. variabilis* continued to be collected. The same site was included as a contemporary site for those species in the subsequent analyses.
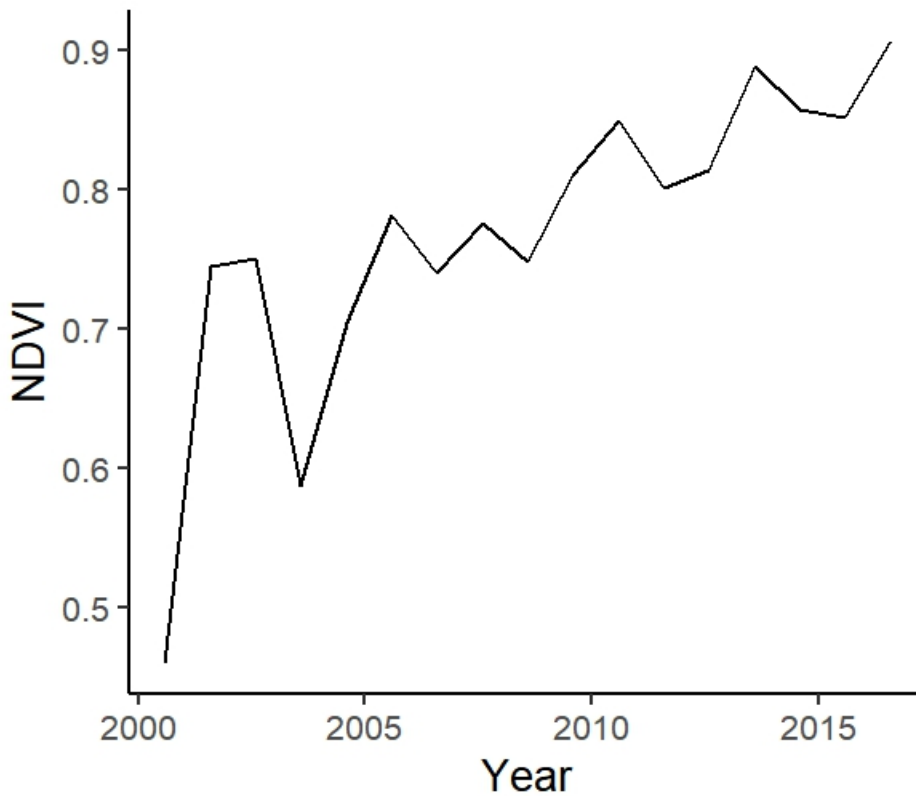
FIGURE 9. Intra-annual median NDVI values at CH0 during the peak active season (June–August) for Gulf Coast ticks (*A. maculatum*). NDVI values are shown from 2000–2016 using harmonized spectral bands from Landsat 7 ETM+ and Landsat 8 OLI imagery.

4.3.2 NON-SIGNIFICANT RELATIONSHIP BETWEEN *A. MACULATUM* AND THE NORMALIZED DIFFERENCE VEGETATION INDEX

Overall, 987 *A. maculatum* were collected between 2017 and 2020 using both regular flagging and special sampling to increase *A. maculatum* collections. Among these collections,

912 individuals were collected from locations that met the population threshold of six or more adults. These were collected from 9 transects in 2017, 11 in 2018, 15 in 2019, and 7 in 2020. Numbers collected ranged from 6 to 113 within a year, with a mean of about 28 ticks per transect. Two of these locations were considered off-transect, meaning that they were not areas typically flagged and coordinates were not available. In 2019, BI1 and BI3 were subsampled using a cluster sampling approach that differed from the linear transects at regularly flagged sites. Four transects each at BI1 and BI3 were pooled to represent those barrier island populations. Spatial thinning was then applied as described in Section 4.2.3. After cleaning and thinning the data, twelve spatial points were included in the final *A. maculatum* dataset, representing a total of 689 ticks. These counts were transformed to a presence/absence matrix for each of the twelve retained transects and the years sampled, with "NA" values reported for sites that were not sampled in a given year. Only one additional point was included for *A. maculatum* when the threshold was lowered to ≥ 2 adults. The same process of spatial point selection was applied to the four other tick species. In contrast to *A. maculatum*, changing the population threshold increased the number of *I. affinis* sites from 9 (threshold ≥ 6) to 17 (threshold ≥ 2). Because *A. maculatum* were the focus of this study and other species were included for comparison only, the remaining analyses included only sites with tick populations based on the established threshold of six or more adults. After processing datasets, only three *I. scapularis* sites met the population criteria; after thinning, all sites for *Ixodes* species included *I. affinis*. Therefore, *Ixodes* spp. here were represented by *I. affinis*.

For all species, a total of 60 spatial points were included after thinning, of which 34 were unique. Duplicated points had populations of multiple species present, which were collapsed to create the multi-species presence/absence matrix. One barrier island site was subsequently excluded because the site changed from an island to predominantly open water at the sampled coordinates following a major storm in 2017. After excluding the barrier

island site, 33 sites were included in the analyses.

Significant correlations were observed between many of the 19 bioclim variables, as well as between bioclim variables and soils, with the exception of pH in soil water (pHH_2O). None were significantly associated with presence of *A. maculatum*. These variables were then excluded from analysis because of overall low variation and independence at the spatial scale of interest. The average NDVI for sites pooled by species' population presence indicated differences between species across all months, with higher values for *A. americanum* and *Ixodes* spp., and lower values for *A. maculatum* and *D. variabilis* (Figure 10.).
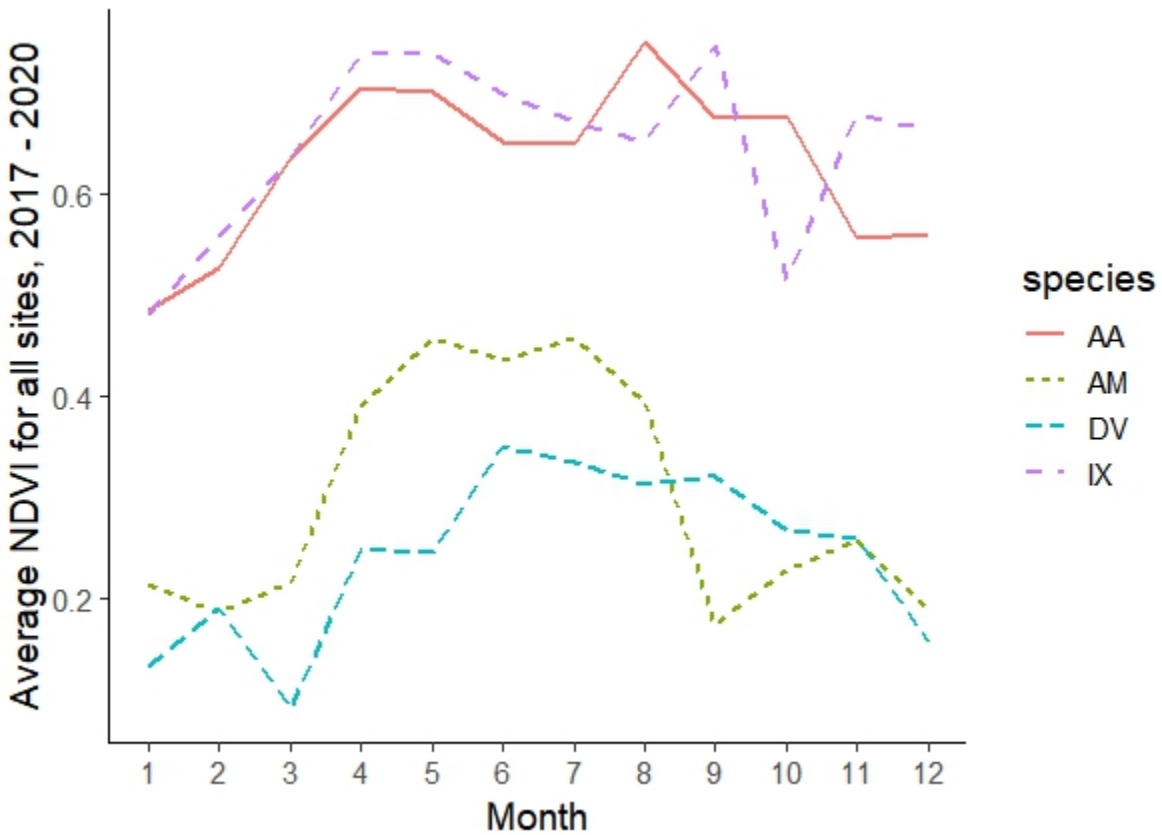
FIGURE 10. Average NDVI by month for all sites from 2017–2020 based on MODIS NDVI bands (500 m resolution) at sites with tick populations. Species codes are: AA = *Amlyomma americanum*, AM = *A. maculatum*, DV = *Dermacentor variabilis*, and IX = *Ixodes* spp.

The GLMM model for 30 m Landsat 8 NDVI values showed non-significant positive relationships between NDVI and all species. The distribution of NDVI values was generally greater than 0.5 in any given year for most sites, with the exception of three barrier island sites. In addition, all occurrences of *A. maculatum* populations were at sites with peak NDVI

values > 0.53. Since I was most interested in vegetated landscapes, namely distinguishing between the transition from early successional stages to mid-succession after canopy closure, a second set of models was generated using a subset of the data. This was done to minimize the effects of the non-significant positive relationship on the predictions at greater NDVI measures. The subset models filtered out sites with < 0.53 peak NDVI, a threshold that was chosen to retain all *A. maculatum* sites. Zeroes made up 77% of the data after filtering, justifying use of the log-log link once again. No significant relationship was observed between *A. maculatum* presence and NDVI in the model using the NDVI range 0–1, $z = 0.967$, $p = 0.3337$. The subset model also showed a non-significant negative relationship between *A. maculatum* populations and peak NDVI using NDVI values above 0.53, $z = -0.215$, $p = 0.830$.

Amblyomma americanum, in contrast, populated many more sites across years 2017–2020. NDVI peak values during these years ranged from -0.363 to 0.918. The model based on all NDVI values for *A. americanum* showed a non-significant positive relationship between *A. americanum* populations and NDVI, $z = 1.518$, $p = 0.129$. When the subset model was run, filtering out any data from sites < 0.53 peak NDVI, the results were inconclusive, as both the intercept and the variable (NDVI) were significant and the model failed to converge.

4.4 DISCUSSION

No significant relationships were detected between the environmental variables evaluated and *A. maculatum* presence within the regional study. A major limitation in studying *A. maculatum* habitat through remote sensing is the difficulty in identifying populations on the ground, particularly those that remain stable long enough to provide multiple years of data, along with accurate spatial coordinates. Ideally, a study design would be able to incorporate ground-truthed data to create models combing field data and remotely-sensed data. However, given the overall impermanence of many *A. maculatum* sites, designing and

completing such an experiment would require concentrated effort beginning in a short time frame after the population was first identified.

This study used a rigorous definition of populations to identify population presence/absence and limited locations to transects with coordinates that were known to be accurate within 30 m of the transect origin. With these data, a negative relationship with NDVI was observed when NDVI values over 0.53 were considered, but this relationship was not significant likely because of limitations described above, as well as limitations with the index. This NDVI range is important to distinguish between a late stage old field succession to a secondary succession habitat, as was observed with the site CH0 (Section 4.2.1). NDVI is sensitive to bare soil and becomes saturated at higher NDVI values in dense vegetation, which makes this index notoriously problematic except as a coarse measure, as it is used here. Relaxing the population definition could expand the number of spatial points for presence-only modeling. Alternatively, more locations could be included if all individual occurrences rather than populations are incorporated, and the number of occurrences is increased by using those from outside databases such as the Global Biodiversity Information Facility, the National Ecological Observation Network, TickSpotters (Kopsco et al., 2021), and iNaturalist. Such an approach would also introduce biases that must be handled carefully by addressing uncertainty about correct species identification as well as accurate coordinates for the collection location.

Going further with a temporal investigation of NDVI changes over years in relation to tick phenology can reveal the relationship between vegetation and tick populations. The goal here was to be able to identify a variable that would have a strong enough relationship to discriminate between suitable and unsuitable habitat for the ultimate purpose of mapping these with confidence. The best way to accomplish this would be to develop a field study that could more closely link data at a fine scale on the ground to remotely sensed variables such as NDVI, Leaf Area Index, or another appropriate measure. Canopy closure has been

identified as a factor in *A. maculatum* population decline and extirpation (Nadolny, 2016). Vegetation studies to monitor canopy cover over time, or the flux of this measure in relation to disturbances, could shed more light on the apparent relationship between GCTs and succession. Remote sensing would still be useful in this regard if unmanned aerial vehicles were deployed to capture point clouds of the vegetation using light detection and ranging. This task is relatively less labor-intensive than traditional vegetation sampling, but adds significant costs to the project. When refined, future work following some of these approaches can be applied to identify new populations using spatial imagery.

CHAPTER 5

SIMULATING THE EFFECTS OF PROPAGULE PRESSURE ON GENETIC DIVERSITY WITH AGENT-BASED MODELING

5.1 INTRODUCTION

Agent-based modeling (ABM), or individual-based modeling (IBM), is a stochastic simulation modeling approach that allows individual variation in behaviors to generate emergent patterns in a system (Sokolowski & Banks, 2009). ABMs are useful for modeling complex ecological systems, particularly those that would be hard to evaluate in field studies, where agents model organisms that are driven by different cues and motivations. Questions about landscape and dispersal effects on the genetic patterns of the Gulf Coast tick (GCT), *Amblyomma maculatum* are good candidates for evaluation using ABM. For example, a pattern indicating a founder effect was identified in Benham et al. (2021). The development of this model specifically addresses how common the founder effect might be, and how environment and propagule pressure can affect such patterns. The model described here was designed with the Mid-Atlantic United States (U.S.) region in mind, and it is specifically suited to address population genetics questions from this region (Benham et al., 2021; Nadolny et al., 2015). As such, the regional limitations should be considered before the model is applied to other locations. The phenology parameters in particular have been tuned to a regionally-specific set of surveillance data.

Several ABM or IBM models have been proposed to evaluate the effects of landscapes and demographic processes on genetic diversity. Among these, the individual-based CDPop models have been used in a number of applications, primarily for conservation

planning (Landguth & Cushman, 2010). CDPop brought together the concept of landscape resistance/cost-distance with organismal gene flow to create an individual-based landscape genetics model. Initially, the full map had to be populated and demographics were not considered (Landguth & Cushman, 2010). A later update, CDMetaPop implemented in Python coding language, added expansions to allow users to model landscape change and demographic stochasticity along with updated genetic components (Landguth et al., 2017). One of the limitations of the CDMetaPop model is that only one species can be simulated. Demographic and life history features, such as dispersal behavior, are explicitly defined for a single species, the one for which genetic and other outcomes will be monitored. This makes it difficult to tie the individual movement of a parasite to movements of host animals that would be necessary to accomplish dispersal, when both organisms have unique and possibly conflicting responses to habitat change. Also, CDMetaPop still populates the system upon initialization with species numbers subject to demographic change throughout the simulation. One of the more powerful features of this model is demographic response to a changing environment, which can allow for simulations of species removal (Landguth et al., 2017). What is missing, however, is a mechanism for ongoing introduction of individuals into the system to simulate the start of an invasion process.

A similar type of model, SimAdapt, was created in the program Netlogo (Rebaudo et al., 2013). Netlogo software provides an environment in which to create and visualize ABM models using the Logo coding language (Wilensky, 2021). SimAdapt allowed users to monitor the genetic effects of landscape configuration and change over time. However, the original design was limited to non-overlapping generations of organisms, which was integral in the genetic assumptions. Like CDMetaPop, SimAdapt allows a species to respond to a changing environment through mutation, but does not accommodate ongoing introductions. One of the advantages of this model is that SimAdapt implements novel coding for genetic structure in Netlogo. Ultimately, though, it does not meet the requirements needed to model organisms

that have several overlapping life stages and can be subject to ongoing introductions from outside populations.

Since the movement dynamics of ectoparasites like GCTs are dependent either on explicit modeling or implicit assumptions about host movement, a more realistic model has to take into account at least two organisms: tick and host. TICKSIM, another agent-based model designed in NetLogo, was initially developed for the purpose of modeling these complex interactions between ticks and host, with a submodel tracking prevalence of the tick-borne pathogen *Ehrlichia chaffeensis* through populations of both tick (*A. americanum*) and host (*Odocoileus virginianus*) (Gaff, 2011). TICKSIM has since been modified to explore questions related to population establishment of generic invading species, specifically trying to pinpoint the minimum number of ticks needed to establish a new population in a simple spatial configuration with unconstrained (random) host movement (Nadolny & Gaff, 2013). The latest iteration of the TICKSIM model introduced mitochondrial DNA haplotypes and habitat interactions using a generic tick life cycle to explore dynamics of species invasions under different habitat conditions (Nadolny & Gaff, 2018*a*). Generally, the TICKSIM model in all of its iterations provides a general tick phenology and tick-host interactions that can be adjusted to match species-specific parameters. The TICKSIM model is well-suited to answering questions specific to tick-host interactions because of the built-in phenology and basic interactions programmed into the model. However, to follow up with theories presented in Chapter 3, key changes must be made to the model to reflect GCT phenology, ongoing introduction of new adult ticks to the system (propagule pressure), and interactions between ticks, hosts, and landscapes.

Presented here is a modified TICKSIM model updated to match a hypothetical 2-year GCT life cycle in the Mid-Atlantic region, a change from a generalized 3-year life cycle modeled in earlier versions (Gaff, 2011; Nadolny & Gaff, 2013, 2018*a*). Several other changes have been made to the model to expand the spatial extent, increase the number

of haplotypes in the system, introduce adult ticks over time as the model runs, and have both ticks and hosts interact with the landscape. The change in landscape effects on the host also incorporates seasonal dynamics in which mortality increases in winter. Host-landscape interactions are controlled by patch suitability, which affects small host energy and survival. The energy of the larger host is affected primarily by movement (energy loss) and predation (energy gain). Two types of hosts are still present in the model, as was the case in earlier models. Consistent with earlier models, each of these hosts only occur as mature individuals, even though there is a mechanism to increase small host populations. Further, assumptions about these hosts have been changed by modifying the large, long-distance dispersing host to act as a predator of the smaller host, simulating the possible role of coyotes (*Canis latrans*) in the GCT system. The reasoning for this change is to examine what effect the host for adult ticks might be on the system overall if that host preys on the host of immature ticks. Host behaviors, including predation, are flexible and can be modified with few changes to the code. The predator role chosen for this model is not meant to imply that this is the only, nor the most likely, relationship between two types of hosts. Rather, the model is meant to test the effects predator-host on other hosts, since coyotes are a host of adult GCTs and the associated pathogen *Hepatozoon americanum* (Kocan et al., 1999; Teel et al., 2010). Small mammals make up an estimated 25–35% of the diet of North American coyotes (Jensen et al., 2022). Although deer and other large mammals are likely also important to GCT dispersal, direct interactions between host species, such as small mammals and coyotes, have not been modeled in previous versions of TICKSIM. Introducing a host that also interacts with the smaller host as a predator allows for the model to simulate the competing effects of these interactions on GCT populations. Additionally, pathogen dynamics have been removed from this model, which would have been a mechanism for increasing mortality of the small mammal host. In the absence of interaction-based effects on mortality, the inclusion of a predator helps to control the small mammal population throughout the model

runs. Overall, the modifications to the model allow us to explore more specific hypotheses that affect quantitative measures of GCT population abundance and intraspecific diversity.

5.2 BACKGROUND INFORMATION

Ticks are vectors of pathogens that can cause disease in humans and a range of other mammal hosts. GCTs are the primary vector of *Rickettsia parkeri*, an intracellular bacterium that causes *R. parkeri* rickettsiosis, a spotted fever illness in humans (Paddock et al., 2004). Experimental transmission has been demonstrated for *Ehrlichia ruminantium* the causative agent of Heartwater, a disease affecting cattle, and GCTs also harbor the previously mentioned *H. americanum*, a disease of both wild and domestic canids. The range expansion of the GCT poses the risk that the pathogens could be introduced, via transport in the ticks, to new areas where they can come into contact with naive host species.

Although GCTs can be considered native to the U.S., having been present in the Americas, including the southeastern U.S., since at least 1844 (Teel et al., 2010), their dispersal and subsequent establishment in other areas of the U.S. can be evaluated using biological invasion theories. GCTs have several commonalities with non-native invaders, especially their association with disturbed habitat and the apparent fecundity in suitable habitat (Nadolny & Gaff, 2018*b*). Species invasions occur when individuals are redistributed into new areas where populations are not yet established. Once there, they subsequently establish new populations. GCT population establishment is a process that is dependent on a combination of site factors, including GCT biology and host behaviors that move ticks from one location to another. Ticks are limited to short-distance movements on their own and must rely on hosts or other means of transportation to travel long distances to new sites. Different hosts likely influence different colonization patterns. For example, hosts that can carry ticks long distances are essential to contributing to range expansion, whereas smaller hosts with limited ranging distances can be key to survival and establishment in a site with

new drop-offs (Nadolny & Gaff, 2018*a*). Coyotes, for example, have an average home range of 18.7 km^2 (Jensen et al., 2022). To simulate the invasion process, several parameters must be included in a model: introduction, interactions with hosts and the environment, tick fecundity, and subsequent population establishment (Blackburn et al., 2011).

One of the most important variables that contribute to population establishment in any invasion is propagule pressure. In quantitative terms, propagule pressure is the product of the number of individuals (propagule size) and the frequency of introductions (propagule frequency) (Wittmann et al., 2014). In GCTs, the assumption is that introductions occur via drop-offs of adult female ticks that have already mated and fed, as mating occurs on-host in metastriate ticks. In GCTs specifically, females begin taking their blood meal where conspecific males have already initiated feeding (Teel et al., 2010). Based on this feeding and mating behavior, the male parent of any offspring is likely from a location near where the female originated, even with long-distance host migration. Maternal lineages can be tracked through mitochondrial DNA (mtDNA), because mitochondria are inherited from the female. Mitochondrial haplotypes can be characterized by single base pair changes in the 16S rRNA gene of the mitochondria (Benham et al., 2021; Nadolny et al., 2015). The establishment of multiple mitochondrial lineages indicates success of a larger number of females, whereas reduced haplotype richness suggest few females have successfully contributed to subsequent generations.

The model described here is designed to look at haplotype richness as a result of variations in propagule pressure. The key response I was looking for in the ticks was the relationship between propagule pressure and the resulting haplotype richness and evenness within a site. Exploring this system through modeling is necessary to unravel the expected effects of different components of propagule pressure on genetic outcomes, where definitive empirical data are largely absent regarding primary hosts and their movement patterns.

5.3 MODEL DESCRIPTION

1. *Purpose and patterns*

The purpose of this model is to evaluate the effects on ongoing introductions of adult GCTs into a system to simulate the effects of propagule pressure on genetic diversity given a range of starting conditions. Secondarily, the model will use different landscapes to look for ecological effects on GCT establishment and genetic diversity based on responses of the mammal hosts and GCT hatching success to environmental conditions. A major pattern of interest, based on rare observations in natural systems (Benham et al., 2021), is the likelihood of a single haplotype gaining dominance. Here I tested some questions about how often this would occur using a system with simplified landscape and host interactions. The stochastic nature of this model is especially useful to study this pattern. Mitochondrial genes are well-conserved, meaning that they tend to be protected from natural selection pressures. Instead of natural selection acting on mtDNA, genetic drift is the primary neutral process that affects intraspecific diversity, along with background mutation rate. Genetic drift is one of the key neutral processes that could cause haplotype diversity to fluctuate. Genetic drift is closely linked to population demographics, specifically population effective size, which is the actual number of reproducing females in the population. However, ecological filters can also act to modulate invasion processes and have significant effects on the colonization success of introduced species (Wittmann et al., 2014).

To evaluate the interactions between propagule pressure and environment on the genetic patterns of GCT population establishment, the effects of 6 parameters were measured: landscape, predator abundance, host density, propagule size (total number of ticks per drop-off), propagule frequency, and land use. The effects of drop-off rates on two outcome variables, abundance and haplotype diversity of adult GCTs, were

also considered. Patterns of interest in the outcome variables include dampening of GCT abundance, haplotype richness, and the emergence of a dominant haplotype as evaluated through rank-abundance model fitting.

2. *Agents/Individuals, state variables, and scales*

<u>Agents</u>

The entities modeled include GCTs at all life stages (egg, larvae, nymph, adult), and two types of mammal hosts, small and large, with different dispersal abilities. GCT-specific state variables were life stage, sex, maternal identification and haplotype, individual identification number, activity, and current host (if applicable). Life stage determined tick activity, with eggs only having one activity (dormant), then transitioning to larvae to begin questing. Questing larvae have a probability of attaching to a host on the same patch, with a higher likelihood of attaching to small rather than large mammals (Table 11.). If they successfully attach, activity switches to feeding, after which they drop-off and enter a resting/dormant period. Each life stage from larvae to adult proceeds through the same activities, although the duration of feeding and resting varies by life stage. After adults feed, females will reproduce and males will die at the end of the blood meal. All of the offspring (eggs) will occupy the same patch and inherit the same haplotype as the mother. Eggs will also have sex assigned upon creation. The number of eggs each female produces is controlled by a slider. An important note here is that GCTs typically lay an average of 8,000 eggs per female (Teel et al., 2010). Some assumed mortality is included here that is not explicitly modeled.

Agent parameters

State variables for small mammals included energy level, range area to limit movement, a maximum number of ticks each host could hold, and the ID of the ticks currently on the animal. Energy for small mammals is tied to habitat suitability, a patch variable, so that if the small mammal spent too much time in unsuitable habitat, energy would eventually run out, killing the host and any ticks present on it. State variables for large mammals were similar except that they had to consume smaller mammals for energy, so they also have a variable to keep count of the number of small mammals eaten. A lack of energy resulting from lack of small mammals to feed on, can trigger the large mammal to leave the system. Larger mammals also respond to a parameter called restlessness, which operates like mortality for the ticks and smaller mammals. Restlessness is a way to approximate a range of stimuli that would trigger a coyote to range beyond a given area, thus leaving the system. Since this model does not track individuals outside of the bounds of the system, restlessness is functionally a mortality procedure. Large mammals also have a maximum number of ticks, a list of ticks currently feeding, and a total count of all ticks that have ever been on that host. Additional variables that control large mammals are a system parameter for drop-off frequency, which controls the number of large mammals that emerge into the system based on a probability per time step. With these immigrations, a variable number of ticks are also introduced as feeding adults attached to the large mammal. The haplotype diversity of immigrating ticks varies depending on the maximum founder diversity parameter.

Spatiotemporal units

The first simulation day of the year is set to June 1, which is the start of peak season for adult GCTs in the Mid-Atlantic U.S. (Nadolny & Gaff, 2018b). Additional

TABLE 11. Initial model parameter settings. Bold text indicates new parameters or changes to parameter values from prior models (Nadolny & Gaff, 2018*a*). Abbreviations for adults and immatures: A and I.

Entities	Parameters	Category or value/unit
Environment	Simulation extent (ha)	**640**
	Number of cells	**7396**
	Hectares/patch	**0.087**
	Starting time	**June 1**, Year 1
	Simulation duration	1130 time steps (days)
Patches	**Landscapes**	See Table 12.
	Suitability	See Table 13.
	Cell size	30 m (900 m$\hat{2}$)
	Occupied	Any ticks present
	Population	> 6 adult ticks
Large host (predator)	Initial population	**0**
	Movement	**within 20 patches**
	Restlessness	0.09/day
	Max ticks per host	**500**
	Group size	5
Small host	Initial population	1000
	Movement	**1 suitable neighboring patch**
	Mortality per time step	0.002
	Density	**up to 15/ha**
	Dispersal	at max density
	Max ticks per host	**200**
Ticks	Mortality per time step	0.05
	Immature attachment on sm host	0.9
	Immature attachment on lg host	0.01
	Adult attachment on sm host	0.9
	Adult attachment on lg host	0.01
	Initial population	0
	Eggs per female	**3000**
	Time from egg to hatching	**7**
	Molt time from larva to nymph	**7**
	Molt time from nymph to adult	**258**
	Maximum questing time	**A: 35 days; I: 25 days**
	Length of blood meal	**A: 10–17 days; I: 4–8 days**
	n unique haplotypes	**0–100**
	Haplotypes per drop-off	3
	Drop-off frequency	0.1
	Adults per drop-off	15
	Hatch success	See Table 13.

state variables control the spatial and temporal scale of the system are year number, day of year, and cell size. Cell size is scaled based on the resolution of the imported raster files. Cell size is used to calculate the range area of small mammals, which limits their movements in any given time step. This model replicates the landscape at a scale of 1:17,000, approximately the size of a typical field site and the surrounding landscape, enclosing just over 640 hectares total. The maps are based on a 1 m resolution land cover image aggregated by a factor of 30, with the function modal to take the most frequent land cover value from the cells being aggregated using R package raster (Hijmans et al., 2023) in R 4.2.2 (R Core Team, 2023). The total extent includes 7396 Netlogo patches equivalent to 7396 × 30 m squares, which is 6,400,459.75 m^2 or 640 hectares. Year number and day of year manage phenology and mortality for the agents. Each time step in the model is 1 day. The model duration can run indefinitely, but was set to stop after 1130 time steps, or approximately 3 simulation years starting from June 1 in Year 1, and ending July 19 in Year 4. The active season for adults based on field collections in the Mid-Atlantic U.S. typically runs from April to September, with peak densities in June and July. The end of the model is set to coincide with the end of peak adult activity for the fourth generation.

Environment

Patch variables include land use, appeal, and suitability. The composition of landscapes (Table 12.) are based on land use/land cover (LULC) rasters (CBPO [Chesapeake Bay Program Office], 2022). Appeal and suitability are determined based on land use types of each patch (Table 13.). Suitability determines small mammal energy and whether GCTs can reproduce on a patch. Appeal attracts large mammals to edge habitat. Appeal is based on proximity to suitable habitat and is highest in patches that are immediately adjacent to suitable patches.

TABLE 12. Landscape composition by raster layer for six GCT landscapes. Landscape codes refer to sites mentioned in Chapter 3. Core sites are those where suitability = 1. Edge patches include any unsuitable patch adjacent to core patches.

	GCT Landscapes					
	TP1	BI1	BI3	DN1	HM2	CH3
n land use classes	8	8	14	15	8	18
n core patches	2232	1791	2313	1360	1857	513
n unsuitable patches	5264	5605	5083	6036	5539	6883
% suitable	0.30	0.24	0.31	0.18	0.25	0.07
n edge patches	1254	138	878	1074	1987	989
% edge	0.17	0.19	0.12	0.15	0.27	0.13

TABLE 13. Suitability and hatch success probability designations for land use classes.

Land Use Classes	Suitability	Hatch success
water	0	0
forest	0	0.6
succession	1	0.6
other forest	0	0.6
non-forest riverine wetlands	1	0.2
terrene wetlands	1	0.2
crop	0	0
pasture	1	0.6
road	0	0
structure	0	0
impervious	0	0
tree canopy over impervious	0	0
tree canopy over turf	0	0.84
turf	1	0
pervious developed	1	0
harvested	1	0.2
extractive	0	0

3. *Process overview and scheduling*

Birth/Immigration

Populations at startup can be set for all species, including all life stages of ticks, with default settings defined in Table 11.. Large mammals immigrate into the system as adults based on drop-off-frequency, which controls a procedure called eruption. This procedure also introduces new GCT adults attached to the large mammal hosts. GCT haplotypes are randomly set from 0 to 100.

Small mammals are born when existing individuals have reached an energy level of 50. These hosts do not have life stages so all are equivalent after birth. This means that after the time step in which they are born, small mammals act as mature adults. A small mammal host can act as a host for ticks, move the same distance as any other small mammal, and intake energy within one day of its birth in the system. Although this is not realistic, it helps to simplify the model without any major effects expected on the overall relationship between ticks and small mammals. More essential to the model than strict fidelity to small mammal maturity times is the simulation of small mammal population dynamics overall. These dynamics control when and where a tick might find its host, and whether the host itself survives in the system long enough to provide a good blood meal. A carrying capacity based on patch size and monthly mortality coefficients control the maximum number of small mammals in the system. Individuals will not be born if the population is at carrying capacity in a given time step.

Death

Each agent is initially subjected to a cull based on mortality or restlessness and, for hosts species, low energy levels. GCTs will die if they are active (not resting) beyond November 1. Only adults and nymphs will overwinter in resting mode. For

hosts, if energy exceeds 50, then an individual's energy is adjusted down to the 50, the maximum for the species. When energy is too low, small mammals die and large mammals leave the system. Large mammal mortality is coded as restlessness, which ultimately means death in the system, but is based on theoretically leaving the map extent and not returning, as described in Section 2. Any ticks feeding on hosts that die or leave are also killed.

An additional density-dependence control works on small mammals, which requires them to disperse if density of the patch they are on exceeds the maximum density for that species. First, they will try to move to one of 8 neighboring patches. However, if all neighboring patches are full, the individual will die.

4. *Design concepts*

Basic principles

This model is updated from the TICKSIM model (Nadolny & Gaff, 2013); more conceptual background is presented in detail there. The updates focus on improving the dynamics of new tick introductions to the system at a spatial scale comparable to a field site. Changes were made to patches, tick phenology, host birth and mortality, as well as timing of introductions. The environment was modified to include a substantially larger spatial extent with a patch size comparable to the 30 m resolution of typical land cover data. The number of haplotypes in the system were increased to 100, but these would be randomly assigned when GCTs were created, rather than divided equally, to mimic a typical distribution as observed in Benham et al. (2021) and Chapter 3. Haplotypes are introduced into the system in two ways: either at setup by explicitly creating GCTs at any life stage, or by immigrating as an adult with a large mammal host, in which the host acts as transportation for the adult GCTs. The immigrant introduction is part of the update and was designed specifically to measure the effects of propagule

pressure on haplotype diversity. Prior model versions only introduced ticks at creation or through reproduction from ticks already created in the system. Finally, interactions between hosts exist in the form of predation and density-dependence. Small mammal density is limited by season, dropping to 1/10 of the summer maximum during winter.

Stochasticity

Ticks brought in by large mammals, the "drop-offs", are subject to three different procedures to generate haplotypes depending on starting conditions. Generally, haplotypes of introduced ticks will be randomized within certain limits. The first limit is the number of ticks introduced in any drop-off event, which was set to a random number from 0 to 7 by default. Second, founder richness limits the number of haplotypes that can be introduced in a single drop-off event, which is also subject to the number of individual ticks that can be introduced.

Drop-off frequency is a parameter that can be set to determine how often drop-offs occur. Drop-off frequency is also a measure of propagule pressure. Drop-off frequency and founder richness are expected to influence the intraspecific diversity at the end of the model run. In order for drop-offs to occur, a host must arrive from outside of the system with ticks already feeding on the host to provide an opportunity for immigrating ticks to drop-off in a suitable location. The timing of these arrivals was random, although GCT adults could not be introduced into the system outside of the active season for adult ticks.

Interactions between ticks and hosts, and hosts with each other, all occur in response to individual variation in terms of host movement, tick life stage, tick activity (questing or not), and location of the individual agents. Agent location was randomized at startup, with the constraint that small mammals and GCTs will only populate suitable habitat patches.

Timing of the tick life cycle allows for variation within set time frames. This includes the length of time each life stage of tick will feed on a host, rest (or for adults: lay eggs and/or die), molt, and begin questing again. Egg survival depends on the location that an adult female drops off of the host she was feeding on.

Emergence

This model was designed to evaluate intraspecific diversity as an outcome of two components of propagule pressure (model variables in parenthesis): propagule size (number of ticks per drop-off) and propagule frequency (drop-off frequency) (Wittmann et al., 2014). These outcomes are subject to the simplified stochastic effects of tick, host, and habitat interactions.

Sensing

Ticks sense large and small mammals as potential hosts, only if they are occupying the same patch. The overall chance of sensing a host on the same patch was 5%, a change from previous TICKSIM models. This change was based on the broader scale of the landscape in the update compared to the previous model, in which ticks could detect any host on the same patch and attach based on attachment success (Nadolny & Gaff, 2018a). Patch sizes in the update represent a larger area, therefore the updated sensing probability corresponds to a tick being able to sense a host within about 45 m^2, or up to 6 m away. Attachment success follows sensing, and was based on the host type and the tick life stage (Table 11.).

Small mammals sense conspecifics and suitable patches. They will preferentially choose the nearest neighbor patch with the highest suitability value. When the number of small hosts on a single patch exceeds small host density, they are forced to disperse to nearby patches.

Large hosts sense small mammals, suitable patches, and appealing patches. These hosts emerge into the system in an edge patch, which are those patches with highest appeal. Large hosts act as predators to the small hosts and will enter suitable areas during each time step to hunt, during which they can consume up to two small hosts. At the end of each time step they return to one of 20 patches within their location based on patch appeal.

<u>Interaction</u>

Agents perform a series of action procedures to move around the environment and interact with other agents. Any ticks that are questing (based on tick activity) can attach to a host that shares the same patch as the tick during a time step. Ticks that attach can change their activity to "feeding" and both the host and the tick track the identity of one another (i.e. agent ID in the system) in this exchange.

Simplified energy budgets generate a cost or reward to movement and interactions for the hosts. Small mammals pay a fixed energy cost to move through unsuitable patches, and have a small gain in energy for moving through suitable territory. Large mammals likewise lose energy for their movement regardless of the patch they move through. Large mammals will move four times during each time step. These hosts, which are also predators, only gain energy from eating small hosts. In each time step, they move to an appealing patch, move to a nearby suitable patch, and repeat those steps once more to increase the odds of encountering a small host.

Small mammals have a dispersal procedure that limits the number on any patch based on density. GCTs change activity and lifestage according to procedures developed in previous TICKSIM models (Nadolny & Gaff, 2013, 2018a), and as described above with regard to questing and feeding. GCTs can only go into resting mode if they successfully feed, after which they molt to the next life stage or, if adults

lay eggs (females only) and die.

Observation

The simulation was monitored using plots and a viewer that showed the spatial extent of the model. Three plots were set up to track: 1) tick populations including larvae, nymphs, adults, and total questing ticks, 2) total tick population (all life stages), large mammal hosts, and small mammals hosts (scaled by 1×10^{-2} for plotting), and 3) a count of ticks with a subset of haplotypes (1–16). A viewer window showed the starting landscape colored by land use classes. Patch colors would change over time, similar to the TICKSIM model (Nadolny & Gaff, 2018a), to show occupied patches as light red and populated patches ($>= 6$ ticks) in dark red, as well as locations for all patches. During BehaviorSpace runs, variables that were reported included haplotypes of all adult ticks present during the run, the total count of ticks, small mammals, large mammals, the cumulative number of adult ticks immigrating into the system, the cumulative number of drop-off events, and finally, the number of patches occupied and populated along with land use type for these patches.

5. *Initialization*

On setup, a specified number of agents of each species are created (GCT by life stage, small mammals) with their species-specific variables. Small animal host numbers are controlled by a slider. Large mammals enter the system periodically based on a drop-off frequency, so are not present at initialization. Each new individual tick in the system will be assigned a haplotype randomly from 101 possible haplotypes (0–100), as well as other tick variables such as life stage, sex, and activity. The initial number of possible haplotypes is based on upper estimates from the datasets presented in Chapter 3 using SpadeR (Chao et al., 2016) (Table 14.).

A landscape raster is loaded into the viewer to specify land use classes, which are

then assigned a suitability and appeal value (Table 13.). Edge habitat adjacent to suitable patches has the highest appeal, which attracts large hosts.

TABLE 14. Haplotype richness estimates from empirical data.

	Estimate	s.e.	95% Lower	95% Upper
Chao1[a]	59	14.4	45.5	112.3
Chao1-bc	54.2	10.2	44.4	91.5
iChao1	63.5	9.7	51	91.6
ACE[b]	53.2	7.6	45	78.3
ACE-1[b]	58.1	12.1	45.9	100.9

[a] (Chao, 1984)

[b] (Chao & Lee, 1992)

6. *Input data* Raster datasets were imported into the model representing land use classes for six field sites in eastern Virginia using ArcGIS Pro (Esri, 2022) to prepare Chesapeake Bay Program land use land cover classes (CBPO, 2022). Rasters were generated by defining a map extent of about 640 hectares around the transect origins and exporting these rasters in GEOTIFF format. Rasters were loaded into R 4.2.2 (R Core Team, 2023), aggregated to 30 m resolution, and exported as .ASC files. The final .ASC files were loaded into Netlogo using the 'gis' extension (Russell & Hovet, 2021).

The model was finalized in Netlogo 6.3 (Wilensky, 2021). Model runs were completed using BehaviorSpace for Netlogo. R (R Core Team, 2023) was employed for all statistical

analyses of simulation runs.

5.4 MODEL EVALUATION

5.4.1 PARAMETER SETUP

After the model was finalized, parameters were initially checked using two experiments to evaluate the effects of number of eggs laid per female, drop-off frequency, and landscape on the total number of ticks and occupied patches in the model. These runs were completed as a final calibration check before running the full sensitivity analysis. The first set of simulations ran for 3 replicates each, for a total of 324 simulation runs. Three parameters were changed: eggs, drop-off frequency, and landscape. Each run started with 20 adults present upon initialization. The number of eggs was changed in increments of 1000, from 1000 to 3000. Six sites (landscapes) were compared in this experiment: BI3, BI1, TP1, HM2, CH3, and DN1. These correspond to field sites described in Chapter 3. Drop-off frequencies were 0, 0.05, 0.1, 0.125, 0.15, and 0.2. Total ticks and occupied patches were plotted for each simulation run with all 324 simulations pooled. The number of eggs had a clear effect on tick abundance during each simulation, but all variations from 1000 to 3000 had populations survive from year-to-year (Figure 11.). Results by landscape were mixed depending on the sites. Two sites, HM2 and CH3, failed to maintain populations throughout most of the runs, as the number of occupied patches remained low from year to year (Figure 12.), as did the total number of ticks (Figure 13.). Neither of these sites had ticks by the end of the simulations, so there were also no occupied patches. Four other sites, BI3, BI1, TP1, and DN1 all remained relatively stable for the duration of each simulation, with four annual peaks in abundance (Figures 12. and 13.).
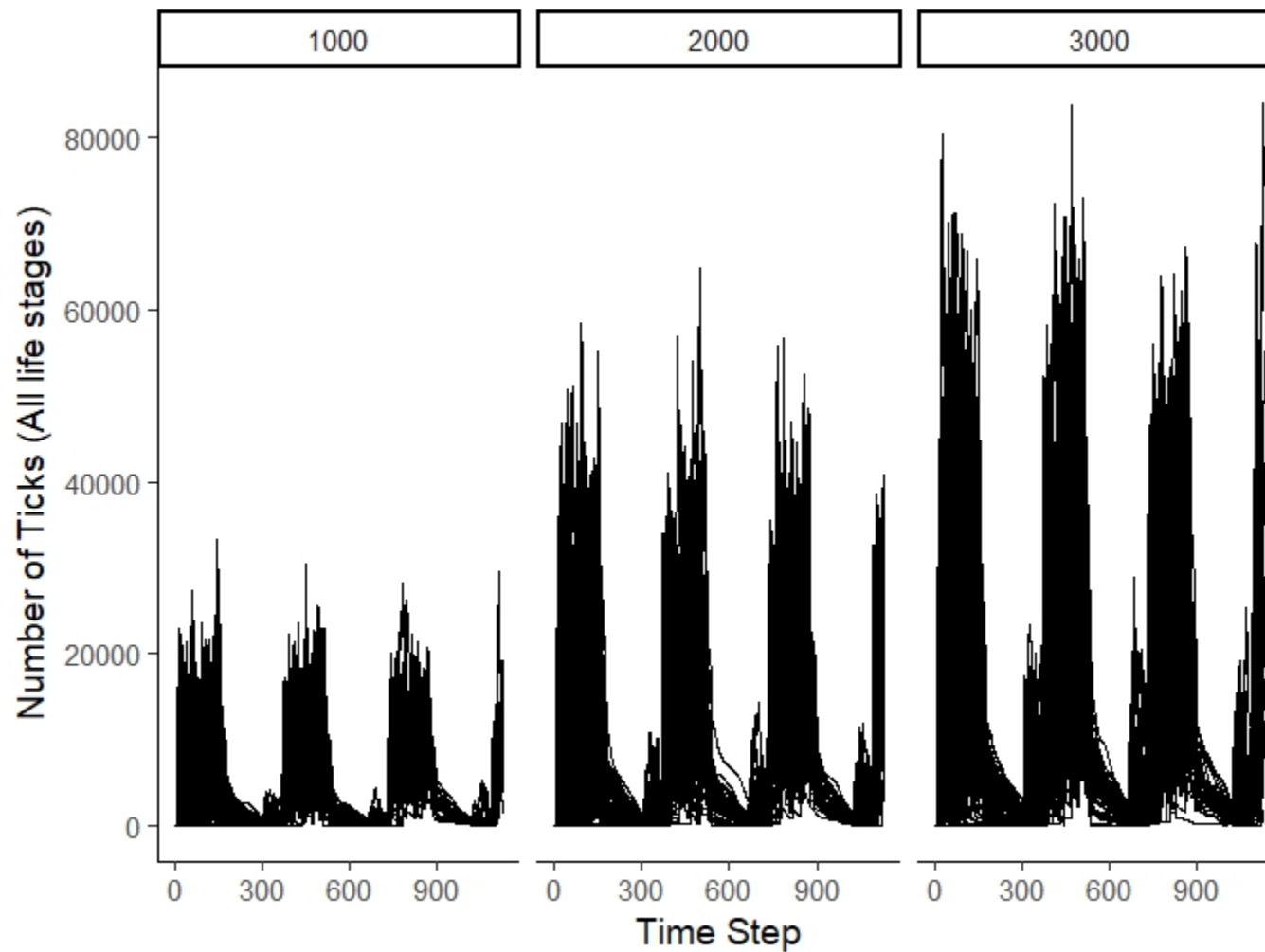
FIGURE 11. Number of ticks of all life stages by the number of eggs per female (1000, 2000, 3000). Plots show results from all 324 simulation runs.
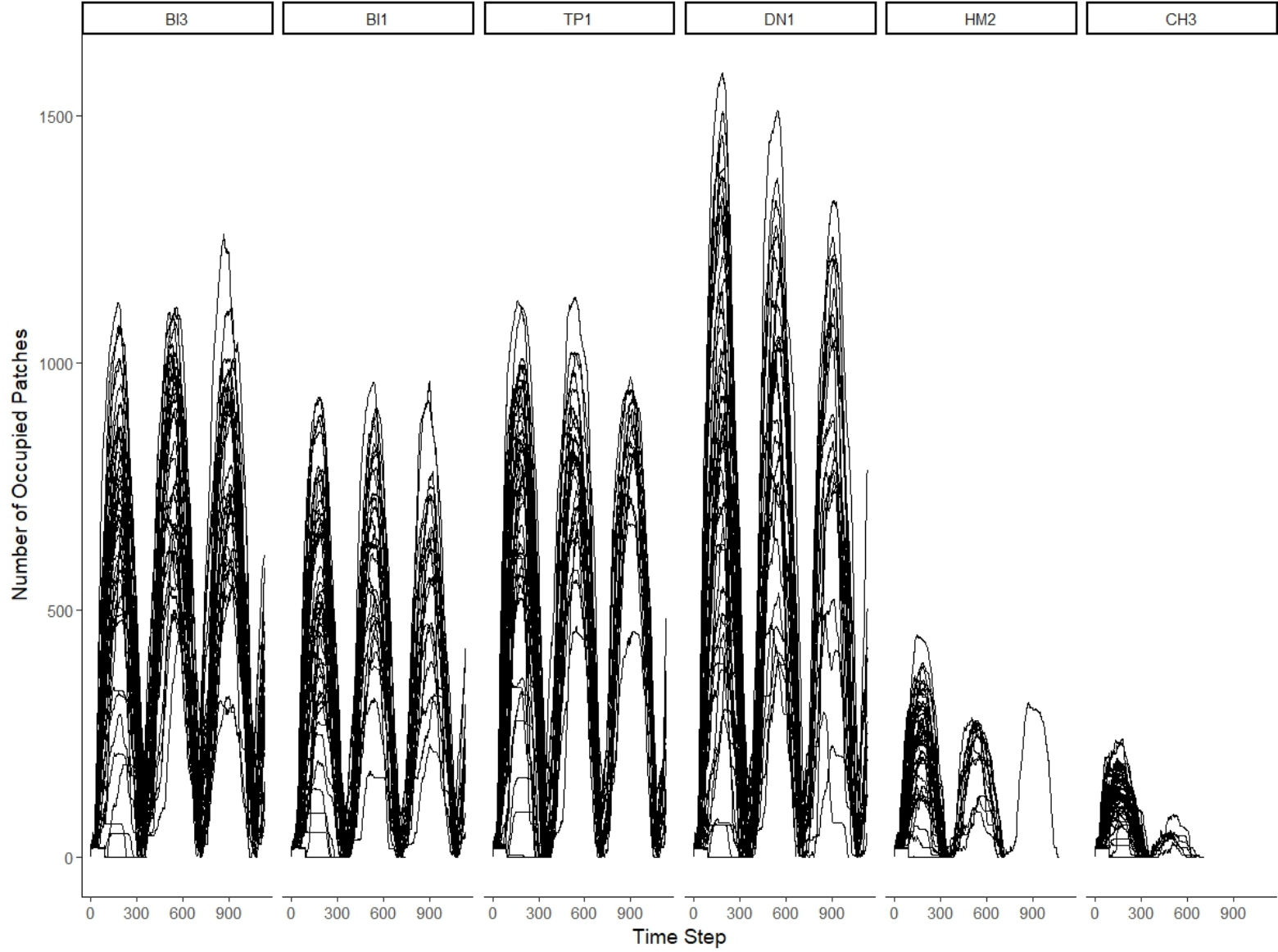
FIGURE 12. Number of occupied patches per time step for each site. Plots show results from all 324 simulation runs.
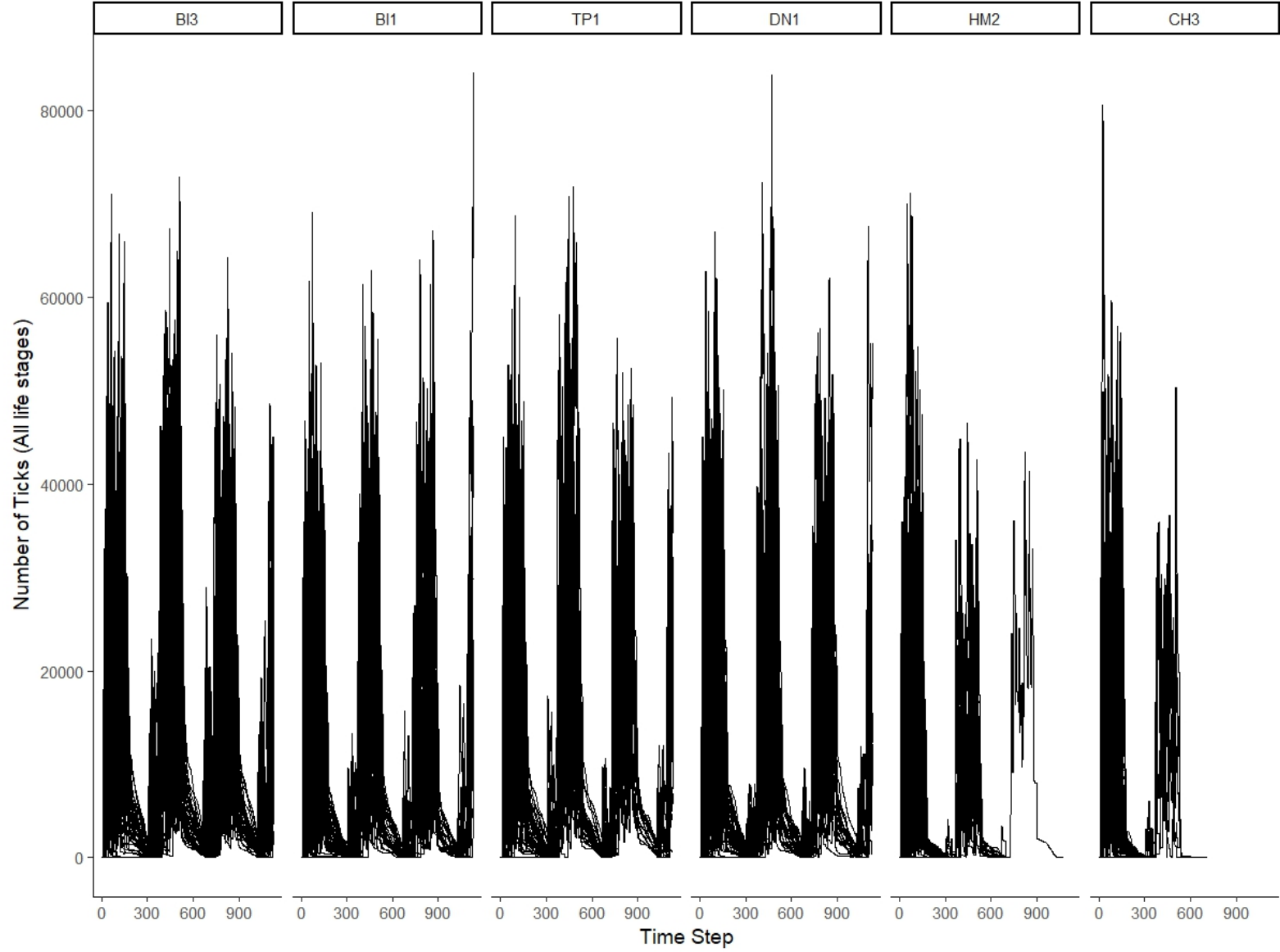
FIGURE 13. Number of ticks per time step for each site. Plots show results from all 324 simulation runs.

A second BehaviorSpace experiment was completed for 135 runs, with 3 replicates for each set of parameters, for three of the original six sites: BI1, BI3 and TP1. For this set of experiments, drop-off frequency was tested in combination with number of eggs. No adults were populated into the system at the start of the model runs. Instead, all ticks that entered the system were adult drop-offs. The drop-off frequencies were 0.05, 0.1, 0.125, 0.15, and 0.2. Number of eggs per female were again set to 1000, 2000, and 3000. These runs were intended to confirm that an increasing number of ticks immigrated into the system over time as a result of varied drop-off frequencies (Figure 14.). In addition, this experiment also confirmed that each of the three landscapes selected were all experiencing roughly similar immigration rates as drop-off frequencies changed (Figure 15.).
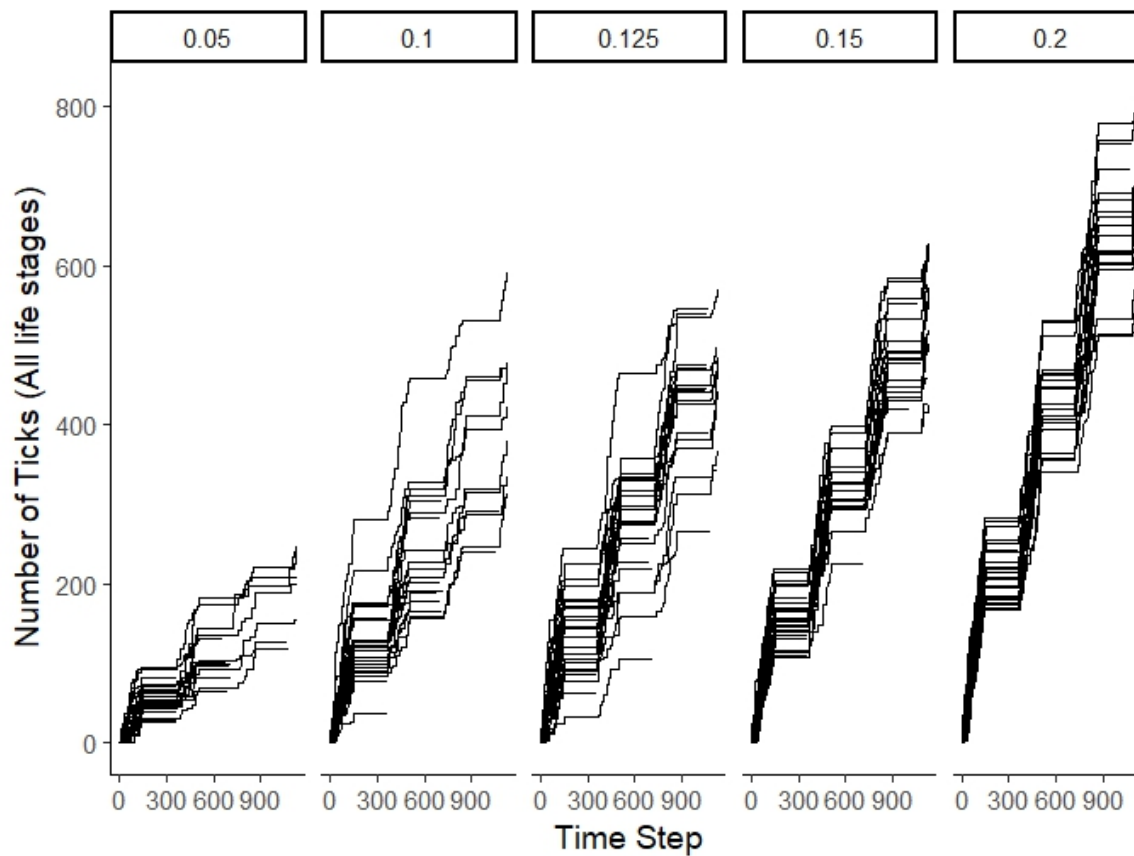
FIGURE 14. Number of ticks immigrating into the system over time by drop-off frequencies. Simulated drop-off frequencies are: 0.05, 0.1, 0.125, 0.15, and 0.2. Each combination of parameters was run for 3 replicates.
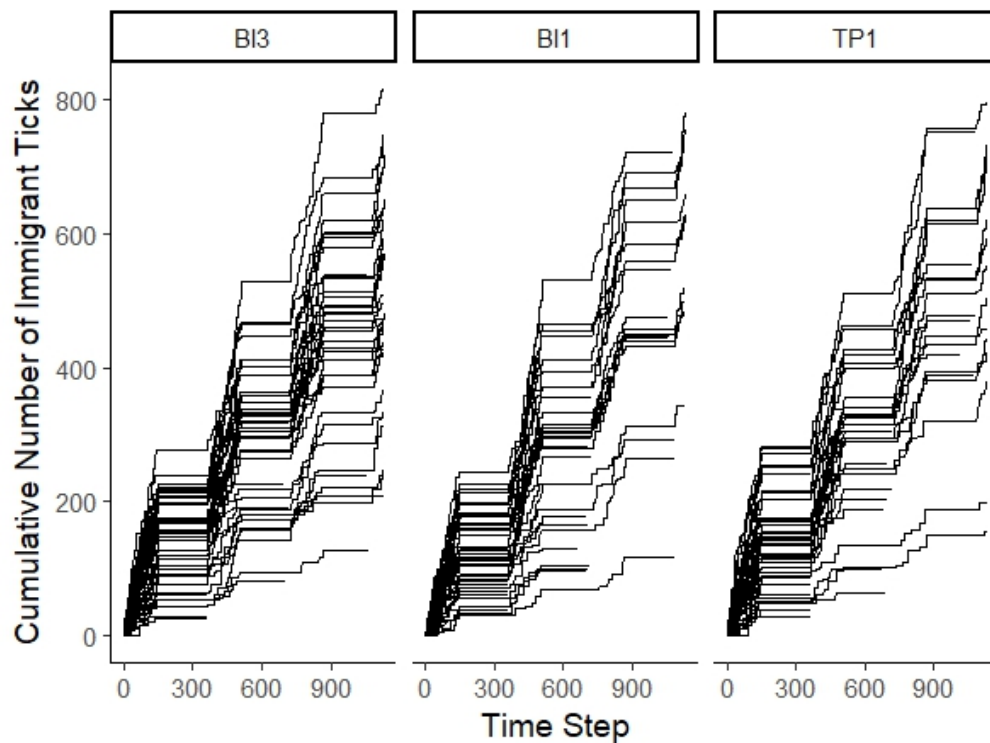
FIGURE 15. Number of ticks immigrating into the system over time for each site. Sites included BI3, BI1, TP1. Each combination of parameters was run for 3 replicates.

After confirming that the basic parameters of the model were responding as expected, a more comprehensive sensitivity analysis was conducted to see which parameters had the greatest effects on several outcome variables.

5.4.2 SENSITIVITY ANALYSES

Sensitivity analyses were conducted to test the sensitivity of the model to incremental

parameter changes. The model included new variables of drop-off frequency, host density dependence, and landscape suitability. The major outcome variables were the tick counts, resulting phenology of all life stages of ticks, the genetic diversity among adult ticks from the start to the end of the simulation run, and occupancy patterns during the final active season in the simulation.

Initially, Spearman rank correlations were computed using the 'corr.test' function in base R 4.2.2 for each of the input variables and its effect on each response variable. The default settings for the input variables were set to those in Table 11.. The parameters in Table 15. were changed one at a time. The model was run 25 times for each parameter set.

TABLE 15. Parameter changes for Spearman rank correlation test.

	Min	Max	Increments or values
Drop-off frequency	0.05	0.2	0.5
Ticks per drop-off	5	20	5
Small host density limit	5	15	5
Predator group size	1	25	5
Core patches	1360	2313	2232, 1791, 2313, 1360
Edge patches	878	1382	1254, 1382, 878, 1074
Eggs	1000	3000	2000

Not surprisingly, drop-off frequency had the greatest effect on drop-off events and also on richness (Table 16.). The next strongest effect on richness was the number of ticks per drop-off, even with the overall number of haplotypes per drop-off limited to 3 or fewer. These were the two parameters controlling influx of ticks into the system, and replaced earlier models that populated the system with an initial number of ticks at startup. Drop-off

frequency was significantly associated with all of the outcome variables measured, including a negative association between drop-off frequency and the number of small hosts, because each drop-off occurs with a predator entering the system.

A significant negative relationship occurred between the number of edge patches and richness. In fact, edge negatively affected all outcomes except drop-off events and the number of immigrants. The reason for this relationship could be because more edges in the landscape tend to be associated with smaller core areas and more fragmentation. Edges also resulted in fewer ticks overall, and fewer patches throughout the landscape that were occupied by ticks. This occurred despite edges being the point of origin for the large host into a system, similar to a corridor for movement, and those hosts were essential to the tick drop-offs in the model. The size of predator groups had significant but not particularly strong effects on the tick outcome variables, but interestingly did not affect small hosts, in contrast with what was observed with visit frequency. Finally, small host density limits were the most important variable in determining the number of populated patches at the end of the run, consistent with previous results (Nadolny & Gaff, 2018a).

One of the primary goals of the model was to evaluate the effect of propagule pressure on GCT genetic diversity under a range of environmental conditions. To further explore the model, 100 replicates each were run on four different landscape scenarios while changing two key measures of propagule pressure: drop-off frequency and the number of ticks per drop-off. Partial rank correlation coefficients were generated using the epi.prcc function in the 'epiR' package (Stevenson et al., 2023) in R 4.2.2 (Table 17.).

TABLE 16. Rho values for Spearman rank correlations. Asterisks indicate significant correlations. The strongest correlations for each outcome variable are in bold.

	Drop-off frequency	Ticks per drop-off	Eggs	Small host density limit	Predator group size	Land use classes	N core patches	N edge patches
Richness	**0.874***	0.650*	0.242*	0.264*	0.310*	-0.177	0.326*	-0.236*
Drop-off events	**0.943***	0.148	-0.057	0.007	0.349*	-0.218*	-0.108	-0.06722
Immigrants	0.941*	**0.949***	-0.082	-0.037	0.321*	-0.123	-0.055	0.011621
Ticks	0.696*	0.715*	**0.764***	0.197	0.301*	-0.175	0.062	-0.336*
Occupied	0.809*	0.733*	0.782*	**0.873***	0.167*	0.179	0.026	-0.659*
Populated	0.558*	0.584*	**0.648***	0.635*	0.286*	-0.196	0.293*	-0.238*
Small hosts	-0.666*	0.069	0.026	**0.943***	0.009	-0.328*	0.849*	-0.282*

TABLE 17. Partial rank correlation coefficient test statistics. Two parameters controlling propagule pressure (drop-off frequency and max ticks per drop-off), and three habitat parameters based on four landscape scenarios were tested. Asterisks indicate significant correlations. The strongest relationships for each outcome variable are bold.

	Drop-off frequency	Max ticks per drop-off	LULC classes	n core patches	n edge patches
Richness	**40.180***	34.403*	-1.554	3.887*	-4.701*
Drop-off events	**84.937***	1.047	-1.089	1.265	0.288
Immigrants	**108.226***	94.509*	-0.322	0.774	-0.325
Ticks	**9.565***	1.187*	-2.004*	1.919	-0.865*
Occupied	11.847*	**18.208***	-9.557*	6.766*	-3.529*
Populated	**51.718***	45.295*	2.046*	0.296	-15.198*
Small hosts	-18.082*	0.57	-49.649*	**99.965***	-0.242

Without considering the changes in the number of eggs laid by each female, both the number of ticks and the number of populated patches are more strongly influenced by drop-off frequency than by any other parameter. With all parameters combined in a partial rank correlation analysis, the number of immigrants into the system was also more strongly associated with drop-off frequency than the number of ticks per drop-off, although both parameters were significant and had large effects on the outcome. Small host density was strongly associated with the number of core, or suitable, habitat patches, and had a negative relationship with the number of land use classes in the simulation.

5.5 APPLICATION

5.5.1 EFFECTS OF PROPAGULE PRESSURE ON DIVERSITY

The frequency of drop-offs was the most important factor in haplotype diversity after 3 years. Higher drop-off frequencies resulted in steeper positive trends in the relationship between haplotype richness and population numbers (Figure 16.), and between haplotype richness and the total number of ticks at the end of the runs divided by propagule sizes (Figure 17.). Propagule sizes were influenced by drop-off frequencies and the the maximum number of ticks per drop-off, subject to stochastic influences on both parameters. Plotting richness against propagule pressure ($I * D$) showed the clearest relationship among the variables (Figure 18.). The practical application for tick control and management would be to use this model to estimate propagule pressure for different sites based on genetic diversity. Understanding the introduction effort of this species in different sites regionally, as well as between regions where new introductions are being detected, would facilitate interventions designed to control population establishment or expansion. For example, surveillance projects can identify candidate sites for experimental control efforts where relatively low propagule pressure is suspected to contribute to low diversity (Benham et al., 2021). Experimental control could include a range of host or habitat interventions (White & Gaff, 2018). In areas where prescribed burning is already used as a management tool, seasonality and frequency of burns may have distinctly different effects, even where it appears that burning has not eliminated populations. Outcomes could be monitored by using tick densities and diversity estimators to understand the impact of control efforts on the populations. Where propagule pressure is expected to be relatively low, ongoing immigration is less likely to contribute to noise in the data. This model can be used to set up on-the-ground experiments, which would also be useful in model validation.
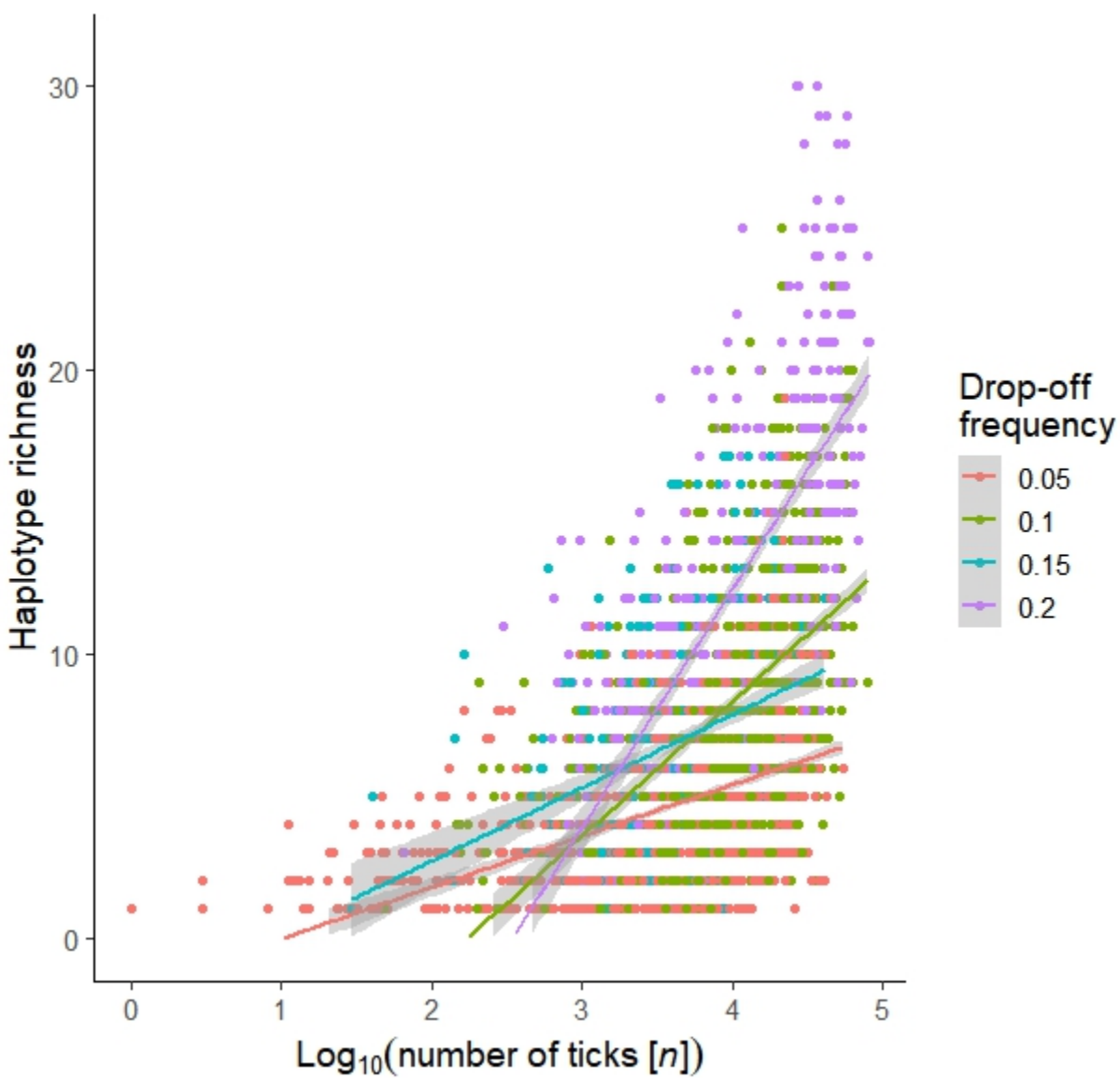
FIGURE 16. Haplotype richness by $\log_{10}$ number of ticks (n) in the final step. Parameters were varied for 1901 simulations. Log scale was used to minimize overplotting.
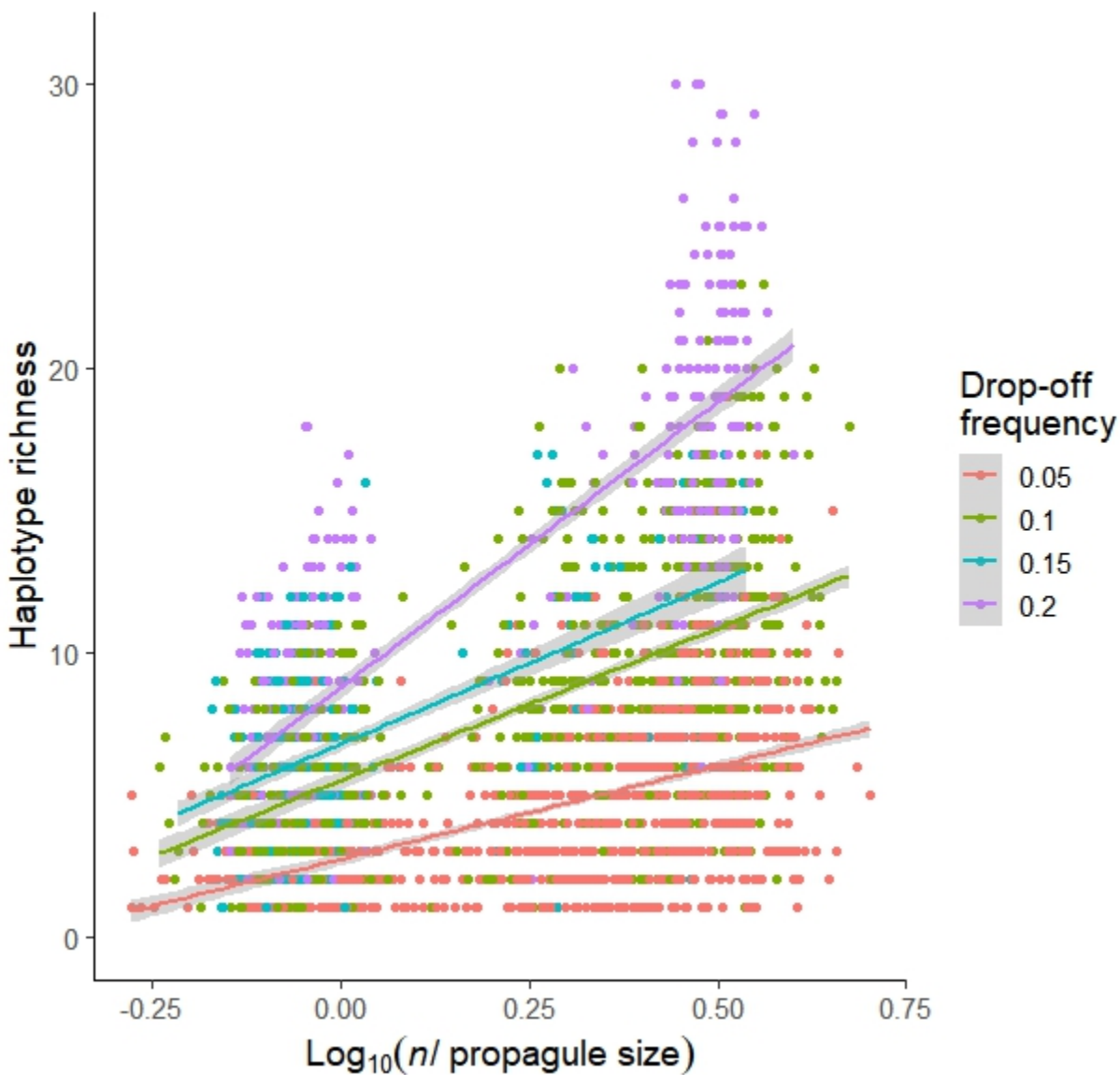
FIGURE 17. Haplotype richness by $\log_{10}(n/\text{propagule size})$. Propagule size is the quotient of the number of immigrants divided by drop-off events (I/D). Log scale was used to minimize overplotting.
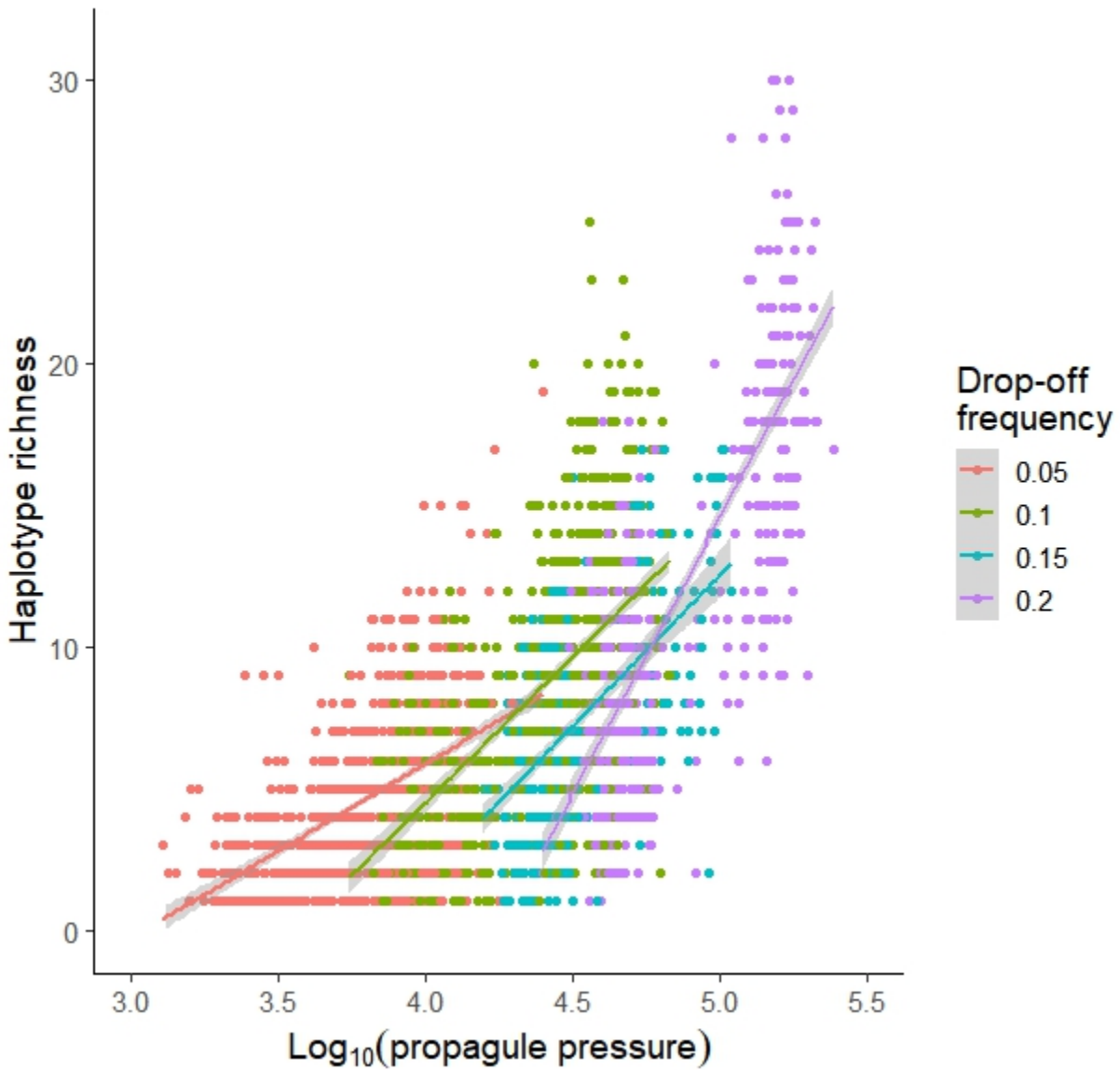
FIGURE 18. Haplotype richness by $\log_{10}$(propagule pressure). Propagule pressure is calculated as $(I * D)$, where I is the total number of immigrants into the system and D is the number of drop-off events that occurred during the run. Log scale was used to minimize overplotting.

5.5.2 RANK ABUNDANCE MODELS

Rank abundance models were generated by creating matrices of haplotype abundances by simulation run and running the radfit function in vegan (Oksanen et al., 2022). Four sets of parameters were run with drop-off frequency set to 0.1 and the maximum number of ticks per drop-off varied in increments of 5 for values 5–20. Two sets of rank abundance models were compared, with 5 and 10 ticks per drop-off in Figure 19., and 15 and 20 ticks per drop-off in Figure 20..

In Chapter 3, haplotype evenness at three sites, measured by rank abundance plots, fit the Zipf model. These sites included one which was thought to show the pattern of a founder effect because of dominance of a single haplotype, and the absence of that same haplotype at other sites in the area (Benham et al., 2021). The Zipf model fits best when evenness is skewed by the abundance of the dominant haplotype, which could be consistent with an earlier introduction of that haplotype.

In the simulation runs with fewer ticks per drop-off, the Zipf model fit more often (6/48) (Figure 19.) than in simulations with more ticks per drop-off (2/49) (Figure 20.). The more frequent fit of the Zipf model likely results from the constraint of propagule size (ticks per drop-off), which makes it more likely that females that reproduce successfully will do so in temporal sequence, i.e. in a series of drop-offs rather than as large cohorts. This fits with the expectation that the Zipf model corresponds to temporal succession (Whittaker, 1965; Wilson, 1992). The preemption model was more common overall (21/48 and 30/49) than any others, in contrast with empirical data for which the null model was generally the best fit (Chapter 3). This could indicate more ecological constraints in the simulation compared to the field, perhaps resulting from landscape effects or the predatory behavior of the large hosts on smaller hosts.
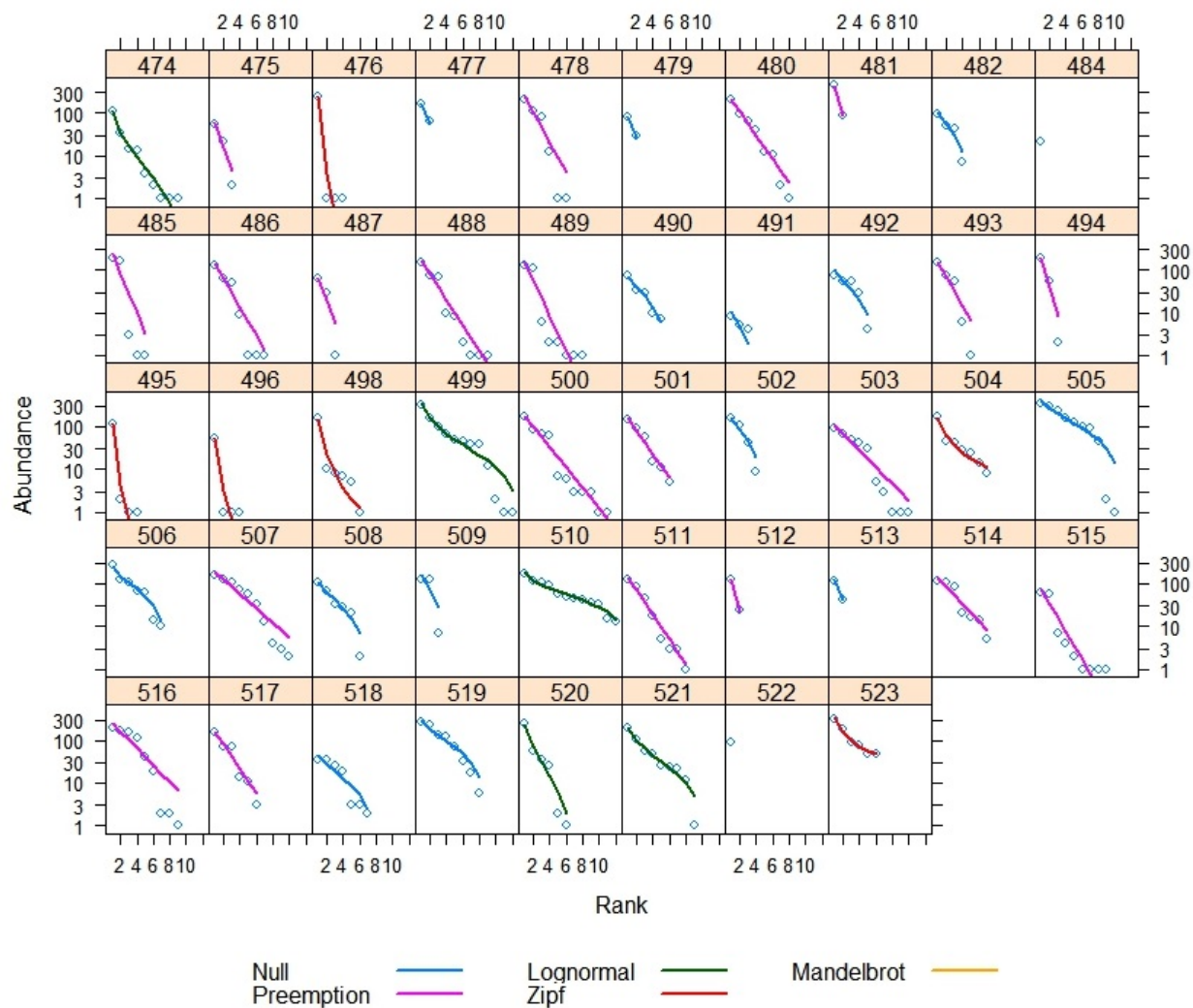
FIGURE 19. Rank abundance best fit models for a subset of 100 model runs with maximum ticks per drop-off set to 5 and 10. Subset includes only runs with $n > 10$. Rank abundance models show the overall evenness of each run by ranking haplotypes from most to least abundant and fitting them to a GLM model for comparison.
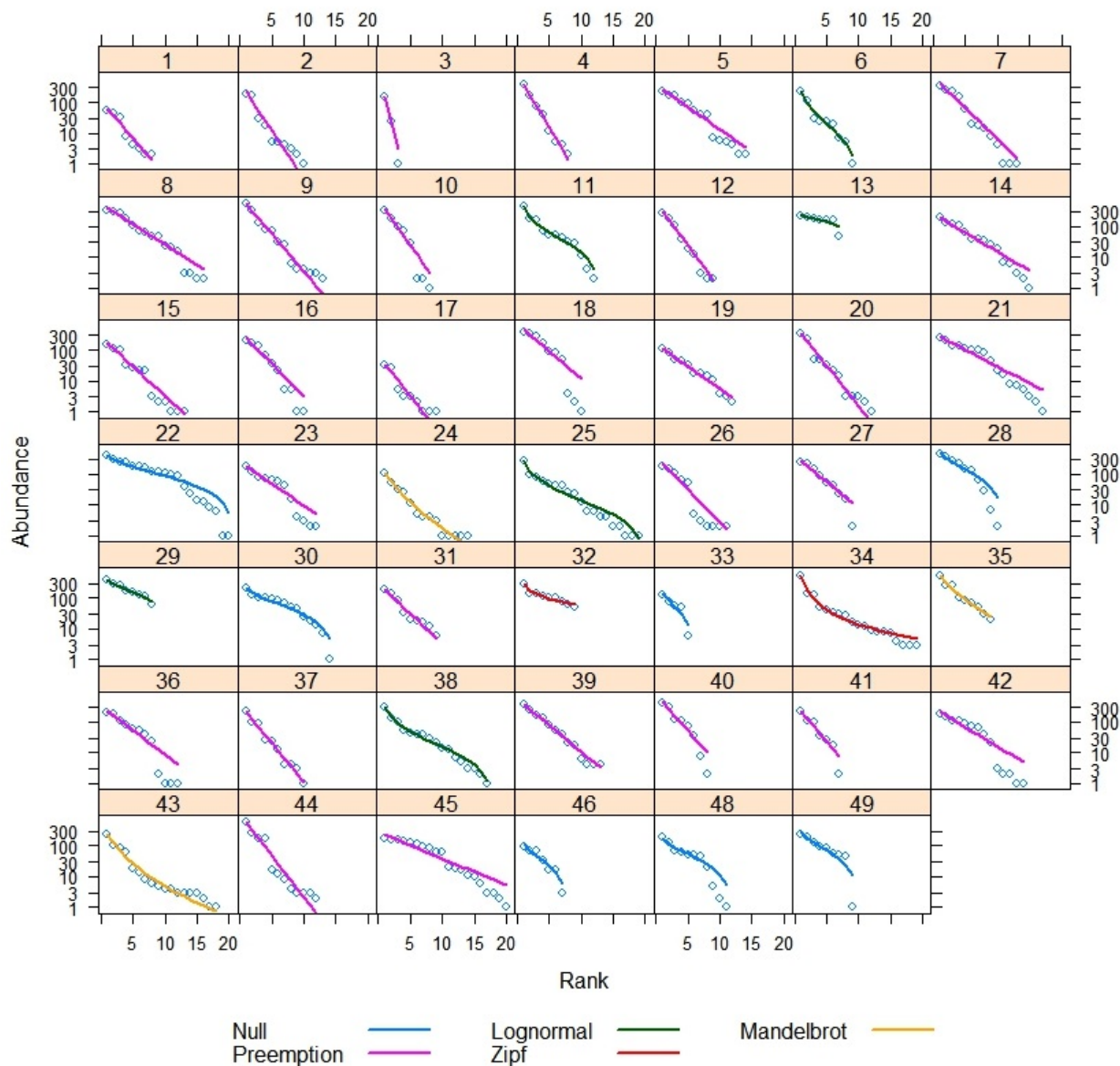
FIGURE 20. Rank abundance best fit models for a subset of 100 model runs with maximum ticks per drop-off set to 15 and 20. Subset includes only runs with $n > 10$. Rank abundance models show the overall evenness of each run by ranking haplotypes from most to least abundant and fitting them to a GLM model for comparison.

5.5.3 UPDATED PHENOLOGY

The model presented here makes assumptions regarding GCT natural history and phenology by using both literature (Nadolny & Gaff, 2018b; Teel et al., 2010) and field observations of adult and immature GCT activity in the Mid-Atlantic U.S. Data on immature tick phenology is limited to specimens collected from small mammal live-trapping, whereas adult ticks can be collected while questing by using the flagging technique. For example, the time for eggs to hatch, molting from larvae to nymph, questing time, and length of a blood meal were all drawn from literature (Teel et al., 2010). Generally, the shortest published time period was chosen for each of these parameters so that the phenology would best approximate local observations. The questing times specifically were shortened so that activity would cease during the winter months, as longer questing times generally lengthened active periods. The molt time from nymph to adult is the most speculative value, as it assumes a long stasis between seasons, generally starting from August to November before the individuals emerge as adults during the next active season.

Phenology of GCTs appears to vary by region (Nadolny & Gaff, 2018b; Teel et al., 2010). The phenology presented here is a proposed hypothesis for the Mid-Atlantic region, and only one of many possibilities. However, it represents a more specific phenology for GCTs than prior models, which generalized across multiple species (Nadolny & Gaff, 2018a). Tick numbers are shown here for all life stages across the duration of the model, with tick numbers averaged across 100 simulation runs (Figure 21.). The average phenology for all life stages is shown for year 3, after a third generation of adults emerges (Figure 22.). To highlight the emergence times for each life stage, simulation year 3 is also plotted with close-up plots showing time steps 640–700 (Figure 23.) showing larval emergence shortly after some adults have emerged and laid eggs. The next close-up shifts to time steps 640–750 (Figure 24.) to show nymph emergence, which only occurs after some larvae have emerged, fed, and molted.

Parameters values for the phenology runs are set to those in Table 11., with the exception of a smaller number of eggs (1000) to minimize the numbers of larvae and thus limit the scale of the y-axis.
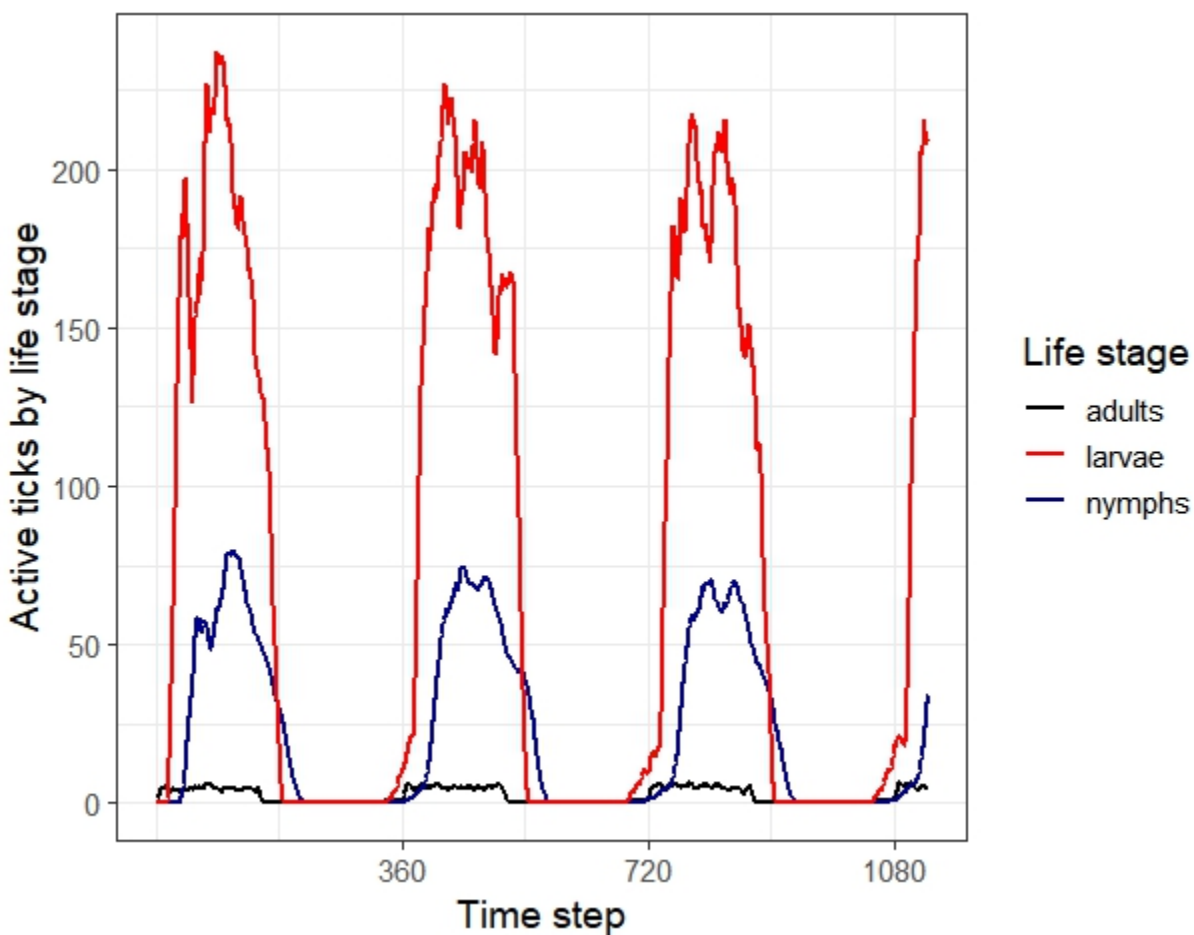
FIGURE 21. Simulated phenology of active ticks (questing or feeding) by life stage across simulation days. Number of active ticks is averaged across 100 simulation runs.
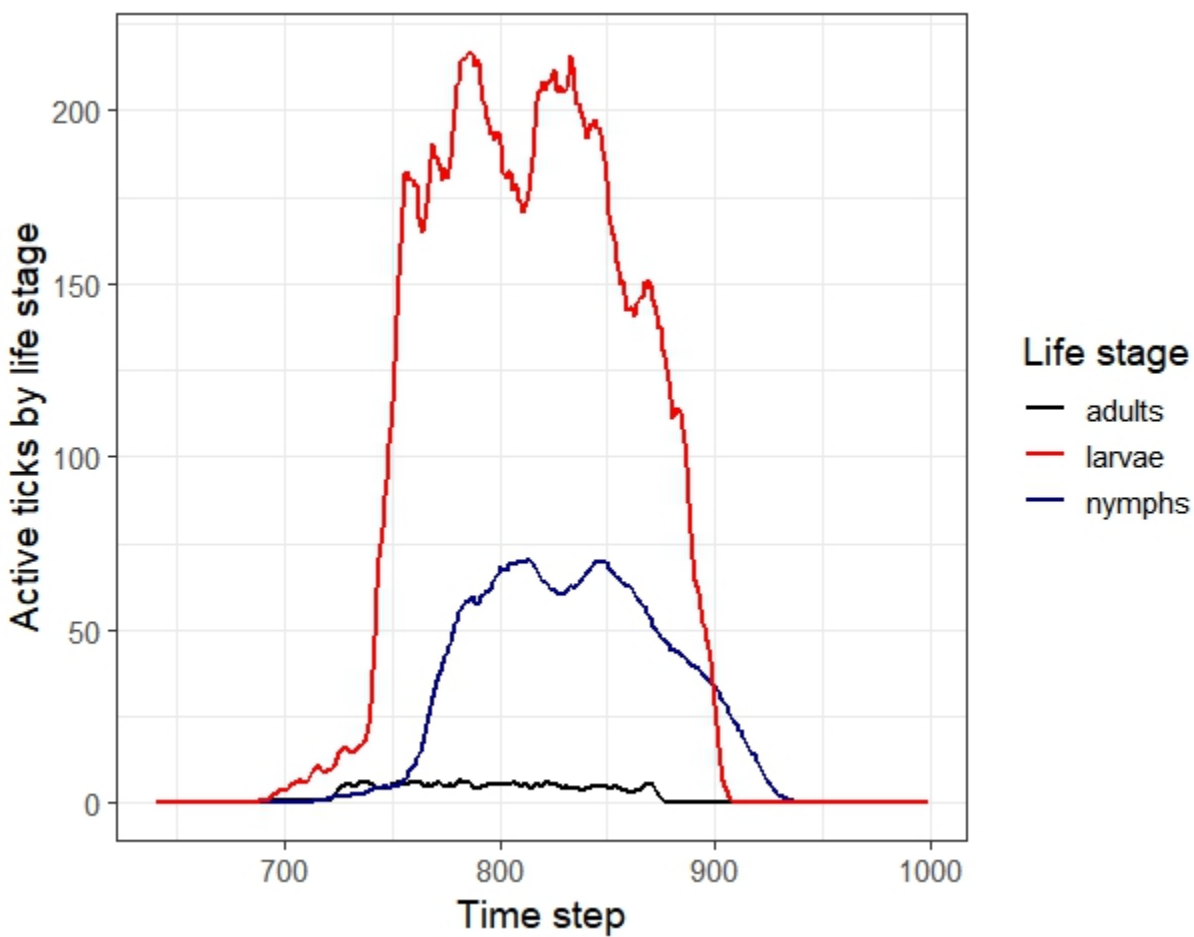
FIGURE 22. Average activity by life stage for one full year beginning in simulation year three (Y3). Time steps are shown from 640–999, corresponding to March 10, Y3 to March 9, Y4.
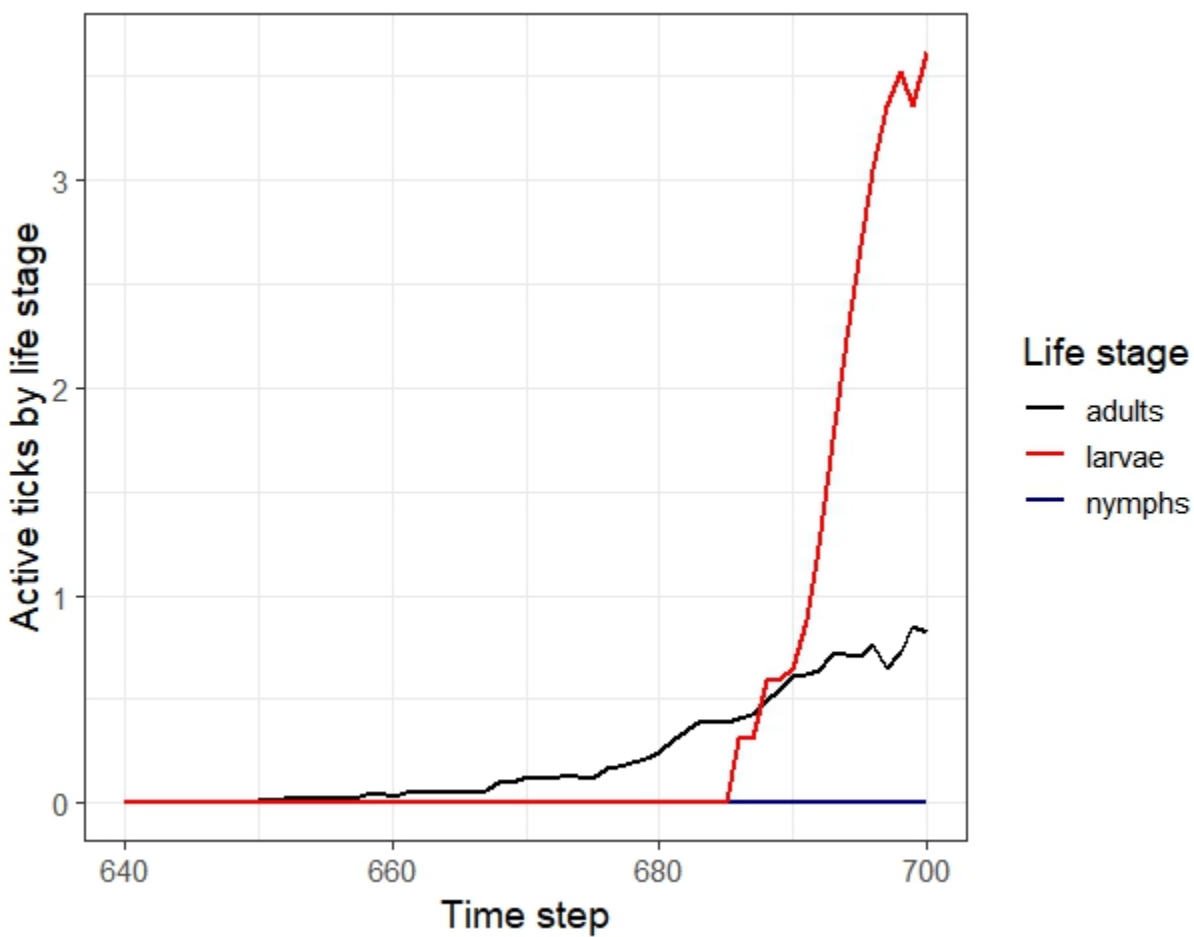
FIGURE 23. Close-up of emergence by life stages for adults and larvae. Model time steps 640–700 are shown here, corresponding to March 10 to May 9. Active nymphs are not plotted because they emerge after time step 700.
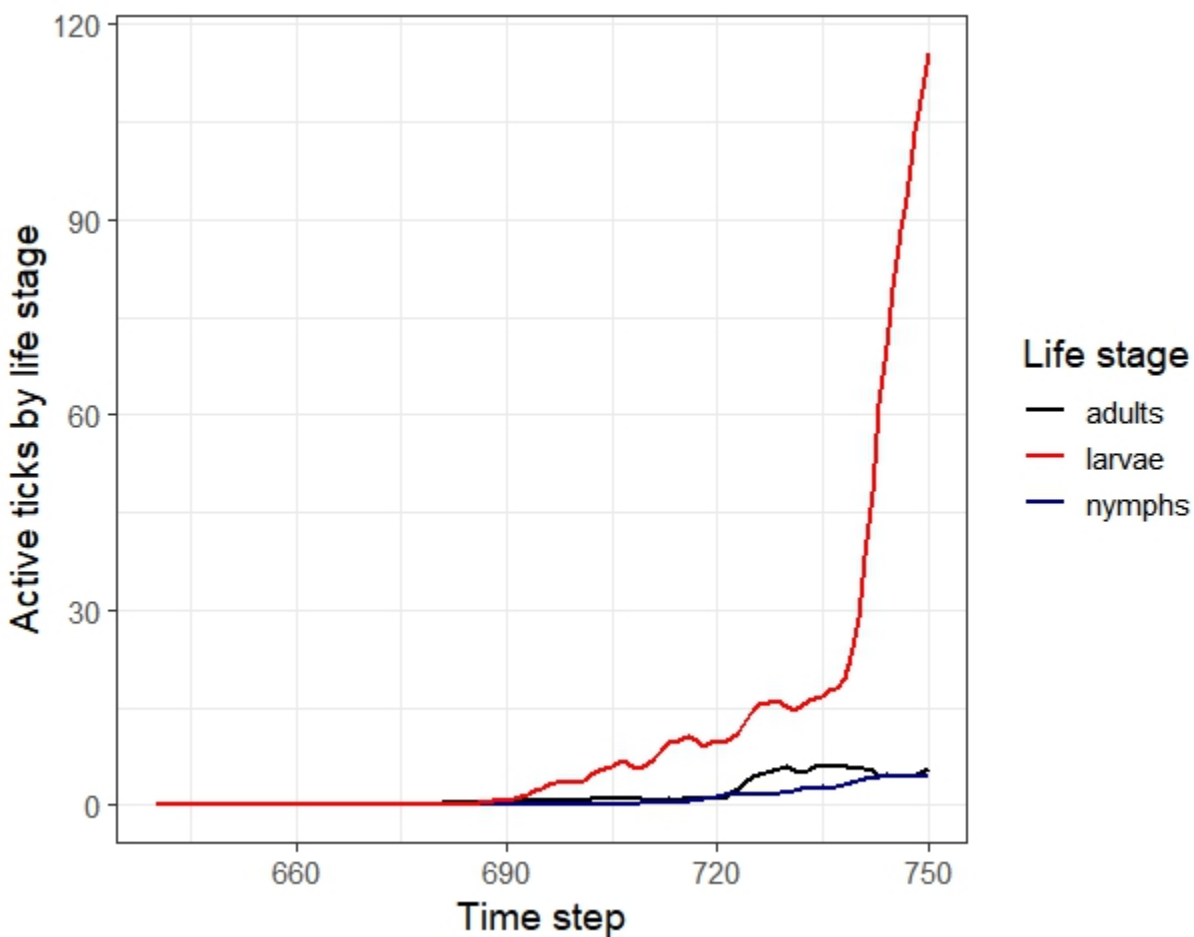
FIGURE 24. Close-up of emergence by life stages for all active life stages. Only time steps 640–750 are shown, corresponding to March 10 to June 28.

The resulting phenology was not entirely consistent with field collection, although this was primarily because little knowledge exists about immature phenology in the region. In the simulations, the active season for adults spans about 225 days on average, from time steps

corresponding to approximately March 21–November 1 (day-of-year 81–306). These dates line up with the typical April–September active season, with notable collections outside of this window in February and October (Gaff, unpublished). Less data are available for immature ticks in the field, as these are typically only collected on-host, often between July and August (Gaff & Espada, unpublished). In the model presented here, larvae emerged as early as April 27 and remained active as late as December 5, whereas nymphs were active from May 11 to January 7. After November, the model forced active ticks to either die or go into stasis until the next season, but eggs were not prevented from hatching, nor were those larvae prevented from molting after November 1. This likely explains the continued activity beyond November 1, which could be remedied in later updates as needed.

5.6 DISCUSSION

The model presented here provides a starting point for exploring the various effects of drop-off rates, host interactions, and natural history of Gulf Coast ticks on genetic outcomes. In addition to the applications described in Section 5.5, using this model to estimate propagule pressure can also help inform efforts to understand how GCT introductions contribute to the spread of *R. parkeri*. The updates here are compatible with infection dynamics from prior versions of TICKSIM models (Gaff, 2011; Nadolny & Gaff, 2013) and expand on these other models with the added parameters related to introduction effort, and the broader landscape extent. Integrating tick and host infection back into the model would enable an initial assessment of how new parameters affect infection prevalence, including ongoing drop-offs and different landscape configurations. Additionally, adding genetic tracking to the pathogen would help to explore a key question whether there is some congruence in genetic diversity in the ticks and the pathogens in a site in generations following an introduction, and which parameters might cause divergence between the respective genetic patterns. These questions are key to understanding the geographic relationship between GCT

and *R. parkeri* prevalence.

Compared to other genetics models, this model uses a simple approach to track mitochondrial haplotypes. However, this approach reflects the current state of population genetics in GCTs as many recent reports in *Amblyomma* spp. more broadly still rely on mitochondrial DNA (Benham et al., 2021; Bitencourth et al., 2017; Fournier et al., 2019; Nadolny et al., 2015). Viable microsatellite loci have only recently been proposed for *Amblyomma maculatum* and population patterns for these loci have not yet been thoroughly explored (Allerdice, 2021). The results of the simulations from the model presented here can be examined through classic population genetics software, e.g. Arlequin (Excoffier & Lischer, 2010), as well as through diversity analyses using programs for ecological analyses, including R packages like vegan (Oksanen et al., 2022) in R. Changes to the types of genetic markers for this model would require the development of a submodel for reproduction. Such changes might justify shifting to another modeling platform such as CDMetaPop (Landguth et al., 2017) if a careful effort is made to account for host interactions using the available parameters or model improvements.

Some unexpected negative associations between tick abundance and landscape configuration emerged in this model. These warrant further study, particularly why edge appears to be associated with a decline in richness, abundance, and occupied/populated patches. Drop-offs are limited in this model to large host movement, which is roughly based on coyote group sizes, predatory behavior, home ranges (Jensen et al., 2022), and associations with edge habitat (Webster et al., 2022). Large hosts in the program spend each turn in both edge and core (small mammal) habitat. They always populate the edges first when they emerge into the system, because the assumption is that they are moving from outside areas and dropping off new ticks. Because of these dynamics, ticks can be dropped off in edge habitat, but immatures are unlikely to find a small mammal host in the same habitat as they emerge. In this sense, edges (or edge-preferring hosts) may act as an ecological trap

for ticks that rely on multiple hosts with differing habitat preferences. Although GCTs are generalists that will feed on a large variety of hosts (Teel et al., 2010), this model presents an interesting predicament. If GCTs do have a suite of available or preferred hosts whose behaviors and habitat preferences conflict, then that could partially explain why populations are relatively sparse compared to other tick species.

The model is built with flexibility to test any landscape in the given spatial extent, including randomly generated landscapes that meet preset requirements (e.g. number and size of habitat patches or connectivity between patches). Further, suitability, hatch success, and appeal can all be modified to fit different hypotheses. This means that a much larger number of sites can be readily tested to see if the negative correlations persist, and the same sites presented in this simulation can also be evaluated using different hypothetical suitability settings. In addition, any landscape metric that can be extracted from a raster dataset, including fragmentation and percolation, can be evaluated using the basic model framework. This model creates the potential to explore a large number of hypotheses regarding the landscape ecology effects on GCTs.

Among the challenges with developing the model was the lack of information about small mammal hosts. Small mammals are known to host large numbers of immature ticks (Cumbie et al., 2020), and have been demonstrated to have a strong effect on GCT population success in agent-based simulations (Nadolny & Gaff, 2018a). The natural history of two suspected important hosts, the marsh rice rat (*Oryzomys palustris*) and the hispid cotton rat (*Sigmodon hispidus*) could be more explicitly modeled if their relationships between both ticks and the landscape are included in ongoing studies of GCTs. Natural history information is available for both species to support this effort (Bergstrom & Rose, 2004; Rose, 2020). Interactions between small mammals and larger hosts that can act as predators will continue to be an interesting area to explore, as predators can have both positive and negative effects on ticks by serving as hosts while potentially suppressing hosts that are critical to other life stages.

Finally, interactions with agents and the landscape can be improved as empirical data are gathered to better quantify how landscape affects movement and demography of different types of hosts, as well as tick survival.

Models are designed to explore a limited set of parameters that are suspected to be most influential to the processes of interest. This model simulates the effects of propagule pressure on GCT diversity in a spatial area that encompasses the habitat within a core sampling area and the surrounding landscape matrix. The demographic processes of ticks and their hosts are layered on top of the landscape, with interactions among all levels. This creates the emergent pattern of tick genetic diversity, which can be analyzed to make inferences about the frequency and type of interactions that are most likely taking place in the field. The critical next step is to gather empirical data to verify assumptions and patterns observed in the model.

CHAPTER 6

CONCLUSION

Unique patterns in haplotype diversity can indicate variation in the underlying processes of a species invasion or range expansion. One site in the Mid-Atlantic United States had a population of Gulf Coast ticks that differentiated that site from others. This differentiation was based on dominance of a single haplotype, which persisted across years, along with the rare occurrence of that haplotype at the other sites (Benham et al., 2021). This indicates that establishment at this site might have occurred by a strong bottleneck effect that either limited the introduction of many haplotypes to the site initially, or led to a large die-off from which only few haplotypes recovered. The evidence favors some limitation on propagule pressure, i.e. a bottleneck in the introduction process, given the relative stability of this unique genetic pattern over time even as the population has fluctuated following large prescribed burns.

The first GCT was collected from TP1 as an adult in 2014. Since this tick was a unfed adult flagged from vegetation, it must have been present in the sites as a nymph or earlier life stage. From this, one can deduce that GCTs were present in the site by 2013 at the latest and were collected in low numbers until 2018 when the initial large population was identified and included in the initial population genetics. The site was acquired as a National Wildlife Refuge in 2001, after which the previously managed cropland was restored with native grasses and maintained as an open grassland habitat. Prior to 2001, crop management activities would have likely interfered with GCT establishment had they been introduced to the site, because practices such as tilling disrupt the soil surface where ticks spend much of their time off-host. Therefore I assume that GCTs arrived between 2001 and 2013.

The grassland is maintained with burning in two-year intervals since at least 2017. Burns clear most organic matter from the soil, leaving charred debris and mineral soil within the

main grassland tract. Along the edges of the fields, strips of mowed grass, with occasional clumps of taller grasses buffer the burned field area from the gravel roads. GCTs can occasionally be collected in small numbers in this buffer, even before any vegetation begins to reemerge within the core grassland. Burns typically occur early in the year before late April or May. Those burns that occur later, in April or May, are more likely to coincide with emergence of adult GCTs. The grass buffer areas and rodent burrows can act as refugia, providing some protection for GCTs that allows some individuals to survive burns. Overall densities appear to be negatively affected in the season following the burn, however recovery can be rapid in the following season, with up to a tenfold increase in numbers. Future efforts should continue to monitor these population dynamics in relation to habitat disturbance, along with any variation in *R. parkeri* prevalence in the ticks. Prescribed burning has been proposed as a method of tick control, and burns are often anecdotally cited by forest managers as beneficial in terms of reducing tick numbers. Long-term data on population dynamics and pathogen prevalence in a site that appears to persist and recover rapidly after burns can help clarify whether generalizations about burning as tick control are accurate. In addition, a more careful effort should be made to look at how burn frequency and seasonality affect the same dynamics. Changes in the activity of hosts and ticks during the timeframe in which burns tend to occur may affect individual survival, thus resulting in a broader effect on the populations.

Population genetics as a discipline has benefited from a long history of model development to understand demographic processes, dispersal history, as well as overall diversity and connectivity (Avise, 2004). Single-locus population genetics analyses are an important starting point for genetic diversity surveys, however all inferences from a single locus are limited by the variability, mutation rate, and modes of inheritance of that locus. Examining many more loci can improve estimated relationships between populations and even individuals within a population. Given several populations with multiple years of

data presented in Chapters 2 and 3, a natural next step would be to analyze these same samples with additional loci. Specifically, 14 polymorphic microsatellite loci (Allerdice, 2021) could be used to compare against the inferences made here with a 16S rRNA gene fragment by following the same analytical approaches. Further conclusions about relatedness between individuals and demographic history of these sites could be explored using the newly-developed microsatellites. Regarding pathogen exposure risk, using population genetics to uncover population dynamics over time would make it possible to connect tick demographics to pathogen infection rates in tick populations. From this, the strength of the link between the vector and the pathogen could be determined, along with any notable lag between tick population change and changing rates of *R. parkeri* infections in those populations. Microsatellites can also resolve the question of a founder effect by investigating inbreeding and relatedness among TP1 individuals to determine whether MAC6 haplotype ticks at that site are closely-related progeny, possibly from one founding female. Additional questions could be resolved regarding the species identities of ticks with Genbank (Clark et al., 2016) accession numbers: AZ1663, AZ1614, and AZ1640, which were collected from Arizona. The populations where the original named haplotypes were collected included *A. maculatum* sensu lato, a morphologically distinct species or subspecies of *A. maculatum* sensu stricto (or *A. maculatum*, Koch 1844), yet haplotype matches were also collected in our samples from the Mid-Atlantic states, including Delaware, North Carolina, and Virginia, which are all presumed to be *A. maculatum* s.s. consistent with other east coast GCTs.

The most valuable contribution of the agent-based model presented in Chapter 5 is the ability to evaluate the assumptions underlying our interpretations of population genetics results. In particular, the model simulates the range of outcomes that could result from either directly controlling parameters such as those that contribute to propagule pressure, or from the stochastic effects of host and landscape interactions that limit tick numbers within the site. SimAdapt (Rebaudo et al., 2013) provides a template for adding

microsatellite markers to this type of model, including options for controlling mutation rates through the graphical user interface (GUI). Based on prior experience, modifying the reproduction submodel to require male and female ticks to occupy the same patch or host, so that both parents can contribute to offspring genetics, substantially decreases the likelihood of population establishment and persistence. Key changes would have to be made to the reproduction submodel while paying special attention to those parameters that affect population establishment, particularly the number of eggs laid per female and the spatial scale. Such changes would be welcome in the effort to better simulate real-world reproduction, but go beyond the scope of this model, especially given the lack of existing population genetics data for GCTs using microsatellite markers.

As it stands now, the critical focus of the updated TICKSIM model in Chapter 5 was to use a working approximation of the real-world system to separate dispersal from environment in terms of parameters contributing to spread, in addition to those that more directly affect establishment. Each of these elements represent distinct barriers that influence the spread of an organism in the unified framework for biological invasions (Blackburn et al., 2011). The value of separating these components of the invasion process is to be able to determine the strongest limiting factors on the genetic diversity of new populations that result from introduction events. Linking diversity measures to the predictors of invasion success provides a way to then monitor populations more effectively with an understanding of site- and regional-level restrictions on the range expansion. In other words, the question of whether low immigration or environmental filtering play a stronger role in limiting invasion success can be answered, along with understanding to what degree can key parameters be modified and still result in successful population establishment? In the interest of public health, these questions can help direct efforts to control the spread and establishment of GCTs as a vector of medically-important pathogens by identifying the most critical parameters to control.

The model presented in Chapter 5 is regionally- specific and designed to answer questions

related directly to our empirical genetics data, however the parameters are flexible with regard to host behaviors, landscape effects, and haplotype numbers that can be introduced to the system. The parameters tested in the sensitivity analysis can be easily changed using the GUI in Netlogo (Wilensky, 2021). Other parameters listed in Tables 11., 12., and 13. can be adjusted by making minimal changes to the program code. Additional focus should be placed on testing model sensitivity to different landscapes, including changes to the suitability, appeal, and hatch success assumptions outlined in Table 13.. The presence of edge had a significant negative effect on several outcome variables, but edge was defined coarsely as the unsuitable habitat adjacent to suitable patches. In this sense, edge included multiple types of habitat, including some that would likely be unappealing to any of the animals modeled in this system. Reclassifying edge to better define edge as a habitat class or set of classes with unique suitabilities, rather than primarily a proximity-based definition, could make the measure more ecologically relevant. These changes would provide a better understanding of the relationship that emerged in the model. Ground-truthing to identify edge habitat types would be beneficial to the effort to reclassify edge as a true, ecologically-meaningful habitat class.

Field observations suggest a fairly reliable link between certain habitat and the likelihood of locating a Gulf Coast tick population, though it is clear from both the field and from analyses presented in Chapter 4 that such populations can be uncommon even in ideal habitat. An essential next step to improving attempts to use remote-sensing would be to collect data from the field to ground-truth canopy cover and land use classification schemes. Discrepancies appear in the LULC classes (CBPO, 2022), for example the site CH3 is classified as crop in areas where sports fields and adjacent unmowed edge occur. Further, interpolated soil grids (Hengl et al., 2017) failed in important areas of the coastal and barrier island sites, resulting in no data. Field measures would help close the gaps in the data, and provide a way to confirm and more accurately model landscape relationships to satellite

imagery, rather than relying on remote-sensing primarily. Soil organic matter, depth of the litter layer, leaf area, and canopy height and cover would all be useful variables to measure on the ground. Additionally, collecting these data from the sites over time, in conjunction with host and GCT sampling, would help provide a comprehensive dataset to improve our empirical understanding of landscape-host-tick connections, as well as to validate model assumptions. Validating the genetics models with the environmental dataset can enhance the ability of the model to distinguish between propagule pressure and environmental effects. Environmental data from on-site surveys could also help to create better species distribution models, similar to the tick and pathogen models developed for *Dermacentor variabilis* and *Rickettsia montanensis* (Lippi et al., 2021*a*). Such models have not been broadly used for *Amblyomma* species and few of those that attempt to model *Amblyomma* tick distributions also consider the pathogens (Lippi et al., 2021*b*). The opportunity exists to better bridge these modeling approaches in a way that addresses the public health implications, particularly pathogen exposure risks in connection with the distribution of tick vectors.

Landscape or habitat data can be supplemented by finer scale measures of soil and closer monitoring of tick populations in response to habitat change as disturbances are documented in established sites. Identifying suitable habitat from remotely sensed environmental data has proven challenging. The relative rarity of Gulf Coast ticks compared to those more common in the Mid-Atlantic, like the lone star tick (*Amblyomma americanum*), complicates spatial analysis of this species. One of the variables that did initially seem to be useful to detect an association between GCT and site characteristics was NDVI. NDVI is widely understood to be sensitive to bare soil, and prone to oversaturated at higher values, which likely reduced the sensitivity of the GLMM designed to look for a relationship between population presence and NDVI values. Further, the study was hampered by the overall lack of spatial points where population presence was detected. This combination of challenges

and overall limited results ultimately deferred the goal of creating a regional-scale map of suitable sites to use in conjunction with genetics data.

The ultimate challenge of controlling invading tick species can help to achieve the long-term goal of reducing the TBD burden on public health. Active surveillance programs that incorporate tick ecology and genetics are essential to identify, monitor, and manage populations that have the potential to increase human and animal exposure to pathogens. Although some processes remain elusive, the genetic surveillance presented in Chapters 2 and 3 combined with ecological simulations to isolate key influences in the invasion process help lay the groundwork for tick control applications. Ultimately, applying this knowledge to experimental control efforts will be the next step in bringing the the effort of tick control closer to realization.

REFERENCES

Allerdice, M. E. 2021. "Systematics and Population Structure of *Amblyomma maculatum* Group Ticks and *Rickettsia parkeri*, an Emerging Human Pathogen in Southern Arizona, USA." Dissertation. Mississippi State, MS: Mississippi State University.

Allerdice, M. E. J., L. Beati, H. Yaglom, R. R. Lash, J. Delgado-de la Mora, J. D. Licona-Enriquez, and C. D. Paddock. 2017. "*Rickettsia parkeri* (Rickettsiales: Rickettsiaceae) Detected in Ticks of the *Amblyomma maculatum* (Acari: Ixodidae) Group Collected from Multiple addresss in Southern Arizona." *Journal of Medical Entomology* 54: 1743—49.

Altschul, S. F., W. Gish, W. Miller, E. W. Myers, and D. J. Lipman. 1990. "Basic Local Alignment Search Tool." *Journal of Molecular Biology* 215: 403–10.

Avise, J. C. 2004. *Molecular Markers, Natural History, and Evolution.* Sunderland, MA: Sinauer Associates.

Bajwa, W. I., L. Tsynman, A. M. Egizi, R. Tokarz, L. P. Maestas, and D. M. Fonseca. 2022. "The Gulf Coast Tick, *Amblyomma maculatum* (Ixodida: Ixodidae), and Spotted Fever Group Rickettsia in the Highly Urbanized Northeastern United States." *Journal of Medical Entomology* 59: 1434–42.

Barker, C. M. 2019. "Models and Surveillance Systems to Detect and Predict West Nile Virus Outbreaks." *Journal of Medical Entomology* 56: 1508–15.

Bates, D., M. Maechler, B. Bolker, S. Walker, R. H. B. Christensen, H. Singmann, B. Dai, F. Scheipl, G. Grothendieck, P. Green, J. Fox, A. Bauer, and P. N. Krivitsky. 2022. "Lme4: Linear Mixed-Effects Models Using 'Eigen' and S4." R package version 1.1-3.1. https://CRAN.R-project.org/package=lme4.

Benham, S. A., H. D. Gaff, Z. J. Bement, C. Blaise, H. K. Cummins, R. Ferrara, J. Moreno, E. Parker, A. Phan, T. Rose, S. Azher, D. Price, and D. T. Gauthier. 2021. "Comparative Population Genetics of *Amblyomma maculatum* and *Amblyomma americanum* in the Mid-Atlantic United States." *Ticks and Tick-borne Diseases* 12: 101600.

Benjamini, Y., A. M. Krieger, and D. Yekutieli. 2006. "Adaptive Linear Step-up Procedures That Control the False Discovery Rate." *Biometrika* 93: 491–506.

Bergstrom, B. J. and R. K. Rose. 2004. "Comparative Life Histories of Georgia and Virginia Cotton Rats." *Journal of Mammalogy* 85: 1077–86.

Biggs, H. M., C. B. Behravesh, K. K. Bradley, F. S. Dahlgren, N. A. Drexler, J. S. Dumler, S. M. Folk, C. Y. Kato, R. R. Lash, M. L. Levin, R. F. Massung, R. B. Nadelman, W. L. Nicholson, C. D. Paddock, B. S. Pritt, and M. S. Traeger. 2016. "Diagnosis and Management of Tickborne Rickettsial Diseases: Rocky Mountain Spotted Fever and Other Spotted Fever Group Rickettsioses, Ehrlichioses, and Anaplasmosis — United States: A Practical Guide for Health Care and Public Health Professionals." *Recommendations and Reports* 65: 1–44.

Bitencourth, K., M. Amorim, S. V. De Oliveira, R. L. Caetano, C. M. Voloch, and G. S. Gazêta. 2017. "*Amblyomma sculptum* : Genetic Diversity and Rickettsias in the Brazilian Cerrado Biome." *Medical and Veterinary Entomology* 31: 427–37.

Blackburn, T. M., J. L. Lockwood, and P. Cassey. 2017. "The Influence of Numbers on Invasion Success." Pages 25–39 *in* S. C. H. Barrett, R. I. Colautti, K. M. Dlugosch, and L. H. Rieseberg, editors, *Invasion Genetics: The Baker and Stebbins Legacy*. Hoboken, NJ: John Wiley & Sons.

Blackburn, T. M., P. Pyšek, S. Bacher, J. T. Carlton, R. P. Duncan, V. Jarošík, J. R. Wilson,

and D. M. Richardson. 2011. "A Proposed Unified Framework for Biological Invasions." *Trends in Ecology and Evolution* 26: 333–9.

Bowen, B. W., K. Shanker, N. Yasuda, M. Celia, M. C. M. D. Malay, S. von der Heyden, G. Paulay, L. A. Rocha, K. A. Selkoe, P. H. Barber, S. T. Williams, H. A. Lessios, E. D. Crandall, G. Bernardi, C. P. Meyer, K. E. Carpenter, and R. J. Toonen. 2014. "Phylogeography Unplugged: Comparative Surveys in the Genomic Era." *Bulletin of Marine Science* 90: 13–46.

Brenner, A. E. and R. Raghavan. 2021. "Complete Mitochondrial Genome Sequence of the Gulf Coast Tick (*Amblyomma maculatum*)." *Microbiology Resource Announcements* 10: e00431–21.

CBPO [Chesapeake Bay Program Office]. 2022. "One-Meter Resolution Land Use/Land Cover Dataset for the Chesapeake Bay Watershed, 2017/18." Chesapeake Conservancy, U.S. Geological Survey, and University of Vermont Spatial Analysis Lab, Dataset. https://www.chesapeakeconservancy.org/conservation-innovation-center/high-resolution-data/lulc-data-project-2022/.

CDC [Centers for Disease Control and Prevention]. 2019. "Rocky Mountain Spotted Fever: Epidemiology and Statistics." Online. https://www.cdc.gov/rmsf/stats/index.html.

Chao, A. 1984. "Non-Parametric Estimation of the Classes in a Population." *Scandinavian Journal of Statistics* 11: 265–70.

Chao, A. and S.-M. Lee. 1992. "Estimating the Number of Classes via Sample Coverage." *Journal of the American Statistical Association* 87: 210–7.

Chao, A., K. Ma, T. Hsieh, and C. Chiu. 2016. "SpadeR (Species-Richness Prediction and

Diversity Estimation in R): An R Package in CRAN.". http://chao.stat.nthu.edu.tw/wordpress/software_download.

Childs, J. E. and C. D. Paddock. 2003. "The Ascendancy of *Amblyomma americanum* as a Vector of Pathogens Affecting Humans in the United States." *Annual Review of Entomology* 48: 307–37.

Clark, K., I. Karsch-Mizrachi, D. J. Lipman, J. Ostell, and E. W. Sayers. 2016. "Genbank." *Nucleic Acid Research* 44: D67–72.

Clarke, K. R. and R. N. Gorley. 2006. *Primer v6: User Manual/Tutorial* 866. Plymouth: Primer-E.

Cuervo, P. F., F. S. Flores, J. M. Venzal, and S. Nava. 2021. "Niche Divergence among Closely Related Taxa Provides Insight on Evolutionary Patterns of Ticks." *Journal of Biogeography* 48: 2865–76.

Cumbie, A. N., C. D. Espada, R. M. Nadolny, R. K. Rose, R. D. Dueser, W. L. Hynes, and H. D. Gaff. 2020. "Survey of *Rickettsia parkeri* and *Amblyomma maculatum* Associated with Small Mammals in Southeastern Virginia." *Ticks and Tick-borne Diseases* 11: 101550.

de la Fuente, J., R. A. Van Den Bussche, and K. M. Kocan. 2001. "Molecular Phylogeny and Biogeography of North American Isolates of *Anaplasma marginale* (Rickettsiaceae: Ehrlichieae)." *Veterinary Parasitology* 97: 65–76.

Dennis, D. T., T. S. Nekomoto, J. C. Victor, W. S. Paul, and J. Piesman. 1998. "Reported Distribution of *Ixodes scapularis* and *Ixodes pacificus* (Acari: Ixodidae) in the United States." *Journal of Medical Entomology* 35: 629–38.

Dewitz, J. 2021. "National Land Cover Database (NLCD) 2019 Products (Ver. 2.0, June 2021)." U.S. Geological Survey, Dataset. https://doi.org/10.5066/P9KZCM54.

Didan, K. 2021. "MODIS/Terra Vegetation Indices 16-Day L3 Global 0.05Deg CMG V061." dataset. NASA EOSDIS Land Processes DAAC. https://doi.org/10.5067/MODIS/MOD13C1.061.

Dyer, R. J. 2014a. "Gstudio: Analyses and Functions Related to the Spatial Analysis of Genetic Marker Data." R package version 1.3. https://mran.microsoft.com/snapshot/2014-11-17/web/packages/gstudio/index.html.

Dyer, R. J. 2014b. "popgraph: This is an R Package That Constructs and Manipulates Population Graphs." R package version 1.4. https://cran.microsoft.com/snapshot/2015-07-29/web/packages/popgraph/index.html.

Dyer, R. J. and J. D. Nason. 2004. "Population Graphs: The Graph Theoretic Shape of Genetic Structure." *Molecular Ecology* 13: 1713–27.

Dyer, R. J., J. D. Nason, and R. C. Garrick. 2010. "Landscape Modeling of Gene Flow: Improved Power Using Condition Genetic Distance Derived from the Topology of Population Networks." *Molecular Ecology* 19: 3746–59.

Esri. 2022. "ArcGIS Pro 3.0." Software.

Excoffier, L. and H. E. L. Lischer. 2010. "Arlequin Suite Ver 3.5: A New Series of Programs to Perform Population Genetics Analyses under Linux and Windows." *Molecular Ecology Resources* 10: 564–7.

Excoffier, L., P. E. Smouse, and J. M. Quattro. 1992. "Analysis of Molecular Variance Inferred from Metric Distances among DNA Haplotypes: Application to Human Mitochondrial DNA Restriction Data." *Genetics* 131: 479–91.

Ferrari, F. A., J. Goddard, M. Caprio, C. D. Paddock, T. Mixson-Hayden, and A. S. Varela-Stokes. 2013. "Population Analyses of *Amblyomma maculatum* Ticks and *Rickettsia parkeri* Using Single-Strand Conformation Polymorphism." *Ticks and Tick-borne Diseases* 4: 439–44.

Fick, S. E. and R. J. Hijmans. 2017. "WorldClim 2: New 1-km Spatial Resolution Climate Surfaces for Global Land Areas." *International Journal of Climatology* 37: 4302–15.

Florin, D. A., R. J. Brinkerhoff, H. Gaff, J. Jiang, R. G. Robbins, W. Eickmeyer, J. Butler, D. Nielsen, C. Wright, A. White, M. E. Gimpel, and A. L. Richards. 2014. "Additional U.S. Collections of the Gulf Coast Tick, *Amblyomma maculatum* (Acari: Ixodidae), from the State of Delaware, the First Reported Field Collections of Adult Specimens from the State of Maryland, and Data Regarding This Tick from Surveillance of Migratory Songbirds in Maryland." *Systematic and Applied Acarology* 19: 257–62.

Fornadel, C. M., X. Zhang, J. D. Smith, C. D. Paddock, J. R. Arias, and D. E. Norris. 2011. "High Rates of *Rickettsia parkeri* Infection in Gulf Coast Ticks (*Amblyomma maculatum*) and Identification of "*Candidatus* Rickettsia andeanae" from Fairfax County, Virginia." *Vector-Borne and Zoonotic Diseases* 11: 1535–9.

Fournier, G. F. S. R., A. Pinter, R. Santiago, S. Muñoz-Leal, T. F. Martins, M. G. Lopes, K. D. McCoy, C. Toty, M. C. Horta, M. B. Labruna, and R. A. Dias. 2019. "A High Gene Flow in Populations of *Amblyomma ovale* Ticks Found in Distinct Fragments of Brazilian Atlantic Rainforest." *Experimental Applied Acarology* 77: 215–28.

Gaff, H. D. 2011. "Preliminary Analysis of an Agent-Based Model for a Tick-Borne Disease." *Mathematical Biosciences and Engineering* 8: 463–73.

Gergel, S. E. and M. G. Turner, editors. 2017. *Learning Landscape Ecology.* New York: Springer.

Gleim, E. R., L. M. Conner, R. D. Berghaus, M. L. Levin, G. E. Zemtsova, and M. J. Yabsley. 2016. "The Phenology of Ticks and the Effects of Long-Term Prescribed Burning on Tick Population Dynamics in Southwestern Georgia and Northwestern Florida." *PloS ONE* 9: e112174.

Goddard, J. 2007. "Seasonal Activity of *Amblyomma* spp. in Mississippi." *Journal of Vector Ecology* 32: 157–9.

Hallett, L., M. L. Avolio, I. T. Carroll, S. K. Jones, A. A. M. MacDonald, D. F. B. Flynn, P. Slaughter, J. Ripplinger, S. L. Collins, C. Gries, and M. B. Jones. 2020. "codyn: Community Dynamics Metrics." R package version version 2.0.5. https://github.com/NCEAS/codyn.

Hecht, J. A., M. E. J. Allerdice, S. E. Karpathy, H. D. Yaglom, M. Casal, R. R. Lash, J. Delgado-de la Mora, J. D. Licona-Enriquez, D. Delgado-de la Mora, K. Groschupf, A. Mertins, James W. Moors, D. E. Swann, and C. D. Paddock. 2020. "Distribution and Occurrence of *Amblyomma maculatum* Sensu Lato (Acari: Ixodidae) and *Rickettsia parkeri* (Rickettsiales: Rickettsiaceae), Arizona and New Mexico, 2017–2019." *Journal of Medical Entomology* 57: 2030–34.

Heitman, K. N., N. A. Drexler, D. Cherry-Brown, A. E. Peterson, P. A. Armstrong, and G. J. Kersh. 2019. "National Surveillance Data Show Increase in Spotted Fever Rickettsiosis: United States, 2016–2017." *American Journal of Public Health* 109: 719–21.

Hengl, T., J. Mendes de Jesus, G. B. M. Heuvelink, M. Ruiperez Gonzalez, M. Kilibarda, A. Blagotić, W. Shangguan, M. N. Wright, X. Geng, B. Bauer-Marschallinger, M. A. Guevara, R. Vargas, R. A. MacMillan, N. H. Batjes, J. G. B. Leenaars, E. Ribeiro, I. Wheeler, S. Mantel, and B. Kempen. 2017. "SoilGrids250m: Global Gridded Soil Information Based on Machine Learning." *PLOS ONE* 12: e0169748.

Herrick, K. L., S. A. Pena, H. D. Yaglom, B. J. Layton, A. Moors, A. D. Loftis, M. E. Condit, J. Singleton, C. Y. Kato, A. M. Denison, D. Ng, J. W. Mertins, and C. D. Paddock. 2016. "*Rickettsia parkeri* Rickettsiosis, Arizona, USA." *Emerging Infectious Diseases* 22: 780–5.

Hijmans, R. J., A. Ghosh, and A. Mandel. 2022. "geodata: Download Geographic Data." R package version 2 0.5-3. https://CRAN.R-project.org/package=geodata.

Hijmans, R. J., J. van Etten, M. Sumner, J. Cheng, D. Baston, A. Bevan, R. Bivand, L. Busetto, M. Canty, B. Fasoli, D. Forrest, A. Ghosh, D. Golicher, J. Gray, J. A. Greenberg, P. Hiemstra, K. Hingee, A. Ilich, C. Karney, M. Mattiuzzi, S. Mosher, B. Naimi, J. Nowosad, E. Pebesma, O. P. Lamigueiro, E. B. Racine, B. Rowlingson, A. Shortridge, B. Venables, and R. Wueest. 2023. "raster: Geographic Data Analysis and Modeling." R package version 2 3.6-14. https://CRAN.R-project.org/package=raster.

Huang, S., L. Tang, J. Hupy, and G. Shao. 2021. "A Commentary Review on the Use of Normalized Difference Vegetation Index (NDVI) in the Era of Popular Remote Sensing." *Journal of Forestry Research* 32: 1–6.

Huang, Z. Y. X., van Langevelde F., A. Estrada-Peña, G. Suzán, and de Boer W.F. 2016. "The Diversity-Disease Relationship: Evidence for and Criticisms of the Dilution Effect." *Parasitology* 143: 1075–86.

Jensen, A. J., C. J. Marneweck, J. C. Kilgo, and D. S. Jachowski. 2022. "Coyote Diet in North America: Geographic and Ecological Patterns During Range Expansion." *Mammal Review* 52: 480–96.

Kearse, M., R. Moir, A. Wilson, S. Stones-Havas, M. Cheung, S. Sturrock, S. Buxton, A. Cooper, S. Markowitz, C. Duran, T. Thierer, B. Ashton, P. Meintjes, and A. Drummond. 2012. "Geneious Basic: An Integrated and Extendable Desktop Software Platform for the Organization and Analysis of Sequence Data." *Bioinformatics* 28: 1647–9.

Keirans, J. E. and E. H. Lacombe. 1998. "First Records of *Amblyomma americanum*, *Ixodes* (*Ixodes*) *dentatus*, and *Ixodes* (*Ceratixodes*) *uriae* (Acari: Ixodidae) from Maine." *The Journal of Parasitology* 84: 629–31.

Ketchum, H. R., P. D. Teel, C. J. Coates, O. F. Strey, and M. T. Longnecker. 2009. "Genetic Variation in 12S and 16S Mitochondrial rDNA Genes of Four Geographically Isolated Populations of Gulf Coast Ticks (Acari: Ixodidae)." *Journal of Medical Entomology* 46: 482–9.

Kocan, A. A., M. Breshears, C. Cummings, R. J. Panciera, S. A. Ewing, and R. W. Barker. 1999. "Naturally Occurring Hepatozoonosis in Coyotes from Oklahoma." *Journal of Wildlife Disease* 28: 86–9.

Kopsco, H. L., R. J. Duhaime, and T. N. Mather. 2021. "Crowdsourced Tick Image-Informed Updates to U.S. County Records of Three Medically Important Tick Species." *Journal of Medical Entomology* 58: 2412–24.

Lado, P., S. Nava, L. Mendoza-Uribe, A. G. Caceres, J. Delgado-de la Mora, J. D. Licona-Enriquez, D. Delgado-de la Mora, M. B. Labruna, L. A. Durden, M. E. J. Allerdice, C. D. Paddock, M. P. J. Szabó, J. M. Venzal, A. A. Guglielmone, and L. Beati. 2018. "The *Amblyomma maculatum* Koch, 1844 (Acari: Ixodidae) Group of Ticks: Phenotypic Plasticity or Incipient Speciation?." *Parasites & Vectors* 11: 610.

Landguth, E., A. Bearlin, C. C. Day, and J. Dunham. 2017. "CDMetaPOP: An Individual-Based, Eco-Evolutionary Model for Spatially Explicit Simulation of Landscape Demogenetics." *Methods in Ecology and Evolution* 8: 4–11.

Landguth, E. L. and S. A. Cushman. 2010. "CDPOP: A Spatially Explicit Cost Distance Population Genetics Program." *Molecular Ecology* 10: 156–61.

Landguth, E. L., B. C. Fedy, S. J. Oyler-McCance, A. L. Garey, S. L. Emel, M. Mumma, H. H. Wagner, M.-J. Fortin, and S. A. Cushman. 2012. "Effects of Sample Size, Number of Markers, and Allelic Richness on the Detection of Spatial Genetic Pattern." *Molecular Ecology Resources* 12: 276–84.

Leal, B., E. Zamora, A. Fuentes, D. B. Thomas, and R. K. Dearth. 2020. "Questing by Tick Larvae (Acari: Ixodidae): A Review of the Influences That Affect Off-Host Survival." *Annals of the Entomological Society of America* 113: 425–38.

Lippi, C. A., H. D. Gaff, A. L. White, H. K. S. John, A. L. Richards, and S. J. Ryan. 2021*a*. "Exploring the Niche of *Rickettsia montanensis* (Rickettsiales: Rickettsiaceae) Infection of the American Dog Tick (Acari: Ixodidae), Using Multiple Species Distribution Model Approaches." *Journal of Medical Entomology* 58: 1083–92.

Lippi, C. A., H. D. Gaff, A. L. White, and S. J. Ryan. 2021*b*. "Scoping Review of Distribution Models for Selected *Amblyomma* Ticks and Rickettsial Group Pathogens." *PeerJ* 9: e10596.

Maestas, L. P., S. R. Reeser, P. J. McGay, and M. H. Buoni. 2020. "Surveillance for *Amblyomma maculatum* (Acari: Ixodidae) and *Rickettsia parkeri* (Rickettsiales: Rickettsiaceae) in the State of Delaware, and Their Public Health Implications." *Journal of Medical Entomology* 57: 979–83.

McRae, B. H. 2006. "Isolation by Resistance." *Evolution* 60: 1551–61.

Mixson, T. R., S. L. Lydy, G. A. Dasch, and L. A. Real. 2006. "Inferring the Population Structure and Demographic History of the Tick, *Amblyomma americanum* Linnaeus." *Journal of Vector Ecology* 31: 181–92.

Molaei, G., E. A. H. Little, N. Khalil, B. N. Ayres, W. L. Nicholson, and C. D.

Paddock. 2021. "Established Population of the Gulf Coast Tick, *Amblyomma Maculatum* (Acari: Ixodidae), Infected with *Rickettsia Parkeri* (Rickettsiales: Rickettsiaceae), in Connecticut." *Journal of Medical Entomology* 58: 1459–62.

Monzón, J. D., E. G. Atkinson, B. M. Henn, and J. L. Benach. 2016. "Population and Evolutionary Genomics of *Amblyomma americanum*, an Expanding Arthropod Disease Vector." *Genome Biology and Evolution* 8: 1351–60.

Muñoz-Pajares, A. J. 2013. "SIDIER: Substitution and Indel Distances to Infer Evolutionary Relationships." *Methods in Ecology and Evolution* 4: 1195–200.

Nadolny, R. M. 2016. "A Hitchiker's Guide to Invasion Biology: Describing the Ecological Mechanisms Underlying the Range Expansions of Two Ixodid Tick Species." Dissertation. Norfolk, VA: Old Dominion University.

Nadolny, R. M. and H. D. Gaff. 2013. "Identifying Requirements for the Invasion of a Tick Species and Tick-Borne Pathogen through TICKSIM." *Mathematical Biosciences and Engineering* 10: 625–35.

Nadolny, R. M. and H. D. Gaff. 2018a. "Modelling the Effects of Habitat and Hosts on Tick Invasions." *Letters in Biomathematics* 5: 2–29.

Nadolny, R. M. and H. D. Gaff. 2018b. "Natural History of *Amblyomma maculatum* in Virginia." *Ticks and Tick-borne Diseases* 9: 188–195.

Nadolny, R. M., H. D. Gaff, J. Carlsson, and D. T. Gauthier. 2015. "Comparative Population Genetics of Two Invading Ticks: Evidence of the Ecological Mechanisms Underlying Tick Range Expansions." *Infection, Genetics and Evolution* 35: 153–62.

Nadolny, R. M., C. L. Wright, D. E. Sonenshine, W. L. Hynes, and H. D. Gaff. 2014. "Ticks

and Spotted Fever Group Rickettsiae of Southeastern Virginia." *Ticks and Tick-borne Diseases* 5: 53–7.

Oksanen, J., G. L. Simpson, F. G. Blanchet, R. Kindt, P. Legendre, P. R. Minchin, R. O'Hara, P. Solymos, M. H. H. Stevens, E. Szoecs, H. Wagner, M. Barbour, M. Bedward, B. Bolker, D. Borcard, G. Carvalho, M. Chirico, M. De Caceres, S. Durand, H. B. A. Evangelista, R. FitzJohn, M. Friendly, B. Furneaux, G. Hannigan, M. O. Hill, L. Lahti, D. McGlinn, M.-H. Ouellette, E. Ribeiro Cunha, T. Smith, A. Stier, C. J. Ter Braak, and J. Weedon. 2022. "vegan: Community Ecology Package." R package version 2.6-4. https://CRAN.R-project.org/package=vegan.

Paddock, C. D., R. W. Finley, C. S. Wright, H. N. Robinson, B. J. Schrodt, C. C. Lane, O. Ekenna, M. A. Blass, C. L. Tamminga, C. A. Ohl, S. L. F. McLellan, J. Goddard, R. C. Holman, J. J. Openshaw, J. W. Sumner, S. R. Zaki, and M. E. Ermeeva. 2008. "*Rickettsia parkeri* Rickettsiosis and Its Clinical Distinction from Rocky Mountain Spotted Fever." *Clinical Infectious Diseases* 47: 1188–96.

Paddock, C. D. and J. Goddard. 2015. "The Evolving Medical and Veterinary Importance of the Gulf Coast Tick (Acari: Ixodidae)." *Journal of Medical Entomology* 52: 230–52.

Paddock, C. D., P. W. Greer, T. L. Ferebee, J. Singleton, Jr., D. B. McKechnie, T. A. Treadwell, J. W. Krebs, M. J. Clarke, R. C. Holman, J. G. Olson, J. E. Childs, and S. R. Zaki. 1999. "Hidden Mortality Attributable to Rocky Mountain Spotted Fever: Immunohistochemical Detection of Fatal, Serologically Unconfirmed Disease." *The Journal of Infectious Diseases* 179: 1469–76.

Paddock, C. D., J. W. Sumner, J. A. Comer, S. R. Zaki, C. S. Goldsmith, J. Goddard, S. L. F. McLellan, C. L. Tamminga, and C. A. Ohl. 2004. "*Rickettsia parkeri:* A Newly

Recognized Cause of Spotted Fever Rickettsiosis in the United States." *Clinical Infectious Diseases* 38: 805–11.

Phillips, V. C., E. A. Zieman, C.-H. Kim, C. M. Stone, H. C. Tuten, and F. A. Jiminéz. 2020. "Documentation of the Expansion of the Gulf Coast Tick (*Amblyomma maculatum*) and *Rickettsia parkeri*: First Report in Illinois." *Journal of Parasitology* 106: 9–13.

Potapov, P., X. Li, A. Hernandez-Serna, A. Tyukavina, M. Hansen, A. Kommareddy, S. T. A. Pickens, H. Tang, C. E. Silva, J. Armston, R. Dubayah, J. B. Blair, and M. Hofton. 2020. "Mapping Global Forest Canopy Height through Integration of GEDI and Landsat Data." *Remote Sensing of Environment* 253: 112165.

R Core Team. 2023. *R: A Language and Environment for Statistical Computing*. Vienna, Austria: R Foundation for Statistical Computing.

Rebaudo, F., A. Le Rouzic, S. Dupas, J.-F. Silvain, M. Harry, and O. Dangles. 2013. "SimAdapt: An Individual-Based Genetic Model for Simulating Landscape Management Impacts on Populations." *Methods in Ecology and Evolution* 4: 595–600.

Ribeiro, J. M., N. J. Bayona-Vásquez, K. Budachetri, D. Kumar, J. C. Frederick, F. Tahir, B. C. Faircloth, T. C. Glenn, and S. Karim. 2022. "A Draft of the Genome of the Gulf Coast Tick, *Amblyomma maculatum*." *Ticks and Tick-borne Diseases* 14: 102090.

Rose, R. K. 2020. "The Natural History of the Marsh Rice Rat, *Oryzomys palustris*, in Eastern Virginia." *Banisteria* 54: 57–68.

Roy, D. P., V. Kovalskyy, H. K. Zhang, E. F. Vermote, L. Yan, S. S. Kumar, and A. Egorov. 2016. "Characterization of Landsat-7 to Landsat-8 Reflective Wavelength and Normalized Difference Vegetation Index Continuity." *Remote Sensing of Environment* 185: 57–70.

Russell, E. and J. Hovet. 2021. "GIS Extension for NetLogo.". https://github.com/NetLogo/GIS-Extension.

Schloerke, B., D. Cook, J. Larmarange, F. Briatte, M. Marbach, E. Thoen, A. Elberg, O. Toomet, J. Crowley, H. Hofmann, and H. Wickham. 2021. "GGally: Extension to 'ggplot2'." R package version 2.1.2. https://CRAN.R-project.org/package=GGally.

Simondi, S., G. Quero, V. Bonnecarrere, and L. Gutierrez. 2016. "haplotyper: Tool for Clustering Genotypes in Haplotypes." R package version 0.1. https://cran.r-project.org/web/packages/haplotyper/index.html.

Smith, B. and J. B. Wilson. 1996. "A Consumer's Guide to Evenness Indices." *Oikos* 76: 70–82.

Sokolowski, J. A. and C. M. Banks. 2009. "Agent-Based Modeling and Social Networks." Pages 63–79 *in* J. A. Sokolowski and C. M. Banks, editors, *Modeling and Simulation for Analyzing Global Events*. Hoboken, NJ: John Wiley & Sons.

Sonenshine, D. E. 1979. "Ticks of Virginia (Acari: Metastigmata)." Technical Report 13. Blacksburg, VA: Virginia Polytechnic Institute and State University.

Sonenshine, D. E. 2018. "Range Expansion of Tick Disease Vectors in North America: Implications for Spread of Tick-Borne Disease." *International Journal of Environmental Research and Public Health* 15: 478.

Sonenshine, D. E. and G. F. Levy. 1971. "The Ecology of the Lone Star Tick, *Amblyomma americanum* (L.), in Two Contrasting Habitats in Virginia (Acarina: Ixodidae)." *Journal of Medical Entomology* 8: 623–35.

Springer, Y. P., L. Eisen, L. Beati, A. M. James, and R. J. Eisen. 2014. "Spatial Distribution

of Counties in the Continental United States with Records of Occurrence of *Amblyomma americanum* (Ixodida: Ixodidae)." *Journal of Medical Entomology* 51: 342–51.

Stevenson, M., E. Sergeant, T. Nunes, C. Heuer, J. Marshall, J. Sanchez, R. Thornton, J. Reiczigel, J. Robison-Cox, P. Sebastiani, P. Solymos, K. Yoshida, G. Jones, S. Pirikahu, S. Firestone, R. Kyle, J. Popp, M. Jay, C. Reynard, A. Cheung, N. Singanallur, A. Szabo, and A. Rabiee. 2023. "epiR: Tools for the Analysis of Epidemiological Data." R package version 2.0.57. https://CRAN.R-project.org/package=epiR.

Teel, P. D., H. R. Ketchum, D. E. Mock, R. E. Wright, and O. F. Strey. 2010. "The Gulf Coast Tick: A Review of the Life History, Ecology, Distribution, and Emergence as an Arthropod of Medical and Veterinary Importance." *Journal of Medical Entomology* 47: 707–22.

Trout, R. T., C. D. Steelman, and A. L. Szalanski. 2010. "Population Genetics of *Amblyomma americanum* (Acari; Ixodidae) Collected from Arkansas." *Journal of Medical Entomology* 47: 152–61.

Webster, S. C., J. C. Beasley, J. W. Hinton, and M. J. Chamberlain. 2022. "Resident and Transient Coyotes Exhibit Differential Patterns of Movement Behavior across Heterogeneous Landscapes in the Southeastern United States." *Ecology and Evolution* 12: e8725.

White, A. and H. Gaff. 2018. "Review: Application of Tick Control Technologies for Blacklegged, Lone Star, and American Dog Ticks." *Journal of Integrated Pest Management* 9: 12.

Whittaker, R. H. 1965. "Dominance and Diversity in Land Plant Communities." *Science* 147: 250–60.

Wilensky, U. 2021. "NetLogo.". http://ccl.northwestern.edu/netlogo/.

Wilson, J. 1992. "Methods for Fitting Dominance/Diversity Curves." *Journal of Vegetation Science* 2: 35–46.

Wittmann, M. J., D. Metzler, W. Gabriel, and J. M. Jeschke. 2014. "Decomposing Propagule Pressure: The Effects of Propagule Size and Propagule Frequency on Invasion Success." *Oikos* 123: 441–50.

Wright, C. L., H. D. Gaff, D. E. Sonenshine, and W. L. Hynes. 2015. "Experimental Vertical Transmission of *Rickettsia parkeri* in the Gulf Coast Tick, *Amblyomma maculatum*." *Ticks and Tick-borne Diseases* 6: 568–73.

Wright, C. L., R. M. Nadolny, J. Jiang, A. L. Richards, D. E. Sonenshine, H. D. Gaff, and W. L. Hynes. 2011. "*Rickettsia parkeri* in Gulf Coast Ticks, Southeastern Virginia, USA." *Emerging Infectious Diseases* 17: 896–98.

Wright, S. 1932. "The Roles of Mutation, Inbreeding, Crossbreeding and Selection in Evolution." *Proceedings of the XI International Congress of Genetics* 8: 209–22.

Yang, L., S. Jin, P. Danielson, C. Homer, L. Gass, S. M. Bender, A. Case, C. Costello, J. Dewitz, J. Fry, M. Funk, B. Granneman, G. C. Liknes, M. Rigge, and G. Xian. 2018. "A New Generation of the United States National Land Cover Database: Requirements, Research Priorities, Design, and Implementation Strategies." *ISPRS Journal of Photogrammetry and Remote Sensing* 146: 108–23.

APPENDIX

PERMISSION TO REPRINT PUBLISHED MATERIAL

Chapter: 2

Article: Comparative population genetics of *Amblyomma maculatum* and *Amblyomma americanum* in the mid-Atlantic United States

Journal: Ticks and Tick-Borne Diseases

License #: N/A, authors retain rights to reprint in thesis or dissertation without explicit permission.

See the following webpage for more information:

https://www.elsevier.com/about/our-business/policies/copyright#Author-rights

Date Received: February 3, 2023

Author rights in Elsevier's proprietary journals	Published open access	Published subscription
Use and share their works for scholarly purposes (with full acknowledgement of the original article): 1. In their own classroom teaching. Electronic and physical distribution of copies is permitted 2. If an author is speaking at a conference, they can present the article and distribute copies to the attendees 3. Distribute the article, including by email, to their students and to research colleagues who they know for their personal use 4. Share and publicize the article via Share Links, which offers 50 days' free access for anyone, without signup or registration 5. Include in a thesis or dissertation (provided this is not published commercially) 6. Share copies of their article privately as part of an invitation-only work group on commercial sites with which the publisher has a hosting agreement	√	√

VITA

Sara Simmons Benham

Department of Biological Sciences

Old Dominion University

Norfolk, VA 23529

PREVIOUS DEGREES

M.S. Biology, July 2017, Southeastern Louisiana University.

B.S. Natural Resources, March 2012, Oregon State University.

PUBLICATIONS

[**Submitted 2023**] Benham, S.A., S. Dutta, R. Maddamsetti, C. Wright, A. Anderson, D.T. Gauthier and H.D. Gaff. "Contrasting Tick Species Behaviors: A Course-Based Undergraduate Research Experience (CURE)." *Spora*.

Benham, S.A. et al. 2021. "Comparative Population Genetics of *Amblyomma maculatum* and *Amblyomma americanum* in the Mid-Atlantic United States." *Ticks and Tick-Borne Diseases* 12:101600.

Simmons, S.A. and J.L. Bossart. 2020. "Apparent Resilience to Fire of Native Bee (Hymenoptera: Apoidea) Communities From Upland Longleaf Pine Forests in Louisiana and Mississippi." *Southeastern Naturalist* 19:567–581.

SCHOLARSHIPS

CDC Southeastern Center of Excellence PhD studentship, 2023   tuition and stipend

Virginia Space Grant Consortium Graduate Research Fellowship, 2020–2022 $12,000

BGSO Research Award, 2020 $300

Graduate Teaching Assistant, 2019–2020   tuition and stipend

Modeling and Simulation Fellowship, 2017–2019   tuition and stipend